DOCTOR OF PHILOSOPHY

Experimental and numerical analysis of behaviour of the myxospermous seeds of Capsella bursa-pastoris (L.) Medik. (shepherd's purse) in soil

Deng, Wenni

Award date:
2012

Experimental and numerical analysis of behaviour of the myxospermous seeds of *Capsella bursa-pastoris* (L.) Medik. (shepherd's purse) in soil

Wenni Deng

BEng MSc

A Dissertation Submitted For the Degree Of

Doctor of Philosophy

Division of Civil Engineering

The University of Dundee

November 2012

TABLE OF CONTENTS

LIST OF FIGURES

LIST OF TABLES

NOTATION

LATIN LETTERS

a	Radius of equilibrium of a spherical gel
a_0	Initial gel radius
a_1	Fitted parameter of mucilage rheology
b	Fitted parameter of mucilage rheology
b_0	Parameter depends on the soil-water diffusion function
c	Sitted parameter of soil rheology
C	Mucilage concentration
C_0	Initial water content
C_1	Consistency index
C_{eq}	Equilibrium water content
C_s	Soil seedbank density
d	Fitted parameter of soil rheology
d_s	Distance from amended soil layer to soil surface
D	Diffusion coefficient
D_s	Coordinate of soil column
E	Elastic diffusion coefficients

f	Friction between the gel and the solvent
f_0	Fillable air porosity
g	gravitational acceleration
G	Shear modulus
G'	Storage modulus
G''	Loss modulus
h_s	Amended soil layer thickness
H	Water pressure head
H_p	Water pressure head
i	Constant
J	Diffusion flux
k	Intrinsic permeability
k_0	Constant in gel swelling empirical model
k_1	Fitted parameters for mucilage viscosity as function of frequency
k_2	Fitted parameters for mucilage shear modulus as function of frequency
k_3	Fitted parameters for mucilage loss modulus as function of freqency
k_m	Mass transfer coefficient
k_r	Relative permeability

K	Bulk modulus
l	van Genuchten parameter
m	van Genuchten parameter, $m = 1 - \frac{1}{n}$
M_0	Initial mass of mucilage
M_t	Mass of mucilage at time t
n	van Genuchten parameter, the pore size distribution
n_0	Fitted parameter
n_0	Flow behaviour index
n_1	Fitted parameters for mucilage viscosity as function of frequency
n_2	Fitted parameters for mucilage shear modulus as function of frequency
n_3	Fitted parameters for mucilage loss modulus as function of frequency
p	Fluid pressure
Q	Swelling degree of mucilage
Q_{eq}	Equilibrium swelling degree of mucilage
Q_w	Water flow rate
r	Radial coordinate in polar coordinate system
r_0	Radius of single testa cell
R	Radius

S	Volume fraction
S_0	Soil water sorptivity
S_m	Mucilage saturation
S_t	Total saturation
S_w	Water saturation
t	Time
t_c	Characteristic time constant
$\mathbf{u}$	Velocity of fluid
U	Velocity of fluid, a scalar
$\bar{U}$	Average velocity of water
V_0	Initial volume of mucilage
V_w	Volume of water
V_t	Volume of mucilage at time t
x	Spatial coordinate in the horizontal direction
z	Spatial coordinate in the vertical direction
z_0	Initial mucilage height

GREEK LETTERS

α	van Genuchten parameter, related to the inverse of the air entry suction

γ	Shear strain
$\dot{\gamma}$	Shear strain rate
δ	Phase angle
η	Shear viscosity
η_∞	Viscosity in the upper Newtonian region
η_0	Viscosity in the lower Newtonian
η^*	Complex viscosity
μ	Dynamic viscosity
θ	Water content
θ_r	Residual water content
θ_s	Saturated water content
ρ	Fluid density
σ	Stress
τ	Shear stress
$\tau_{1/2}$	Shear stress at $\eta=\eta_{1/2}$
τ_f	Shear stress at flow point
τ_y	Yield shear stress
ϕ	Porosity

Φ Swelling degree

Ω Area of computational domain

Ψ Soil matric potential

ω Shear frequency

ABBREVIATIONS

BKC Blake-Kozeny-Carman

Cr Chromium

DS Demucilaged seed

FTIR Fourier transform-infrared spectroscopy analysis

GC/MS Gas chromatography-mass spectrometry

HG homogalacturonan

LVR Linear viscoelastic range

MECis Multi-effect-coupling ionic-strength-stimulus

MO Mucilage only

MS Myxospermous seed

PEG Polyethylene glycol

PGA Polyglutamic acid

PHB Ppolydyfroxybutyrate

RG I Rhamnogalacturonan I

RG II Rhamnogalacturonan II

SE Standard error

SEM Scanning electric microscope

THB Tanaka, Hocker, and Benedek

ACKNOWLEDGEMENTS

I would like to express my sincere gratitude and endless thanks to my supervisors Prof. Dong-Sheng Jeng (University of Dundee) and Dr. Pietro Iannetta (the James Hutton Institute) for their encouragement, patience and support throughout the research and writing up the thesis. Dr. Pietro Iannetta helps me a lot in developing the idea, doing experiments and introducing research methods in biological area. During my research, their enthusiasm and broad view on research has had a great impact on me.

I would also like to express my gratitude to Dr. Tracy Valentine and Dr. Euan James (JHI) for their expert guidance in various microscopic approaches to capture images of the shepherd's purse seeds. I would also like to express my gratitude to Dr. Paul Hallett and Dr. Ken Loades (JHI) for guiding me for the laboratory work. I would like to thank Dr. Peter Toorop (Royal Botanic Gardens Kew) for sharing his knowledge of seed dormancy and germination, especially in relation to his research on shepherd's purse and also his collaboration. My gratitude is also extended to Prof. Geoff Squire (JHI) for his great help to improve my English writing.

I would like to thank my colleague Dr. Huijie Zhang for his help in using Comsol Multiphysics software. Thanks to my other colleagues in the Civil Engineering and in the Center for Environmental Change and Human Resilience for their help and support.

I also would like to thank the Center for Environmental Change and Human Resilience (CECHR) for the financial support.

Finally, I am indebted to my parents and brother, without whose tolerance, love and support I would undoubtedly have failed to get this far. Special thanks are given to my dear husband Li Jiao for his support in my study.

I hereby certify that the work embodied in this dissertation is the result of original research and has not been submitted for a higher degree to any other University or Institution.

_____

Wenni Deng

PUBLICATIONS

1. **Deng, W., Jeng,** D.-S., Toorop, P. E., Squire, G. R. and Iannetta, P. P. M.(2012). A mathematical model of mucilage swelling in myxospermous seeds of *Capsella bursa-pastoris* (shepherd's purse). *Annals of Botany,* **109,** 419–427.

2. **Deng, W,** Iannetta, P.P.M., Hallett, P.D., Toorop, P.E., Squire, G. R. and Jeng, D-S. (2012). The rheological properties of the seed coat mucilage of *Capsella bursa-pastoris* L. Medik. (shepherd's purse). Biorheology (Submitted).

3. **Deng, W,** Iannetta, P.P.M., Hallett, P.D., Toorop, P.E., Squire, G. R. and Jeng, D-S. (2012). *Capsella bursa-pastoris* L. Medik. (shepherd's purse) myxospermous seed mucilage mechanically stabilises clay soil. Conference: Agricultural Ecology Research: its role in delivering sustainable. June 15-16, 2011, Dundee, UK.

ABSTRACT

Myxospermy is a term that describes the ability of a seed (or seed pod) to produce mucilage. The myxospermous trait is prevalent among those plant species adapted to surviving in arid sandy soils. The seed mucilage is composed of polysaccharides, which are capable of absorbing large volumes of water and it has been shown to be of significant ecological importance in terms of seed dormancy, germination and dispersion. However, the effects of the mucilage on the physical properties of soil have not been examined. In this thesis, the *Capsella bursa* (L.) Medik. (shepherd's purse) is chosen as a model plant species to be studied. The shepherd's purse seed mucilage consists two distinct layers. The outer layer is composed of only pectin and is readily dispersed/extracted in water. The inner layer is comprised of cellulose fibres which are anchored to the seed coat and these are embedded in pectinaceous matrix. The aim of this study is to discern the physical properties of the seed mucilage especially in relation to its expansion in response to hydration, and to develop a mathematical model that simulates the seed mucilage expansion, and understand the rheology of the mucilage. Furthermore, this insight is extrapolated to understand the role of the extractable component of the seed mucilage (only) and the whole seeds to affect the soil and its potential application as soil conditioner to change soil stability and soil water related properties.

Firstly, the structures underpinning the mucilage swelling process was described using light, electron and time-lapse confocal micrographs. The geometry size, weight of seed and mucilage were measured from images. The amount of mucilage which was present in the inner and out layer was discerned. The mucilage swelling was assessed at different osmotic pressure environment created by Polyethylene glycol (PEG) solution.

The experimental data were then used to create a mathematical model of myxospermous seed mucilage swelling based on diffusion equations. The swelling time of mucilage at different PEG solution was simulated and the influence of mucilage height was assessed. The results showed that mucilage accounted for 25.2 % of seed weight and took 16 x water of its weight. The mucilage had a low osmotic potential property which helped it compete water from environment. The swelling degree was largely reduced as PEG solution concentration increased and the time required to reach equilibrium state was reduced too.

Secondly, the dynamic rheology of extractable seed mucilage was assessed as a function of mucilage concentration (1–10 % [w/w]), temperature (0–80 ℃) and shear frequency (0.1–100 rad s^{-1}). The relationship between the viscoelastic parameters (η, G', G'', τ_y and τ_f) and mucilage concentration were well fitted by power law models. The dynamic rheology results showed that mucilage was a high viscous material and was able to be classified as a 'weak gel' material. The seed mucilage exhibited relative higher viscosity compared with mucilage from other plant parts which indicated the special role of seed mucilage. These properties highlight the possibility that myxospermous seed mucilage may affect soil conditions and therefore present an additional facilitative ecological role.

Thirdly, a comparative analysis of soil water retention, hydraulic conductivity and rheology using clay and sandy-loam soil containing a range of seed mucilage, or myxospermous seed (MS) or demucilaged seeds (DS) was carried out. The applied densities for mucilage were 0.5 and 1 % [w/w] and for seeds (MS or DS) were 5 % and 10 % [w/w]. The water retention curve of soil was fitted by van Genuchten model and their fitted parameters were used in numerical modelling later. The mucilage or seeds had greater influence on sandy-loam soil compared with clay type soil, both the water retention and the rheology properties. It was also found that seeds, whether

myxospermous or not, increase sandy-loam soil water retention and rheology properties while reducing the soil hydraulic conductivity. The myxospermous seeds had higher impact on soil water retention than demucilaged soil and the effect was more significant in drier soil.

At last, a numerical model was developed to simulate the flow of water in seed conditioned soil. The model was developed on the basis of the experimental data and findings of the earlier chapters. The mucilage swelling properties was considered as a blocking effect and modelled by reducing the hydraulic conductivity. The numerical geometry was the same as the soil column used in the water retention tests. The water flow was modelled by Darcy's law combined with continuum equation. The two dimensional symmetry model was established and was solved using COMSOL Multiphysics. The influence of both MS and DS were simulated at different seed density (C_s), different amended soil layer thickness (h_s) and different position from the soil surface (d_s). The velocity of water flow and the relative permeability were compared at different cases. C_s and h had a great influence on water flow velocity in soil while the influence of d_s was not significant. The simulation showed that 2 – 4 % [w/w] at the surface layer of soil may have the most significant influence on water flow in soil.

Chapter 1 **Introduction**

1.1 Overview

Recently, human beings have begun to understand the importance of climate change and the links between activities such as deforestation, water shortage and the unlimited use of non-renewable (fossil) fuels. It has also been learned that leaving unmitigated climate change will have severe and negative impacts on the environment and human resilience. Towards mitigating the impacts of climate, humans have been exploiting natural, organic and renewable materials from plant and animals. Plant derived polymers such as natural gums and mucilage are of interest to a wide diversity of industries because they are biocompatible, inexpensive, and easily available and are preferred to semi-synthetic and synthetic excipients due of their low toxicity and cost. In addition, they are often easily available and viewed favourably by consumers as they are eco-friendly and of therapeutic potential as they are often non-irritant in nature. Demand for these plant cell-wall materials is increasing and new sources synthesised from natural materials are also being developed. Secreted plant mucilages are especially interesting as they present that interface between the biotic and abiotic components of a system. Such mucilages play important ecological functions which enable the plant to adapt to biotic and abiotic stresses, such as pathogen attack and water shortage, respectively. In this context, greater insight into the function of plant mucilages to enable resource use efficiency and stress avoidance may provide interesting insights, from which the challenges posed by environmental changes will be addressed in this study.

Plant mucilages are composed of polysaccharides that may swell considerably when exposed to moisture and in their hydrated form exhibit gelling characteristics. They have been studied in a diverse array of research areas and over many years because of

their unique chemical and physical characteristics. For example, plant mucilages have been extensively explored as new polymer sources as food thickener, gelling agents, and drug delivery agents and even as flocculants in sewage treatment.

Within the scope of this study, the research upon a particular plant trait termed ‘myxospermy’, which translates from the Greek as ‘slime’-‘seed’ (myxo-spermy), will be presented. The term myxospermy reflects the fact that on imbibition (exposure to moisture) the dry mucilage on the seed coat (testa) surface swells and envelopes the seed. Myxospermy is a common plant seed (or seed pod) adaptation to arid habitats, though it may be found in a wide range of very different, that is phylogenetically diverse, plant families. The presence, structure and ecological role of myxospermous seed mucilages have been explored for decades. However, its functional role is only now being discerned. In this study, the myxospermous seeds of the arable weed *Capsella bursa-pastoris* (L.) Medik. (shepherd’s purse) will be used. Shepherd’s purse is one of the most abundant broad leafed arable weeds, and enjoys a global distribution (with the exception of the dry tropics and extremely cold altitudes or latitudes), and successfully coexists with crops (*i.e.* especially within arable fields), as a non-pernicious weed to crop yield. Shepherd’s purse is therefore an especially persistent broad leafed weed. Furthermore, shepherd’s purse has highly genetically synteny with the academic plant genetic model Arabidopsis, but has the advantage of having in-field/*in situ* relevance: as Arabidopsis does not persist as a common arable weed within the arable soil seedbank (despite of possessing myxospermous seeds). Therefore, in this thesis the myxospermous seeds of shepherd’s purse will be used to develop the first mathematical model to characterise and parameterise myxospermous seed mucilage swelling (during hydration). Using this insight as a basis, hypotheses that relate to the potential role of myxospermous seeds and the extracted myxospermous seed mucilage to impact upon soil physical properties and water flow in soil will be assessed.

1.1 Objective

The main objective of this research was to investigate the properties of shepherd's purse seed mucilage as a model, and ultimately to assess the potential of the myxospermous seed mucilage to be used as a novel soil amendment. The swelling properties of seed mucilage were assessed experimentally and mathematically. The mucilage and seeds were assessed for the capacity to affect soil water retention, hydraulic conductivity and rheology. The data obtained from experimental study was used in numerical models to analyse the effect of seeds (with/without mucilage) on water flow in soil. All the numerical models presented in this thesis were developed within the Comsol Multiphysics environment.

1.2 Outline of the thesis

This thesis consists of 7 Chapters: firstly a brief Introduction (present chapter) followed by an extensive literature review (Chapter 2), which describes the plant mucilages in details and the characteristics of myxospermous seed mucilages in particular. This thesis also considers the ecological function of the seed mucilage and explores its potential interaction with soil, and how this may affect those ecosystem services provided by soil. The literature review also presents the state-of-the-art with regard to the application of numerical models to understand and describe mucilage swelling and flow behaviour in porous media. This is followed by three experimental chapters (3 – 5) and a numerical modelling chapter (6). Finally in Chapter 7, the Conclusions and Future Work are presented. The content of the main part of the thesis (Chapters 3 – 6) are described in brief below.

Chapter 3 reported upon studies that assessed the swelling behaviour of shepherd's purse mucilage. This was first assessed experimentally and the data that was acquired

was used to develop the first mathematical model of myxospermous seed swelling. This chapter proposed that seed mucilage swelling may be simulated using a diffusion equation. Chapter 4 found that *in situ*, a significant amount of the seed mucilage dissociates from the seed upon hydration. However the physical role of this dispersed seed mucilage has hitherto not been considered. Therefore, the dynamic rheological properties of this dispersed seed mucilage were assessed, ahead of studying the effects of whole myxospermous seeds upon soil physical properties. These findings were discussed with a view towards the potential of the dispersed mucilage (alone), to affect soil properties. Chapter 5, extending from the knowledge gathered in Chapter 3 and 4, assesses the influence of water soluble mucilage component and seeds on the physical properties of different soil types. This was done in a comparative analysis with soil amended to contain different densities of either myxospermous seeds or demucilaged seeds. The soil physical properties that were assessed include soil water retention, hydraulic conductivity and rheology. In Chapter 6, a numerical model was developed based on the results from Chapter 5. This model simulated water flow in porous media amended with myxospermous seeds to quantify the influence of myxospermous seeds on water flow rate in sandy-loam soil types.

In Chapter 7, future work on mucilage or myxospermous seeds was suggested.

Chapter 2 **Literature Review**

2.1 C*apsella bursa-pastoris* (L.) Medik. (shepherd's purse)

Capsella bursa-pastoris (L.) Medik. is a common weed widely distributed throughout Europe, Asia, America, Australasia and Africa except the tropical lowlands (Aksoy *et al.*, 1998). Within the UK, this species exists in all the habits from south to north (Figure 2.1). It is a member of the Brassicaceae family and is commonly known as shepherd's purse, but it has other names such as shepherd's heart, pepper and salt, lady's purse, mother's heart and rattle pouches according to the seed pod shape (Vandebroek, 2006). This species is variable in size, fruit and leaf form (Vandebroek, 2006; Iannetta *et al.*, 2007). Figure 2.2 shows shepherd's purse and its seed pod in-field. Shepherd's purse plants can produce between 500 and 500,000 seeds (Hurka and Haase, 1982; Iannetta, 2010), depending on the growing conditions. Individuals plants can produce heteromorphic seeds, *i.e.* seeds of different types, in this case both myxospermous (light brown) and non-myxospermous (dark brown) coloured seeds (Iannetta *et al.*, 2010; Toorop *et al.*, 2012; see also Figure 2.3). The light brown colour seeds are most mature and are borne from those pods held lower most on the flowering stem. During seed development, myxospermous seeds are produced *via* the deposition of dry mucilage within those cells that comprise the outer-most (external) layer of the seed coat (testa). In contrast, the non-myxospermous (dark brown) coloured seeds are borne within younger pods held higher on the flowering stem and are less mature and lack this myxospermous capacity. When hydrated in water, the myxospermous seeds can absorb much more water than that of the non-myxospermous seeds (Figure 2.4). The seeds are normally in the shape of an ellipsoid and are 0.9 – 1.1 mm in length and 0.4 – 0.6 mm in width. The weight for dry seeds is in the range of 0.139 – 0.164 mg (n = 60, SE = 0.004; Aksoy *et al.*, 1998). The seeds can be dispersed by wind, rain, by

birds and animals, on vehicle and equipment tires, on human and animal feet. Shepherd's purse is found in both urban and rural wasteland, in cultivated land and roadsides. It exists on soils ranging from clay to sandy-loam with pH 5–8, temperature from 5 – 30 ^{o}C and germinated mostly in spring or autumn. It is more adapted to drier arable habitats with fertile soils than to wet ones (Aksoy *et al.*, 1998; Vandebroek, 2006). Genetically, it has synteny with *Arabidopsis thaliana* (Arabidopsis) which indicates a promising prospect in studies of adaptation and evolution (Acarkan *et al.*, 2000; Willats *et al.*, 2001; Boivin *et al.*, 2004). The young leaves are edible and has a rich content of iron, calcium and vitamin C. It is also used as a treatment of bleeding, diarrhea *etc.* in medicinal use (http://www.botanical.com/botanical/mgmh/s/shephe47.html). Meanwhile, the shepherd's purse seed has been studied as a model species for adaptation *in situ* (Hawes *et al.*, 2005; Iannetta *et al.*, 2007) and a biomonitor for sustainable arable production for its ecological importance (Iannetta *et al.*, 2010). In this study, the shepherd's purse is chosen to be the model plant.

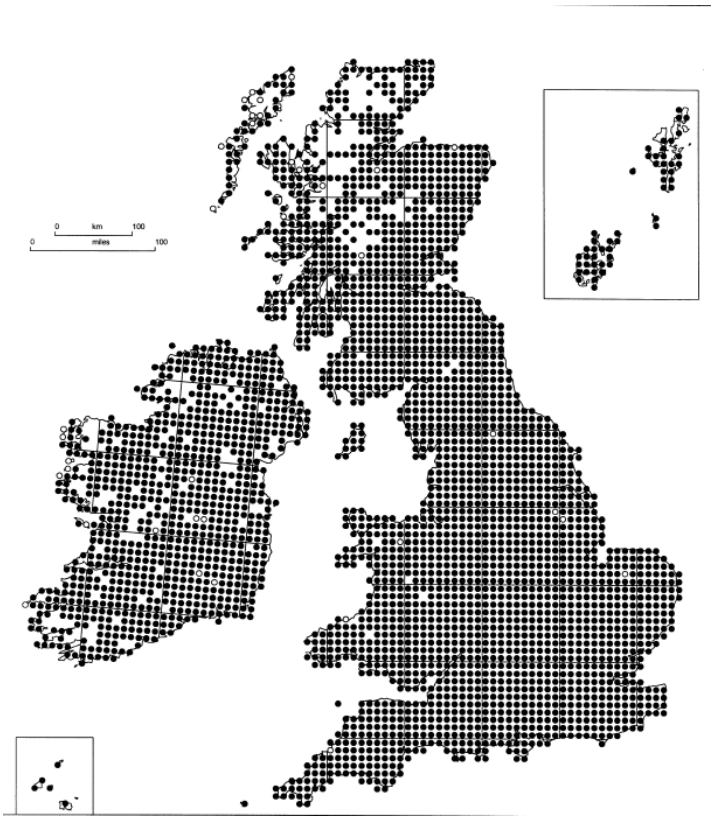

Figure 2.1 The distribution of *Capsella bursa pastoris* in the British Isles (Aksoy *et al.*, 1998).

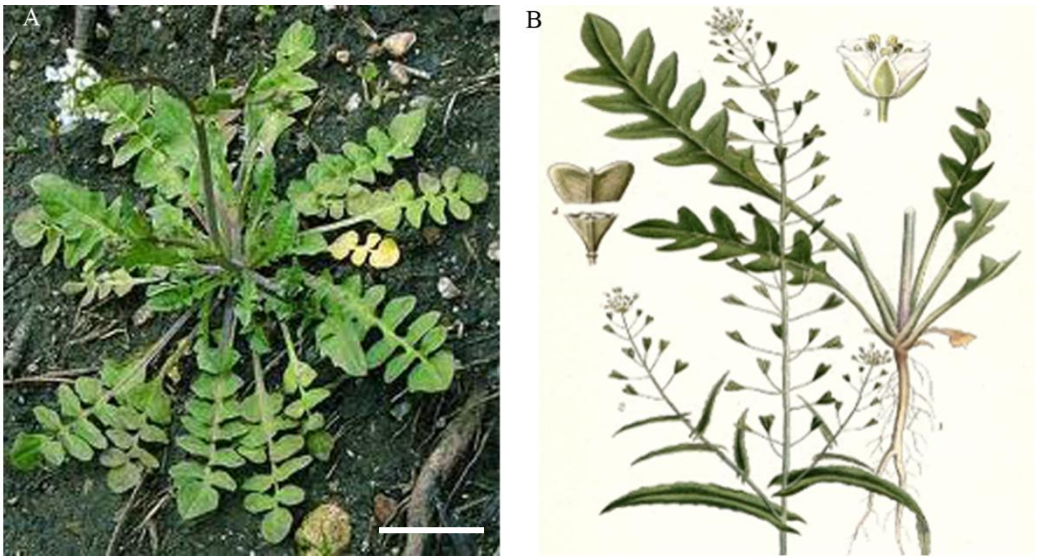

Figure 2.2 A. Shepherd's purse plant in field and B. its stem and seed pod (images from the internet: http://medicinalherbinfo.org/herbs/ShepherdsPurse.html and http://astrologosdelmundo.ning.com/profiles/blogs/las-hierbas-y-plantas-de-6). Scale bar: 5cm.

Figure 2.3 Heteromorphic seeds of Shepherd's purse: non-myxospermous dark brown and myxospermous seeds light brown seeds. Scale bar = 1 mm.

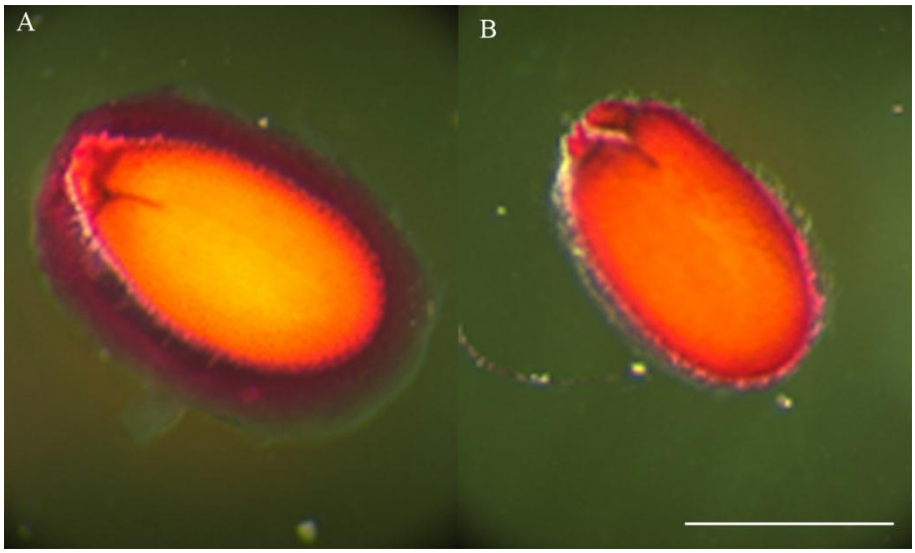

Figure 2.4 Heteromorphic seeds of Shepherd's purse hydrated in water: myxospermous seeds (A) and non-myxospermous seeds (B). The myxospermous seeds exhibit higher swelling property than non-myxospermous seeds. Scale bar = 1 mm.

2.2 Characterisation of seed mucilage and myxospermy

Plant mucilages are mainly hydrophilic polysaccharides secreted during development in various plant tissues, such as roots (marshmallow), seeds (flaxseed, psyllium), leaves (senna) and fruits (aloe). Plant mucilage composition is similar to gums and forms a slimy substance when hydrated. The mucilage is usually produced by metabolism within the cell wall (Frey-Wyssling, 1976; Jani *et al.*, 2009). The plant species which are most widely studied for the properties of mucilage include *Opuntia ficus indica* (cactus pear), *Arachis hypogaea* (peanut) root mucilage, *Linum usitatissimum* (flaxseed) and Arabidopsis (Figure 2.5: images are taken from the internet). Among all the plant mucilages, the seed mucilage confers a trait termed 'myxospermy' and it is the main focus of this research project. Myxospermy is a trait that defines the ability of a seed to become sheathed by a mucilaginous coat upon hydration in water (Frey-Wyssling, 1976; Grubert, 1981). Myxospermy is associated with the seeds of many different species that span phylogenetically distinct plant families and covers vast array of functionally distinct types found in many different niches throughout the world. However, myxospermy seeds are produced mainly in species within the plant families Brassicaceae, Asteraceae, Cistaceae, Solanaceae, Linaceae, and Plantaginaceae (Grubert, 1974; Grubert, 1981). Some of the widely studied weed seed coat mucilages include: Arabidopsis, *Sinapis alba* (yellow mustard), *Ocimum spp* (basil), flaxseed and *Plantago spp.* (psyllium). When myxospermous seeds hydrated in water, the mucilaginous material immediately absorb water to expand and extrude from the seed coat by the rupture of the outer cell wall of the cells which contain it. The following sections will describe the chemical composition, structure and potential ecologic role of the myxospermous seed mucilage in more detail.

Figure 2.5 The most widely studied species which produce mucilage. A. *Opuntia ficus indica* (cactus pear), mucilage from cladodes B. *Arachis hypogaea* (peanut) root, mucilage from root; C. *Linum usitatissimum* (flaxseed), mucilage from seeds; D. *Trigonella foenum-graecum* (fenugreek), mucilage from seeds. (Images are from website: A: http://www.delange.org/IndianFigCactus/IndianFigCactus.htm; B: http://www.ars.usda.gov/Main/docs.htm?docid=16814&page=3; C: http://www.ourprg.com/?p=653; D: http://nl.wikipedia.org/wiki/Bestand:Fenugreek_seeds.jpg).

2.2.1 Seed coat mucilage composition

The components of the seed mucilage have been characterised by various methods, from the simple staining with different dyes such as ruthenium red and toluidine blue (for pectins, Figure 2.7A) and fluorescent calcofluor based stains (for cellulose, Figure 2.7B, and Figure 2.8), to complex analysis including GC/MS analysis and Fourier transform-infrared spectroscopy analysis (FTIR; Windsor *et al.*, 2000; Monsoor *et al.*, 2001; Penfield *et al.*, 2001; Willats *et al.*, 2001). These techniques have shown that the myxospermous seeds mucilage composition is complex, but does contain the polysaccharides pectin, hemicellulose and cellulose as major constituents (Windsor *et al.*, 2000; Monsoor *et al.*, 2001; Penfield *et al.*, 2001; Willats *et al.*, 2001Macquet *et al.*,

2007). Pectins can be characterised as belonging to one of three key distinct classes: homogalacturonan (HG), rhamnogalacturonan I (RG I) and rhamnogalacturonan II (RG II) (Somerville *et al.*, 2004). HG consists of an unbranched chain of (1→4) – β – $_{D}$ – GalA residues that can be methylesterified or acetylated or substituted with xylose or apiose (Willats *et al.*, 2001). RG I has a backbone of alternating (1→2) – α – $_{L}$ – Rha (rhamnose) and (1→4) – β – $_{D}$ – GalA (galacturonic acid) that can be substituted on the RHa residues with side-chain consisting of arabinans, galactans and terminal galactose residues. RG II consists an HG back bone substituted with complex side chains. A schematic represent structure of different types of polysaccharides were illustrated in Figure 2.6 (Vincken *et al.*2003).

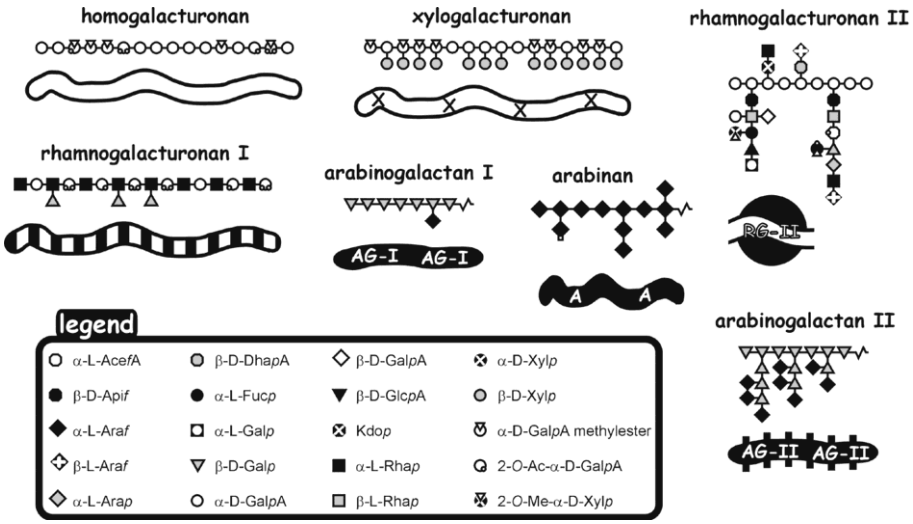

Figure 2.6 This is a schematic representation of the constituents of pectin. The symbols for the various monosaccharide units and predominant linkage types are explained in the accompanying legend (Vincken *et al.*, 2003).

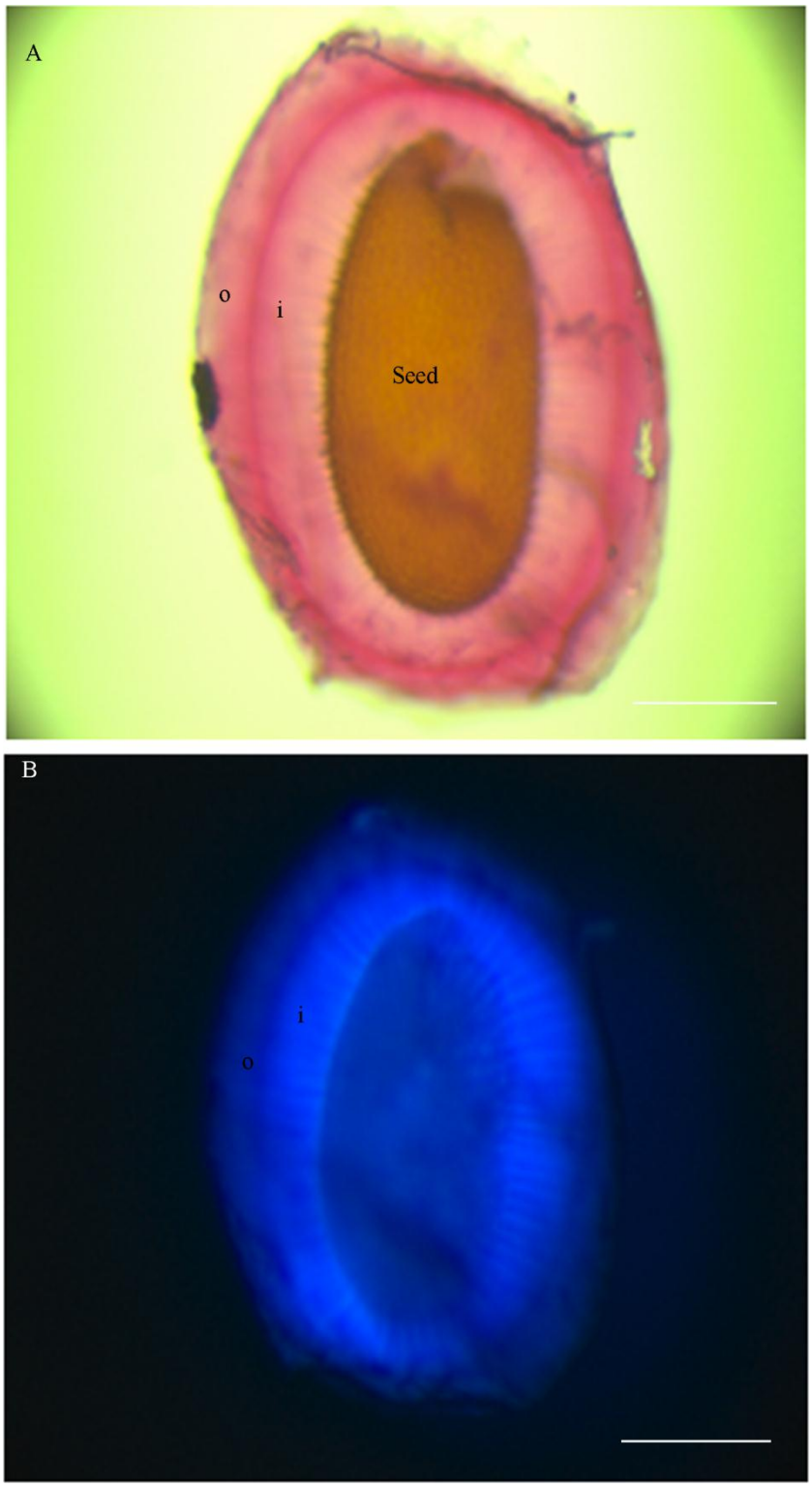

Figure 2.7 (A) Shepherd's purse seed stained with ruthenium red indicating the pectin component of mucilage. (B) Shepherd's purse seed stained calcofluor indicating the cellulose component of mucilage i: inner layer; o: outer layer. Scale bar: 500 µm.

The seed mucilage may be described as bipartite with a scaffold of cellulose fibrils that hold the pertinaceous matrix. The cellulose fibres are organised in discrete twisted bunches, each bunch being anchored to a raised protrusion (the columella), that exists at

the centre of each testa cell. The cellulose fibres radiate out from each cell and there is not much research on the detailed molecular properties of cellulose (Figure 2.8). The hemicellulose component of the mucilage is reported to bridge the cellulose with pectins (Willats *et al.*, 2001; Somerville *et al.*, 2004; Arsovski *et al.*, 2009). In general, the seed mucilage is a specialised, pectin rich, primary cell wall material with high water holding capacity. The polysaccharide and acidic qualities of mucilages make them extremely hydrophilic, such that they hydrate rapidly in the presence of water, forming hydrogels or possibly even superabsorbent polymers (Zohuriaan-Mehr and Kabiri, 2008).

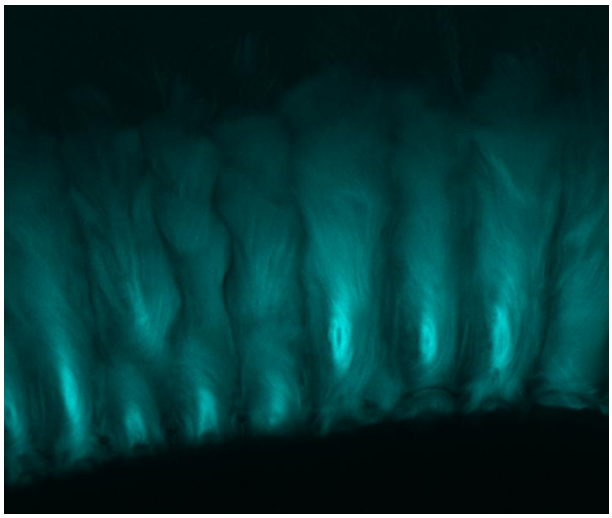

Figure 2.8 Fluorescent UV micrograph of hydrated shepherd's purse seed mucilage. The cellulose fibre component of mucilage has fully swollen and is seen to radiate from the testa (seed coat), each of which emerges from the centre of each testa cell.

2.2.2 Seed coat mucilage structure

During seed coat differentiation, mucilage is synthesized in the Golgi apparatus and deposited to the apoplast adjacent to the radial and outer tangential cell walls (Western *et al.*, 2000). A columella is developed from the thick secondary cell wall and a donut shaped pocket is formed between the membrane, columella and cell walls. The mucilage lies in the pocket in its dry form (Figure 2.10). In addition of water, the mucilage absorb large amounts of water and the primary cell wall is ruptured and mucilage swells to

encapsulate the seeds. After air-drying, the seeds are covered by a thin film clinging to the top of columella (Figure 2.9).

Figure 2.9 Cryo-scanning electron micrograph image shows a fully hydrated shepherd's purse seed imaged after being allowed to dry to show the raised and torn skin. Scale bar = 200 μm.

Staining with ruthenium red shows that the seed mucilage presents two distinct layers (Figure 2.7). The inner layer is an adherent layer which is not easily removed by shaking seed in water, even in strong acids or bases, while the outer layer is very easily removed by shaking the seeds in water. From microscopic observations, the inner layer accounts for most of the mucilage (Penfield *et al.*, 2001; Macquet *et al.*, 2007). It is also reported that the outer mucilage is diffusive and cloudy, while the inner mucilage is much denser and has a clear image of rays which come out from each epidermal cell (Figure 2.7). Furthermore, the two layers of mucilage are varied in polysaccharide composition, function and structural characteristics. The outer layer mucilage is mainly unbranched RG I, a small portion of branched RG I and arabinoxylan forming in a slightly expanded random-coil conformation (Macquet *et al.*, 2007; Arsovski *et al.*, 2009; Haughn and Western, 2012). In contrast, the inner layer is much denser than the

outer layer when stained with ruthenium red. The inner layer of seed mucilage also contains pectin mainly as unbranched RG I, with branched RG I, arabinans, galactans, arabino-galactans and arabinoxylans. The cellulose in the inner layer radiate from the epidermal cells forming cellulose "rays" (Figure 2.8). Macquet *et al.* (2007) reported that 12 – 19 % of the inner layer mucilage is cellulose and they also suggested that the inner layer can be separated into two domains: an inner domain containing cellulose, HG, RG I, galactan and an outer non-cellulose domain containing HG, RG, galactan and arabinan. From the observation using electron microscopy, the structure of shepherd's purse seeds is very similar to that of Arabidopsis, except the latter is smaller. Also, Arsovski *et al.* (2009) found that the swelling rate of the outer layer is much faster than the inner layer for Arabidopsis seeds. As such, the inner layer mucilage appears to present a structure that is more complex than the outer layer, and it is strongly adherent to the seed surface (Macquet *et al.*, 2007; Arsovski *et al.*, 2009; Haughn and Western, 2012).

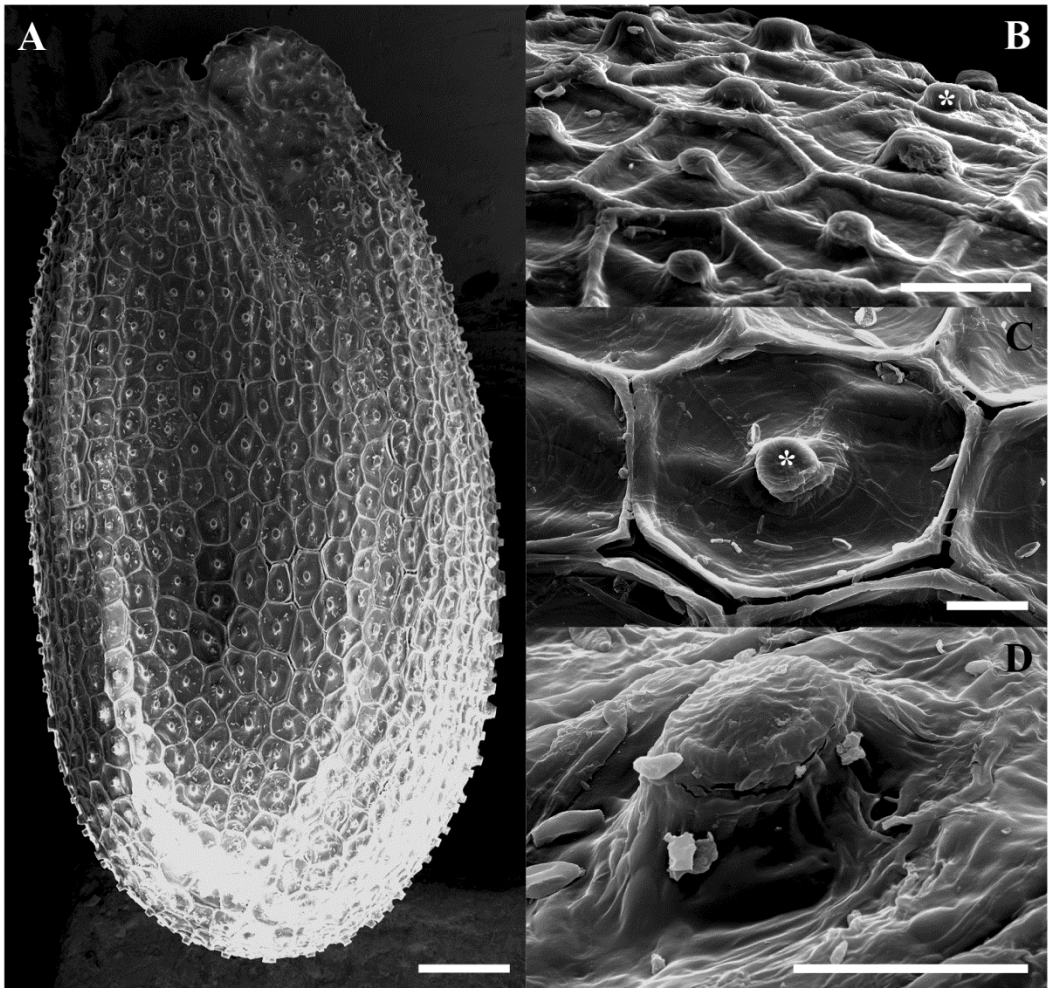

Figure 2.10 Shepherd's purse seed coat structure shown using scanning electron micrographs. A, a whole shepherd's purse seed (scale bars = 100 µm). B to D, the testa cells which form the surface of shepherd's purse seed under increasing magnification. The central columella is identified (*) in B and C while D shows the columnella under highest magnification (scale bars: B = 40 µm; C and D = 10 µm).

2.2.3 The ecological role of seed coat mucilage

Due to the high concentration of hydrophilic polysaccharide constitutents, mucilages generally have a high water-binding capacity and this has led to studies of their role in plant water relations. It has been summarised by Western (2012) and Yang *et al.* (in press) that the seed coat mucilage has the following main ecological functions: (1) assisting seed hydration, even under water deficient or high salinity conditions; (2) facilitating germination or early seedling growth; (3) prohibiting seed germination by preventing oxygen flow; (4) helping germination by promoting seed priming; (5) aiding seed dispersion by adhesion to animal, (6) adhering to soil particles to stop seeds being washed off by water and (7) providing nutrient for bacteria or microorganisms.

Myxospermous seed mucilage hydration and swelling are anticipated to increase seed-soil contact and improve water uptake and perhaps retention; and this has been shown assist seed hydration and germination (Fahn and Werker, 1972; Grubert, 1974; Lu *et al.*, 2010; Yang *et al.*, 2010). Lu *et al.*(2010) measured the effect of the thickness or amount of mucilage on *Diptychocarpus strictus* (Fisch. ex M. Bieb.) seed hydration and germination. They found that the dispersal ability increased as the falling distance of seeds with mucilage was much longer than that without mucilage. Also the rate of dehydration of seed decreased as mucilage thickness increased, because seeds with mucilage still retained > 50 % of their water for more than 240 min while seeds without mucilage became fully dehydrated after the same time. Myxospermous seeds enveloped by a broad layer of mucilage were able to adhere to soil particles with greater efficiency than those with a narrow layer. It has also been noted from ecological surveys that a high proportion of plant species which persist in arid desert environments possess myxospermous seeds or seed-pods (Murbeck, 1919; van Rheede van Oudtshoorn and Van Rooyen, 1999). Furthermore, Yang *et al.* (2010) tested the germination of intact

and demucilaged achenes of *Artemisia sphaerophala* (Asteraceae) under different osmotic potentials and salinity stresses. The results showed that intact achenes germination rate was higher than demucilaged achenes when imbibed to solution of higher osmotic potential, or salinity (PEG and NaCl, respectively). It is also found in Arabidopsis that the germination of mucilage deficient mutant seeds (*ttg1, gl2, myb61*) is more sensitive to water potential than that of myxospermous wild seeds (Penfield *et al.*, 2001; Arsovski *et al.*, 2009; Western, 2012), as their germination rate of the mucilage deficient mutants was reduced significantly in the face of greater competition for water, as generated by increasing PEG concentrations. Therefore, in environments which may be limited in the amount of water for germination and seedling establishment, the mucilage could perhaps be acting as an environmental buffer.

On the other hand, there are two articles which report that mucilage restrict seed germination. The germination rates of *Diptychocarpus strictus, Lesquerella perforate* and *Lequerella stonensis* (Brassicaceae) seeds were reduced as the mucilage thickness increased (Fitch *et al.*, 2007; Lu *et al.*, 2010). This inhibitory effect is especially vivid when there is excess water. It is also possible that the thick mucilages may also restrict the oxygen to the embryo and so inhibit seed germination, though this possibility remains to be proven and in ecological terms would seem to be deleterious, and therefore unlikely.

The mucilage may also impart adherent qualities to improve seed dispersal, as myxospermous seeds became sticky when hydrated and may adhere to animals' feather or fur, or even *via* attachment to soil particles dislodged in a water column/flow. However, the role of mucilage may be varied in different niches (Gutterman and Shem-Tov, 1997), and it is generally believed that the main ecological role of the mucilage is

to empower seed germination *via* improved seed-water retention and enhanced seed-soil particle contact.

Myxospermous seed mucilage has also been reported as a novel form of plant carnivore: studies of shepherd's purse mucilage reported that mucilage can trap larvae due to the large amount of cellulose (Reeves and Garcia, 1969; Page III and Barber, 1975). It is also postulated that the mucilage may act as a 'soil primer' encouraging microbial growth and turnover to facilitate soil formation and seedling growth. Moreover, after the mucilage biodegraded to CO_2 and soluble sugars, it is provided as nutrient source to microbial growth in soil and thus influences the seedling growth (Yang *et al.*, 2012).

2.3 Mucilage swelling properties upon hydration

Plant mucilages can swell immediately when exposed to water, though the swell rate may vary from very slow (hours) to very fast (within a several seconds) in different environments (Arsovski *et al.*, 2009). Consequently, depending on the wetting and water release properties, different mucilages have applications to different processes. For example, for pharmacology, polymers may be used as drug delivery agents (Singh *et al.*, 2007); in bioremediation of petrol chemical contaminated soils, gels may be used to increase oil extraction rate by blocking soil-pores (Zitha *et al.*, 2002; Suzuki *et al.*, 2009); while in agriculture, superabsorbent polymers were applied as a 'soil conditioner' to increase crop product (Wang and Gregg, 1990; Morel *et al.*, 1991; Kazanskii and Dubrovskii, 1992; Al-Darby and AlSheikh, 1995; Al-Darby, 1996; Al-Darby *et al.*, 1996; Karadag *et al.*, 2000; Caesar-Tonthat, 2002; Akhter *et al.*, 2004; Syvertsen and Dunlop, 2004; Andry *et al.*, 2009; Agaba *et al.*, 2011; Yang *et al.*, 2012). There are an abundance of articles on the use and manufacture of synthetic polymers under different conditions, such as pH, temperature and ion concentration. Only scant regard has been paid to understanding existing natural plant polymers, such as exist on the

myxospermous seed coats, and despite a large body of evidence that designs based on naturally occurring structural phenomena has deliver improved and multiple ecosystem services (Bejan, 2000). As for synthetic polymers, research efforts should be applied with great vigour to natural plant polymers, such as myxospermous seed mucilage.

2.3.1 Swelling kinetics

One of the most important characteristics of plant mucilages is their swelling kinetics. Swelling kinetics has been studied both experimentally and mathematically. The swelling degree is always defined as:

$$\Phi = \frac{M_t}{M_0} \tag{2.1}$$

where M_0 and M_t are the mass of the mucilage at initial time and time *t* respectively.

The swelling degree is also given as volume-ratio when the density of the solvent and the mucilage is constant.

$$\Phi = \frac{V_t}{V_0} \tag{2.2}$$

where V_0 and V_t are the mass of the mucilage at initial time and time *t* respectively.

2.3.2 Mathematical modelling of gel swelling properties

The model proposed by Tanaka *et al.*(1973) is based on the theory of elasticity, which was known as the collective diffusion equation. Gels were treated as continuum, as the polymer chains in the gel were connected to each other *via* hydrogen bonding or hydrophobic interaction. Tanaka and Fillmore (1979) derived an equation of motion for network driven by friction between polymer and solvent, and the network stress was

linear to the displacement gradient. However, for large deformations the expression of elasticity can be modified by adding a non-linear terms and expressing these as in material coordinates.

This approach was later applied to solve network displacement by polyacrylamide spheres (Tanaka and Fillmore, 1979). The network displacement was proportional to displacement from the equilibrium state, and the initial displacement was determined from the osmotic pressure of the gel. They assumed that the shear modulus was negligible compared with the bulk modulus. The governing equation for the network displacement in a sphere gel was:

$$\frac{\partial u}{\partial t} = D\frac{\partial}{\partial t}\left\{\frac{1}{r^2}\left[\frac{\partial}{\partial r}\left(r^2 u\right)\right]\right\} \tag{2.3}$$

where $D = \dfrac{K + 4G}{f}$ is the diffusion coefficient, K is the bulk modulus, G is the shear modulus, f is the friction between the gel and the solvent. The displacement was described as:

$$\Delta a(t) = \frac{6\Delta a_0}{\pi^2}\sum_{n=1}^{\infty}\frac{1}{n^2}\exp\left(-\frac{n^2\pi^2 D}{a^2}t\right) = \frac{6\Delta a_0}{\pi^2}\exp\left(-\frac{\pi^2 D}{a^2}t\right) \tag{2.4}$$

where a was the radius of equilibrium of a spherical gel, $\Delta a(t)$ was the radius change at time t, and Δa_0 was the final radius change. Later, Peters and Candau (1988) and Peters *et al.* (1991) extended Tanaka and Fillmore's model for long cylindrical and large disk gel in which the shear modulus cannot be neglected. All these research efforts were executed on an assumption that the motion of the solvent inside the gel network was zero. This assumption, however, was only true for spherical gels. The motion of the solvent contributes directly to the swelling kinetics, except in the case of spherical gels where the swelling process changes both the bulk and shear energy of the polymer network. The solvent motion caused the gel system to minimise the total energy. The

motion field of solvent strongly depended on the geometry of the gel and played an important role in the friction force and the swelling kinetics.

Then, Li and Tanaka (1990) improved the theory and applied it to arbitrary shape. Instead of directly dealing with motion of both network and solvent, they decomposed the swelling process into two imaginary processes. The first process was a pure network diffusion process described by a collective diffusion equation with zero solvent velocity. This process raised the shear energy of the sample. In the second process, the solvent moved together with the network so that the solvent velocity was the same as the network velocity. This process minimized the total energy. The effect of solvent motion was therefore included in their second process. This theory gave good predictions for long cylindrical cells and large disks that undergo small symmetric deformations.

Wang *et al.* (1997) revised the collective diffusion model by adding a convective term. The kinetics of gel swelling was theoretically analysed by considering coupled motions of both the solvent and the polymer network. This model avoided the two process approach of Li and Tanaka (1990), in which the solvent motion was indirectly considered.

Hui and Muralidharan (2005) compared the theories of Biot (1941) and Tanaka *et al.*(1973). However, THB theory ignored the displacement of liquid phase.

Another diffusion model based on Fick's laws had been proposed for modelling the mass transport processes. Fick's first and second law was well-known as Case I or Fickian diffusion for governing the transport of mass through diffusive means. In Eq. 2.5, the diffusion flux J was proportional to the concentration gradient (spatial derivative). Fick's second law predicted the concentration field to change with time as a function of flux change with respect to position:

$$J = -D\nabla C \tag{2.5}$$

$$\frac{\partial C}{\partial t} = \nabla \cdot J \tag{2.6}$$

However, Case I diffusion was not observed in most polymer-solvent systems (Vrentas *et al.*, 1975). Later, Alfrey *et al.* (1966) proposed Case II diffusion to characterise water transport in glassy polymers. Between these two extreme cases was anomalous diffusion. In non-Fickian diffusion (Case II and anomalous), the velocity of the sharp front, which separates the unswollen and swollen polymer, was constant. The mass uptake M was expressed by:

$$M = k_0 t^i \tag{2.7}$$

where k_0, i were constant and t was time, $i = 1/2$ for Fickian diffusion, and $i = 1$ for Case II diffusion, in between was for anomalous diffusion.

De Kee *et al.* (2005) summarised the models for non-Fickian diffusion over the past decades. Thomas and Windle (1980) improved Case II diffusion in glassy polymers by considering mechanical deformation. The solute diffusion rate was compatible with the swelling rate to control the deformation of the surrounding polymers. As a result, the creep deformation depended on both osmotic pressure (caused by diffusion) and the viscoelasticity of the polymer. This model was able to predict most characteristics of Case II diffusion, except the effect of external stress.

However, it was not clear which principle controlled non-Fickian diffusion; while it is accepted that polymer swelling played an important role and the deformation of polymer is driven by osmotic pressure, the transport of solute was driven by both molecular diffusion and a stress associated to swelling. Most of these models modified the classical Fickian diffusion equation to account for the effect of stress. In addition, a

constitutive equation to account for the time evolution of stress was introduced. The modified transport equation then became:

$$\frac{\partial C}{\partial t} = D\nabla^2 C + E\nabla^2 \sigma \tag{2.8}$$

In Eq.2.8, D and E were the molecular and elastic diffusion coefficients that are associated with concentration and stress respectively. When $E = 0$, the equation reduced to Fick's second law. Different viscoelasticity models (Maxwell, Voigt and Jeffrey models) were then applied to associate the stress to time and concentration. The models mentioned above were limited to small deformation in gels. Recently, intense research effort was devoted towards developing models that considered large deformation of gels (Birgersson *et al.*, 2008; Hong *et al.*, 2008; Zhang *et al.*, 2009). Numerical methods were then required to solve the large deformation problem. The free-energy function and kinetic model of Hong *et al*., 2008 was solved using the finite element method in ABAQUS (Zhang *et al.*, 2009). Furthermore, Birgersson *et al.* (2008) carried out analysis of temperature-sensitive two-dimensional gels by using COMSOL MULTIPHYSICS, which was a finite element solver for highly coupled partial differential equations. Instead of modelling gel behaviour at equilibrium, transient models modelled the kinetics of rapid response gels under different environmental conditions. While all swelling activities were complex, they could be explained by the accurate description of three key aspects: (1) the diffusion mechanism of solvent molecules; (2) the relaxation or loosening of polymer chains, and (3) the swelling or/and shrinking of polymer network.

Hong *et al.*(2008) presented a field theory with a non-equilibrium thermodynamic approach, and the theory concerned the coupling of the mass transport and large deformation. In this theory, both the network stretching and mixing of network and

solvent contributed to the free energy of the gels. The large deformation consists of two modes: the rearrangement of molecules and migration of molecules. The former one caused no volume change but shape change, and the latter changed both shape and volume.

Birgersson *et al.* (2008) extended this perspective to macroporous fast-response hydrogels. They analysed thermo-sensitive neutral hydrogels of different shapes. They also dimensionalised the model.

The multi-effect-coupling ionic-strength-stimulus (MECis) model is presented for transient simulation of the kinetic deformation behaviour of the ionic-strength-sensitive hydrogel, and is also based on the laws of conservation of mass and momentum, where the chemical, electrical and mechanical effects are considered on the kinetics of the hydrogel. The simulated kinetic swelling and shrinking characteristics by the MECis model are compared with the experimental data, and it was concluded that the model is able to predict well the responsive variation of the ionic-strength-sensitive hydrogel with time (Li and Tanaka, 1990).

These models usually consist of a similar set of balance equations but differ in the choice of the applied constitutive assumptions, or in the amount and types of chose unknown field quantities.

Models derived from mixture theories were more general than thermodynamic approaches. In mixture theories, gels consisted of a soft porous compressible phase and an incompressible fluid phase, and each phase followed different governing equations. The amount of fluid retained depends on the chemical potential within the sample of interest. Water is attracted inward and balanced by a retractile cross-linking force that restricts water (Bryant *et al.*, 2005).

2.4 Seed coat mucilage rheology

From the chemical analyses, it is known that mucilage contains various hydrophilic polymers which can retain water to form viscous solution or gel. The viscous property is largely influenced by the components of mucilage. Therefore, detailed rheology experiments are required to characterise the properties of mucilage.

Rheology reflects both the deformation and flow behaviour of material. If the fluid viscosity is a constant over the shear stress, the fluid is Newtonian, otherwise the fluid is characterised as non-Newtonian. Figure 2.11 shows the most common rheological behaviour of non-Newtonian fluids. The viscosity increases with increasing shear rate for shear-thickening or dilatant fluids while it decreases for shear-thinning or pseudoplastic fluids. For Bingham-type of fluids, they have to exceed a particular shear stress which is called yield stress to start flow. Most of the polymer solutions are shear-thinning solutions.

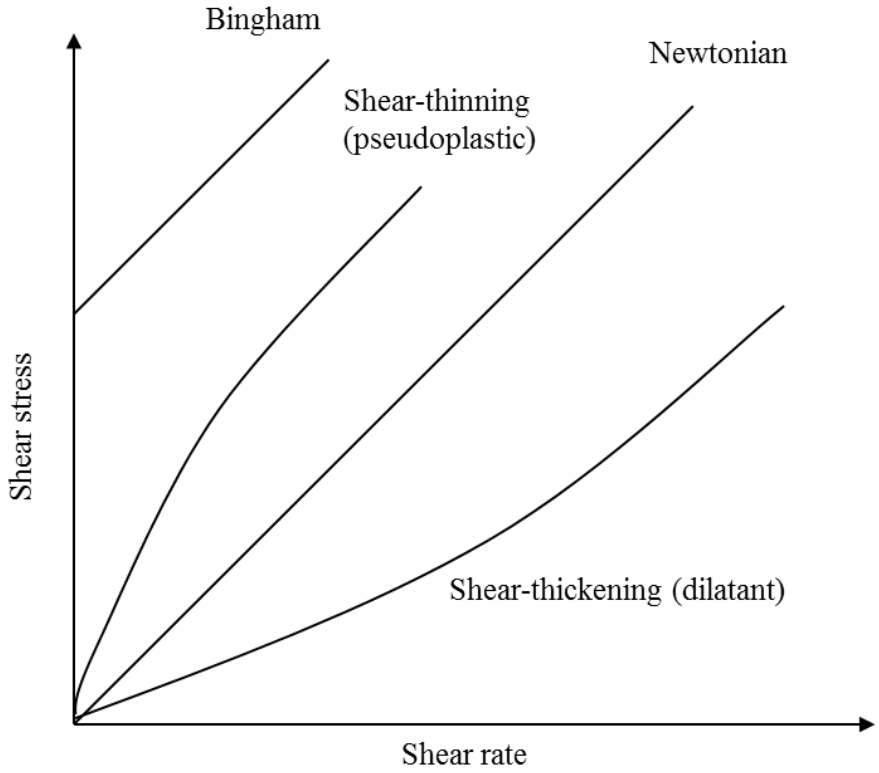

Figure 2.11 Shear stress and shear rate relationships for non-Newtonian fluids.

There are numerous models reported to describe the viscosity behaviour under steady shear conditions. The most commonly used models that describe the relationship between viscosity and shear rate are Carreau, Ellis and power-law models. The formula for each model is listed in Table 2.1. Among all these models, the power-law model is the simplest with only two parameters and is widely used in engineering and scientific applications.

Table 2.1 The most commonly used viscosity models for steady state measurement.

Models	Equations
Carreau model	$\eta = \eta_\infty + \frac{\eta_0 - \eta_\infty}{\left[1+\left(\dot{\gamma}t_c\right)^2\right]^{\frac{1-n_0}{2}}}$
Power-Law Model or Ostwald-de Waele Model	$\eta = C_1\dot{\gamma}^{n_0}$
Ellis model	$\eta = \eta_0\left[1+\frac{\tau}{\tau_{1/2}}\right]^{1-n_0}$

η: viscosity; γ: shear rate; n_0: flow behaviour index; η_∞ and η_0: the viscosities in the upper and lower Newtonian regions respectively; t_c : a characteristic time constant; C_1: consistency index; τ: shear stress; $\tau_{1/2}$: shear stress at which $\eta = 1/2\eta_0$;

The rheological behaviour of mucilage is reported to be shear-thinning or pseudoplastic, and used to enhance viscosity, stability and texture of food products (Wannerberger *et al.*, 1991; Cui *et al.*, 1994a; Fedeniuk and Biliaderis, 1994; Gerhards and Walker, 1997; Chang and Cui, 2011). The understanding of this feature is essential and important as it underpins the extensive use of mucilages in a wide range of technologies, such as oil industry, foods, and processing of plastic. Historically, there are two main types of rheological test that may be applied to mucilages: the steady- and oscillatory-shear tests. In the steady shear test, the shear modulus *G* and shear viscosity η are defined by:

$$G = \tau/\gamma \tag{2.9}$$

$$\eta = \tau/(d\gamma/dt) = \tau/\dot{\gamma} \quad (2.10)$$

where τ is applied shear stress, γ is applied shear strain, $\dot{\gamma}$ is the shear strain rate.

Oscillatory shear measurements are applied to describe the gelling or viscoelastic behaviour of a material by distinguishing a solid from a liquid using the storage and loss modulus (Ross-Murphy, 1994). For dynamic rheological tests, the storage modulus, *G'*, the loss modulus, *G''*, complex viscosity η^* and loss factor tanδ are obtained in the linear viscoelastic range.

The oscillatory rheology tests show that most seed mucilages give a gel type behaviour, with *G'* > *G''*. Typical examples are psyllium mucilage and flaxseed mucilage (Cui *et al.*, 1994b; Farahnaky *et al.*, 2010). But Fedeniuk and Biliaderis (1994) showed that for linseed mucilage *G'* < *G''* with a dilute solution behaviour.

It has been found that seed mucilage rheology properties depend on many factors such as mucilage concentration, temperature, pH and ionic strength (Wannerberger *et al.*, 1991; Ndjouenkeu *et al.*, 1996; Gerhards and Walker, 1997; Medina-Torres *et al.*, 2000; Koocheki *et al.*, 2009; Wu *et al.*, 2010). For example, Farahnaky *et al.* (2010) investigated the dynamic shear properties of aqueous solutions of the mucilage isolated from psyllium at different mucilage concentration, temperature and pH. Guo *et al.* (2008) studied the effect of calcium on the rheological properties of alkaline extracted psyllium polysaccharide. They reported that the aqueous mucilage solutions exhibited shear-thinning and high elastic properties. The viscosity of mucilage always followed Ostwald–de Waele or power law model at different shear rate.

2.5 Mucilage soil interaction

Despite the ecological function of the mucilage in seed germination and dormancy, the mucilage can also change the properties of the soil environment. In many plants, mucilage is secreted from roots and changes the physical and chemical properties of the rhizosphere (the soil-root interface, Read *et al.*, 1999). Similar results were found by studying fungal or bacterial secreted mucilage (Caesar-Tonthat, 2002). Unfortunately, seed mucilage has not yet drawn much attention. The following section summarises the soil mechanical and hydrodynamic properties as modified by mucilage or other plant polysaccharides as a reference to study mucilage soil interaction.

2.5.1 Soil mechanical properties affected by mucilages

Generally, plant mucilage-soil interactions are assessed on the basis of the changes in soil mechanical properties such as soil tensile or compression strength and stability. The mucilages secreted by plant root and microbes in soil and rhizosphere have been studied for the potential to affect soil structure and physical properties (Czarnes *et al.*, 2000). Experiments carried out on both real soils and artificial soils have shown that the addition of mucilage can increase soil aggregation and stability. Root mucilage secreted from maize root cap contributed to the interaction between the plant and soil. The root cap mucilage was characterised as a gel-like material with high viscosity (145 mPa) compared to pure water at low stress. The root mucilage has also been shown to play a major role in maintaining root-soil contact in the rhizosphere (Read *et al.*, 1999). The root mucilage (maize root for example) cannot hold water in the rhizosphere, as it was of low osmotic potential (-7 to -10 kPa, Guinel and McCully, 1986b; -60 kPa at 1.2 mg mL^{-1}, Read *et al.*, 1999), and for good reason as otherwise it may act to limit water supply to the plant. The function of the root mucilage also serves as a lubricant aid with

root penetration, soil aggregate formation, and plant and microbial growth *via* its effect upon nutrient uptake (McCully, 1999; Gregory, 2008).

Morel *et al.* (1991) investigated the effect of the maize root mucilage on soil aggregate stability of two different soil types (silt-clay and silt-loam soil). They pointed out that the freshly released mucilage adheres readily to soil particles binding them together and forming a protective layer against external forces. Barré and Hallett (2009), measured the rheological stability of soils affected by fungal exudates and found that mucilage increased the soils stability. The root and bacterial mucilage can also increase soil binding property after wetting and then re-drying (Watt *et al.*, 1993). In all, root and bacterial mucilages were able to form and maintain soil aggregates.

While there are many studies on the capacity of root or bacterial mucilages to impact upon soil structure, there are only a small number of articles that report on the similar potential of seed mucilages. Even the myxospermous seeds were generally analysed from the perspective of seed germination and dispersion as opposed to seed mucilage-soil interactions. It appears, there is an underlying assumption that myxospermous seed mucilage could have no significant functional effects on that ecosyetem service that may be mediated by soil physical properties. However, I acknowledge that Grubert (1974), did raise the hypothesis that seed mucilage may enhance the binding between seed and soil, though did to provide experimental evidence of this. Later, Gutterman and Shem-Tov(1997) carried out experiments to study the soil binding ability of seed mucilage from *Carrichtera annua* and *Anastatica hierochuntica* in Negev Desert. Their results showed that the role of mucilage differed from season to season. In winter, the main effect is in water retention and soil particle contact, while in summer dew the mucilage allowed water absorption by seeds to facilitate repair of damage and empowered germination by acting a seed-priming mechanism. The capability of

mucilage to change soil properties were affected by the amount of seed mucilage, chemical components and environmental conditions (temperature and water availability).

2.5.2 Soil hydrodynamic properties: as affected by mucilage

The hydrodynamic properties of soil, such as water retention and hydraulic conductivity may be significantly altered by mucilage. These hydrodynamic qualities are modified as a consequence of the water holding capacity, swelling and shrinking of mucilage, which act to alter soil pore space size, length and extent to which they are blocked and/or interconnected. There is only one peer-reviewed study (Bengough, 2012), which used neutron radiography and light transmission methods to report that a plant derived mucilage from roots can change the water retention dynamics of the rhizosphere, relative to those properties of bulk soil.

2.5.3 Hydrogels used as soil amendments for agriculture and horticulture

These natural soil-targeted plant polymers are not generally studied with a view towards their structure and composition being mimicked for redeployment as synthetic form to support plant or crop production. Instead, synthetic polymers such as polyacrylamide based gels are widely used in horticultural and agricultural systems (Syvertsen and Dunlop, 2004). A general term for such synthetic polymers is a “hydrogel”, and these are deployed with the aim of improving one main ecosystem service of soil which is to improve water retention, seed germination, seedling establishment and consequently plant growth and yield, and especially in water deficient areas (Table 2.2). Most of the hydrogels exploited by commerce are polyacrylamide or polyacrylate based due to their particularly high water holding capacity between x10 and x1000 their own dry weight as water. Their water-holding capacity alone may deliver a positive effect for plant growth. Hydrogels such hydrogels also decrease the hydraulic conductivity of the soil,

thus reducing the water drainage rate. In application, only very low concentrations (around 0.01% or 22 kg ha^{-1}), of polyacrylamide gel can improve the physical properties of soil. Table 2.2 lists commercially available hydrogels reported to improve soil physical or chemical properties.

Peer reviewed assessments confirm that the main function of such hydrogels is to increase water storage in soil (Wang and Gregg, 1990; Akhter *et al.*, 2004; Bhardwaj *et al.*, 2007; Andry *et al.*, 2009; Chirino *et al.*, 2011; Singh *et al.*, 2011). The impact of these hydrogels was most significant when used to amend sandy soil in arid areas. Their successful use would also help conserve water since once the water was retained in soil, irrigation frequency can be reduced (Agaba *et al.*, 2011;Akhter *et al.*, 2004; Syvertsen and Dunlop, 2004).

To date, no scientific investigation has reported on the potential of myxospermous seed mucilage to affect important physical properties of soil, which delivers important ecosystem services such water retention, mechanical strength, aggregate stability and hydraulic conductivity. Compared with the synthetic polymers, natural mucilage may have the following advantages: (1) it is nontoxic, renewable and have no adverse impact to environment; (2) it is easily collected and widely distributed, it is cheap to access. The disadvantages lie in: (1) it is not as efficient as a synthetic product in water holding capacity; (2) the mucilage is biodegradable, and may be of limited use after certain time, so new mucilage ought to be put into soil.

Table 2.2 Summary of hydrogels used in different types of soils

Polymer	**Notes on Putative Function**	**Soil Type**	**Reference**
Starch-based polymers followed by a propenoate-propenamide copolymer; polyacrylamide materials	Water uptake and water retention; drying-rehydration	Sand	Wang and Gregg, 1990
Polymerisation of acrylamide (N,N-methylbis-acrylamide) and mixed Na and K salts of acrylic acid	Water storage, water availability to plants, seedling growth and establishment	Sandy-loam and loam soils	Akhter *et al.*, 2004
Acrylamide/acrylate copolymer (PAM); cross-linked copolymer agronomic gel (AGRO).	PAM: no effect on plant growth, water use, N uptake or leaching AGRO: Increase seedling growth, water usage and nitrogen uptake efficiency	Sand	Syvertsen and Dunlop, 2004

Polymer	**Notes on Putative Function**	**Soil Type**	**Reference**
Hydrogel Stockosorb Agro	Delays drought stress effect on seedlings and trees; increased substrate water content, leaf water potential, leaf number, root biomass, CO_2 assimilation and stomatal conductance	Mix of sphagnum peat and perlite (80:20)	Arbona *et al.*, 2005
Cross-linked acrylamide or acrylic acid copolymers	Water retention, hydraulic conductivity	Sandy soil	Bhardwaj *et al.*, 2007
Cross-linked polyacrylate (Acryhope)	Hydrophysical properties	Layered sandy soil	Al-Darby *et al.*, 1996
Carboxymethylcellulose and Isopropyl Acrylamide	Water retention, hydraulic conductivity	Sandy soil	Andry *et al.*, 2009
Luquasorb hydrogel	irrigation frequency, water use efficiency and biomass production	Sand	Agaba *et al.*, 2011

Polymer	**Notes on Putative Function**	**Soil Type**	**Reference**
Hydrogel Stockosorb® and clay	Water holding capacity and morphological and physiological of seedling	Mixture of limed peat and coconut peat	Chirino *et al.*, 2011
Novel nanosuperabsorbent composite (a novel biopolymer of plant origin)	Water Absorption and Retention	Sandy-loam Soil	Singh *et al.*, 2011
Aquanika	Quality of structure and water-air properties of soil	Eroded soil	Paluszek, 2011

2.6 Mathematical models of flow in seeds or mucilage amended soils

In the same way that mathematical models may be used to conceptualise and understand mucilage behaviour, they can be applied to simulate water flows in soils amended to contain mucilages. However, in soil, the mucilage cannot just be treated as a simple particle or transportable solute, but is a non-Newtonian fluid: that is, a fluid with shear-dependant viscosity and it will swell and when hydrated, and could both adhere and migrate *in situ.* In addition, the function of the mucilage to promote (or not), the growth of soil microbes is not taken into account. This too may affect, indirectly, soil physical properties, and there is a broad literature which reports that ability of bacterial growth to block soil pore spaces (Thullner *et al.*, 2004; Kim *et al.*, 2007; Mostafa and Van Geel, 2007; Mostafa, 2009). On the other hand, the degradation of mucilage by bacteria or other microorganisms could also impact on soil-mucilage-water interactions. Thus, the main conclusion excluded to here is that water flow in mucilage amended soils is a complex procedure. However, within hydrological or biological system, there are various processes happening within different domains. These processes are highly complex and require different data for different models.

Various numerical models have been proposed to describe water flow through gel amended soils. These include continuum models, capillary bundle models and pore-scale network models (Sochi, 2010a; Sochi, 2010b). Continuum models are simplified macroscopic approaches which treat the porous media as a continuum and all the parameters are averaged into a bulk term, such as “permeability”. The limitation of this model is that specific important aspects are not quantified and explicitly incorporated into the model details, and includes pore structure, wettability variations or interface behaviour. In the capillary bundle models, flow channels in a porous medium are simulated as a bundle of tubes. In these models, the porous medium is modelled as

straight, cylindrical and identical parallel tubes oriented in a single direction. Again, capillary bundle models fail to simulate the morphology of the pore space and the heterogeneity of the medium. Pore-scale network models are relatively novel methods that accounts for the flow and void space structure at pore level. These models partly accounts for the physics of flow and void space structure at pore level with affordable computational resources.

2.6.1 Continuum models

The most commonly used and simplest model to simulate fluid flow in porous media is Darcy's law. This continuum approach is usually applied with the mass conservation equations. The flow described by Darcy's equation is given as:

$$\frac{\partial(\phi S)}{\partial t} = \nabla \cdot \left[\frac{k_r k}{\mu} (\nabla p + \rho g \nabla D) \right] \tag{2.11}$$

$$\mathbf{u} = -\frac{k_r k}{\mu} (\nabla p + \rho g \nabla D) \tag{2.12}$$

where ϕ is porosity, ρ is the fluid density, S is the volume fraction, $\mathbf{u}$ is the Darcy velocity, μ is the viscosity, k_r is the relative permeability, k is the intrinsic permeability, p is the fluid pressure, g is the gravitational acceleration, D is the coordinate of the direction which g acts.

Darcy's law is starting point for a continuum scale model. Although Darcy's law is able to simulate the flow of underground water in most environments, it makes the following assumptions:

(1) the fluid is Newtonian;

(2) the porous media is isotropic;

(3) the parameters (u, *p*) are described using an averaged value with the porous media;

(4) the flow rate is slow (Re << 1).

Darcy's law has been modified extensively to consider more complex phenomena such as non-Newtonian and multiphase flow.

Other continuum models such as Blake-Kozeny-Carman (BKC) model and Ergun model are also popular in simulating fluid flow through porous media. In BKC model, the fluid viscosity and the porosity and granule diameter of porous media are taken into account. In this model, the porous media pores are considered as a bundle of straight tubes of different cross-section or tortuous tubes with angles. The BKC model is suitable for laminar flow at low Reynolds numbers. In the Ergun model, the fluid viscosity and mass density as well as the porous media porosity, length and granule diameter are considered. Flow of high Reynolds numbers can be simulated using the Ergun model which cannot be modelled by Darcy's law and BKC model.

These models failed to model the non-Newtonian flow because of the complex behaviour of non-Newtonian fluids. When applying these continuum models, some modification are required to consider the non-Newtonian behaviour. One common method is to introduce the effective viscosity of the fluid. By using this method, the continuum models are generalized by replacing the Newtonian viscosity with an effective viscosity, such as the Ellis model and Herschel-Bulkley model (Sadowski, 1965; Sadowski and Bird, 1965; Spena and Vacca, 2001; Balhoff and Thompson, 2004; Woudberg *et al.*, 2006; Uscilowska, 2008; Loix *et al.*, 2009). However, the accuracy of using these models is very limited in predicting the complexity of non-Newtonian fluid.

2.6.2 Capillary bundle models

In capillary bundle models, the flow paths in porous media are modelled as a bundle of tubes. These tubes are considered as straight, cylindrical and parallel tubes oriented in the same direction for simplicity. In these models, the permeability of the porous media is given by the Poiseuille's law:

$$K = \frac{\varepsilon R^2}{8} \tag{2.13}$$

where K and ε is the permeability and porosity of the bundle of tubes respectively, R is the radius of the tubes.

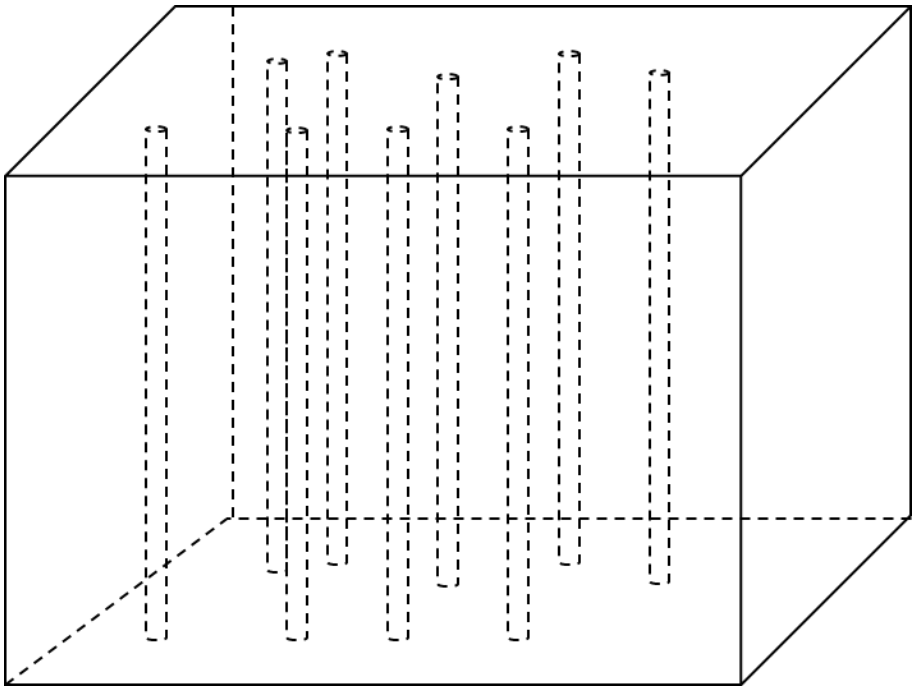

Figure 2.12 Typical capillary bundle model with straight tubes.

Using bundles of capillary tubes of various cross-sections rather than identical tubes are proposed to improve the accuracy of these models. Tortuosity and the connection between tubes can be introduced to improve the model, though bringing complexity to the model.

2.6.3 Pore-scale network models

Pore-scale networking models present the porous media as a series of pore bodies connected by pore throats of various diameters. The throats can have various shapes: circular, square, or triangular cross section. This model is able to simulate both Newtonian and non-Newtonian fluids through porous media. It is easy to get parameters such as relative permeability, flow rate, viscosity through this model. However, the model is usually built up in small scales due to the high computational cost.

In this study, Darcy's law was applied to model the flow in porous media. The relative permeability is defined as the ratio of the effective permeability of a fluid to the absolute permeability of the porous media. The relative permeability is complex that is functions of the saturation, the capillary pressure, viscosity and flow rate.

There are two commonly used empirical models for capillary pressure curve. The relationship between water content (θ) and soil capillary pressure (Ψ) and between unsaturated hydraulic conductivity (K) is important in analysis of water infiltration into soil. The soil water retention and hydraulic conductivity models include van Genuchten and Brooks-Corey model, which are based on empirical curve fitting. van Genuchten model is given as:

$$\theta = \begin{cases} \theta_r + S_e\left(\theta_s - \theta_r\right) & H_p < 0 \\ \theta_s & H_p \geq 0 \end{cases} \tag{2.14}$$

$$S_e = \begin{cases} \dfrac{1}{\left[1 + \left|\alpha H_p\right|^n\right]^m} & H_p < 0 \\ 1 & H_p \geq 0 \end{cases} \tag{2.15}$$

$$k_r = \begin{cases} S_e^{\,l}\left[1-\left(1-S_e^{\frac{1}{m}}\right)^m\right]^2 & H_p < 0 \\ 1 & H_p \geq 0 \end{cases} \tag{2.16}$$

where θ is the volumetric fraction of water, θ_s and θ_r are saturated and residual water fraction respectively, H_p (m) is the pressure head (m), S_e is the effective saturation, k_r is the relative hydraulic conductivity (m/s).

$$\theta = \begin{cases} \theta_r + S_e\left(\theta_s - \theta_r\right) & H_p < -\dfrac{1}{\alpha} \\ \theta_s & H_p \geq -\dfrac{1}{\alpha} \end{cases} \tag{2.17}$$

$$S_e = \begin{cases} \dfrac{1}{\left[1+\left|\alpha H_p\right|^n\right]^m} & H_p < -\dfrac{1}{\alpha} \\ 1 & H_p \geq -\dfrac{1}{\alpha} \end{cases} \tag{2.18}$$

$$k_r = \begin{cases} S_e^{\,l}\left[1-\left(1-S_e^{\frac{1}{m}}\right)^m\right]^2 & H_p < -\dfrac{1}{\alpha} \\ 1 & H_p \geq -\dfrac{1}{\alpha} \end{cases} \tag{2.19}$$

However, the model based on Darcy's law does not consider the gel swelling. Singh (1997) developed two numerical models to simulate the flow through gel-conditioned sand: the "swelling soil model" and the "instantaneous equilibrium model". The swelling soil model was based on the model of Philip (1969, 1972) which simulated the flow through unsaturated clay in one dimension. In this model, the gel swelling was considered as function of time. The soil medium was considered as solid phase and aqueous phase and gel was assumed to be aqueous phase.

Chapter 3 **Swelling of myxospermous seeds mucilage**[1]

3.1 Introduction

Plant mucilage is produced by many different species of plant species and in plant parts that include seeds, leaves and roots (van Rheede van Oudtshoorn and Van Rooyen, 1999). It provides functional advantages such as water storage (especially in succulents; Landrum, 2002), a lubricant for growing roots as they penetrate soil (Guinel and McCully, 1986), and a trap for prey in carnivorous plants (Vintéjoux and Shoar-Ghafari, 2000; Adlassnig *et al*., 2000). Despite the ecological functions plant mucilage may perform, the underpinning capacity of mucilages to hold water, as by myxospermy, has received most attention (Ryden *et al*., 2000; Singh *et al*., 2007; Zimmermann *et al*., 2007). Myxospermy is a trait that defines the ability of a seed to become sheathed by a mucilaginous coat upon hydration in water (Frey-Wyssling, 1976; Grubert, 1981). Myxospermy is associated with the seeds of many different plant families and species in different parts of the world. It predominates among members of the Angiospermae, having been reported for seeds of species within phylogenetically diverse, and predominantly dicotyledonous, plant families such as the Brassicaceae, Asteraceae, Cistaceae, Solanaceae, Linaceae, and Plantaginaceae (Grubert, 1974; Grubert, 1981), and especially species that commonly occur as weeds (Young and Evans, 1973). Angiosperms are characterised by their ability to reproduce and persist using seeds, and while seeds are variable and complex structures, the basic form comprises three main components: embryo, endosperm and seed coat (testa). Seed mucilage is mainly comprised of plant cell-wall polysaccharides (pectin, hemicellulose and cellulose), which are deposited during development within those cells that comprise the seed coat (Western *et al*., 2000; Windsor *et al*., 2000), the myxospermous capability becoming apparent when the mucilage within the apoplastic space hydrates.

1: Published in Annals of Botany

Despite the broad phylogenetic basis for this trait, myxospermy has been mainly characterised from studies of the model plant species *Arabidopsis thaliana* (L.) Heynh. (Arabidopsis; Western *et al*., 2000; Willats *et al*., 2001; Macquet *et al*., 2007; Arsovski *et al*., 2009). However, it has also been noted from ecological surveys that a high proportion of those plant species which persist in arid desert environments possess myxospermous seeds or seed-pods (Murbeck, 1919; van Rheede van Oudtshoorn and Van Rooyen, 1999). A selective advantage of myxospermy as aiding plant fitness in these niches is therefore implicated, possibly through improved germination. For example, the intact achenes of *Artemisia sphaerocephala* (Asteraceae) which contain mucilage in their pericarp, exhibited a higher germination rate than that of demucilaged achenes (Yang *et al*., 2010). It has also been proposed that myxospermous seeds improve contact and adhesion to soil particles (Grubert, 1974).

The ultimate aim of this Chapter is to empower theoretical investigations of myxospermous seed-soil interactions using a mathematical model of myxospermous seed mucilage swelling, which is to be developed in two stages. The first stage, presented here, is based on experimental data of mucilage swelling for the myxospermous seeds of a model weed species (*Capsella bursa-pastoris* (L.) Medik.; shepherd's purse), hydrating in simple environments (seeds immersed in solutions of increasing osmotic pressure). The data are used to create the initial mathematical model of myxospermous seed mucilage swelling, capable of predicting features such as the rate of water ingress, the rate of mucilage swelling and the volume and density of mucilage. In the second phase, the model will be developed and applied iteratively to more complex and variable environments.

Shepherd's purse is a widespread and abundant arable weed (Hawes *et al*., 2005; Iannetta *et al*., 2007; Begg *et al*., 2011), and is presented as a model plant species for

studies of plant adaptation and persistence in arable fields (Iannetta *et al*., 2010). The composition and stages of mucilage swelling for shepherd's purse have been characterised. The general structure and composition are similar to that described for the genetically syntenous species Arabidopsis (Iannetta *et al*., 2010). There are important differences, however, between Arabidopsis and shepherd's purse. Notably, shepherd's purse seed are heteromorphic, occurring in myxospermous and non-myxospermous forms. Seed heteromorphism is proposed as a bet hedging strategy while the absence of the myxospermous capability is correlated with reduced seed dormancy (Toorop *et al*., 2012). Furthermore, shepherd's purse is among the most commonly occurring in-field, broadleaf weed species.

From assessment of the water holding capacity of polysaccharides (Guinel and McCully, 1986; Sealey *et al*. 1995; McCully and Sealey, 1996; McCully and Boyer 1997), seed mucilage may be characterised as a 'gel' (Tibbits *et al*., 1998; Zwieniecki *et al*., 2001) - a three-dimensional, cross-linked, hydrophilic polymer that exhibits the properties of both solid and liquid states. Numerous theoretical models have been proposed to simulate gel swelling under different environmental conditions, which include temperature, pressure, pH and ionic strength (Tanaka and Fillmore, 1979; Peters and Candau, 1988; Birgersson *et al*., 2008; Hong *et al*., 2008; Wallmersperger, 2009; Lai and Li, 2010). Among those of greatest potential utility are models based upon the conservation of energy, mass and momentum. For example, Flory (1953) established a thermodynamic theory from energy conservation laws to define 'equilibrium volume transitions': that is those environmental thresholds at which gel properties alter from one condition to another (such as solid- to liquid-type changes). While this approach provides the equilibrium volume transition of gels, the parameters for these models are difficult to obtain as they are assumed to be based upon molecular interactions. In contrast, the transient volume changes of gels may be captured by diffusion equations

based on the theories of mass conservation (Thomas and Windle, 1982; De Kee *et al*., 2005). In diffusion models, the osmotic pressure of the solute is the driving-force for changes in gel-volume.

Accordingly, a first mathematical model of myxospermous seed mucilage swelling based on equations of water diffusion is presented here. Micrographs of hydrated seeds were used to parameterise the timing of swelling, and the dimensions of those cells that contain the polysaccharide before (dry) and after swelling (hydrated). The proposed mathematical model is compared to data generated from mucilage swelling of seeds imbibed in solutions of different osmotic pressure.

3.2 Materials and methods

3.2.1 Microscopy

Ultra-structural measurements were made from light micrographs of hydrated myxospermous seed, sectioned after embedding in either Tissue-Tek™ (frozen) or wax (at room temperature). For cryo-sections, seeds were hydrated in deionised water for 1 h before immersion in phosphate buffered saline (0.1 M, pH 7) containing 30% [w/v] sucrose, incubated overnight at -4 ^{o}C, then embedded for sectioning in Tissue-Tek™ (#R1180, Agar Scientific) and frozen using liquid nitrogen. Cryosections (8 μm thick) were cut in a cryotome (Cryostat Leica CM3050 S) and placed on SuperFrost™ plus slides (#631-0108, VWR International). Sections were stained with 0.2% [w/v] Toluidine blue (#T3260, Sigma-Aldrich, Poole, UK) for 10 min, rinsed x3 (using running tap water) and dried (5 min) on a slide heater. The sections were observed using a stereomicroscope (Leica MZFLIII attached to Leica DC500 camera). For sectioning of wax-embedded samples, seeds hydrated in water were embedded directly in molten

paraffin wax (VWR International, Poole, UK) within a metal cradle and sectioned using a Leica Microtome (RM2125RT; Wetzlar, Germany).

Observations and measurements of seed surfaces were made from cryo SEM and time lapse confocal images. For cryo-SEM, seeds were rapidly frozen in liquid nitrogen within the freezing-chamber of an Oxford Instruments Alto 2500 Cryo-preparation system. The samples were then transferred under vacuum to the Cryo-stage where they were warmed to -95^{o}C for 5 min to sublime surface water. After sublimation the samples were cooled to -115^{o}C prior to coating with 5 μm gold/palladium. Specimens were examined using a Philips XL30 SEM operating at a voltage of 15 kV. Micrographs were taken with a Focused Ion Beam-Scanning Electron Microscope (FIB-SEM) from samples that were plunge-frozen in liquid nitrogen slush at −210 ̊C and transferred under vacuum using a Quorum Technologies PP2000T Cryo transfer system (Quorum Tech. Inc., Guelph, Canada) to the cryo-preparation chamber of an FEI Quanta200 3D DualBeam FIB-SEM (FEI Europe, Eindhoven, the Netherlands). The sample temperature was raised to -95 ℃ to sublime condensed surface ice and the sample sputter coated with platinum. The sample was passed through the transfer lock to the FIB-SEM cryo-stage, which was held at −145°C and imaging performed using an accelerating voltage of 10 kV. For confocal microscopy, seeds were hydrated in water with 0.2% [w/v] calcofluor (#F3543, Sigma-Aldrich) for 30 min. A small volume of solution was pipetted into the gap between a slide and raised cover-slip to allow visualisation without the seed being compressed by the cover-slip. Calcofluor treated samples were visualised using a UV light source. The seeds were observed with an inverted Nikon Ti-Eclipse or Leica SP2 confocal microscope using a blue diode (405nm) laser (Nikon Instruments Europe BV, Kingston, UK).

3.2.2 Weight of shepherd's purse seed

For each of three replicates, one thousand shepherd's purse seeds were weighed to four decimal places. These seeds were placed into a cylindrical column (2 cm diameter, 1 cm height) cut from a long white plastic pipe, and onto which a disc of plastic mesh (0.2 mm) was glued. Columns were placed in a shallow trough of water (2 mm depth) to allow hydration from the base of the column. Then the column was removed from the water and excess water was removed by filter paper before weighing. The weight of hydrated seeds was measured every hour until a plateau was reached.

The relative weight of the soluble and non-soluble components of shepherd's purse seed mucilage was estimated by weight comparison after seed treatment by cell-wall degrading enzymes (water as a control). Mucilage removal was possible after incubation in Cellic^{TM} CTec (density 1.15 g ml^{-1}, Novozymes A/S, Denmark) at pH 5.5. The degradation of the cellulosic component appeared to facilitate complete removal of the innermost component, which was difficult to remove normally (*i.e.* with aqueous solutions). Two groups of shepherd's purse seeds (each group had six replicates of 5 g) were mixed with distilled water (1:10 [w/v]). One group of seeds was shaken for 48 h at 50^{o}C; , while the other group was treated with Cellic^{TM} CTec (12 % [w/w] of seed weight) and shaken for 48h at 50 ℃. The seeds of each group were washed (x three) before centrifugation (5000 rpm, 20 min). The supernatants from both extractions were collected and freeze-dried for 5 d. The remaining seeds were dried at room temperature for 5 d, before being weighed to record their relative mucilage loss, the weight decline being expressed as a percentage of the original pre-treatment seed weights.

3.2.3 Estimating the osmotic pressure of the shepherd's purse seed mucilage

Approximately 40 shepherd's purse seeds were immersed in 2.5 mL of PEG 6000 solutions containing 0.02 % [w/v] Toluidine Blue for 20 min. The PEG concentrations ranged from 0 – 30 % [w/v] with sterile distilled water. The corresponding osmotic pressure of PEG solutions was calculated according to Michel (1983). Seed mucilage size after swelling was measured from digital images taken using a microscope (Leica MZFLIII with Leica DC 500, Germany) under illumination with white light. Images were analysed using ImageJ software (http://rsbweb.nih.gov/ij/). The shape of shepherd's purse seed is assumed to be ellipsoid (prolate spheroid), with sizes $a = b < c$, where a, b, and c are the seed width, thickness and length, respectively. Thus, the seed volume and surface area are assessed using $4/3\pi abc$ and $2\pi(a^2+c^2\alpha/\tan\alpha)$, $\alpha = \arccos(a/c)$, respectively. Three replicates of 40 seeds were used to estimate mucilage swelling in each PEG solution.

3.3 Modelling Seed Mucilage Swelling

3.3.1 Shepherd's purse seed mucilage swelling: process description

The testa of shepherd's purse seeds is composed of a layer of hexagonal cells within which the mucilage is synthesised and deposited during seed development (Figure 3.1A). The individual testa cells are shown under increasing magnification (Figure 3.1B-D), and key features such as the central columella (Figure 3.1D) are shown relative to the size of the subtending periclinal cell walls (Figure 3.1E). The inner-most periclinal wall (closest to the endosperm and embryo) and short side walls appear as thickened secondary cell walls. The outer periclinal wall is a flexible primary cell wall that appears to be anchored at the top of each short wall that borders each testa cell, and seems also attached to the central columella. The shepherd's purse seed mucilage is

mainly comprised of pectin which is embedded in a matrix of cellulose fibres (PPM Iannetta, The James Hutton Institute, UK, 'pers. comm.'). The swelling process is illustrated in Figure 3.2, which shows the seed coat cell swelling when the water is entered from the left side of the seed. During hydration, the outer periclinal cell wall is raised at the radial cell walls (forming a 'donut' shape), and is subsequently ruptured by the swelling pectin and unfurling cellulose fibres to form a 'boundary layer' which marks the outermost limit of the cellulose network. The pectinaceous component of the mucilage extends beyond the boundary layer to form an outer sheath. An equivalent process, taking up to 20 s, has been reported in Arabidopsis seed mucilage swelling (Arsovski *et al.* 2009). Also, it was reported that the outer layer of mucilage appeared soluble, while the inner layer of mucilage was strongly attached. The inner and outer layers possessed different chemical compositions that affected hydration speed differentially: the inner mucilage hydrated more slowly than the rapidly swelling soluble outer mucilage, which is mainly comprised of unbranched rhamnogalacturonan I. However, the whole process can be simulated as water movement through the periclinal cell wall and the resultant swelling of the contained mucilage.

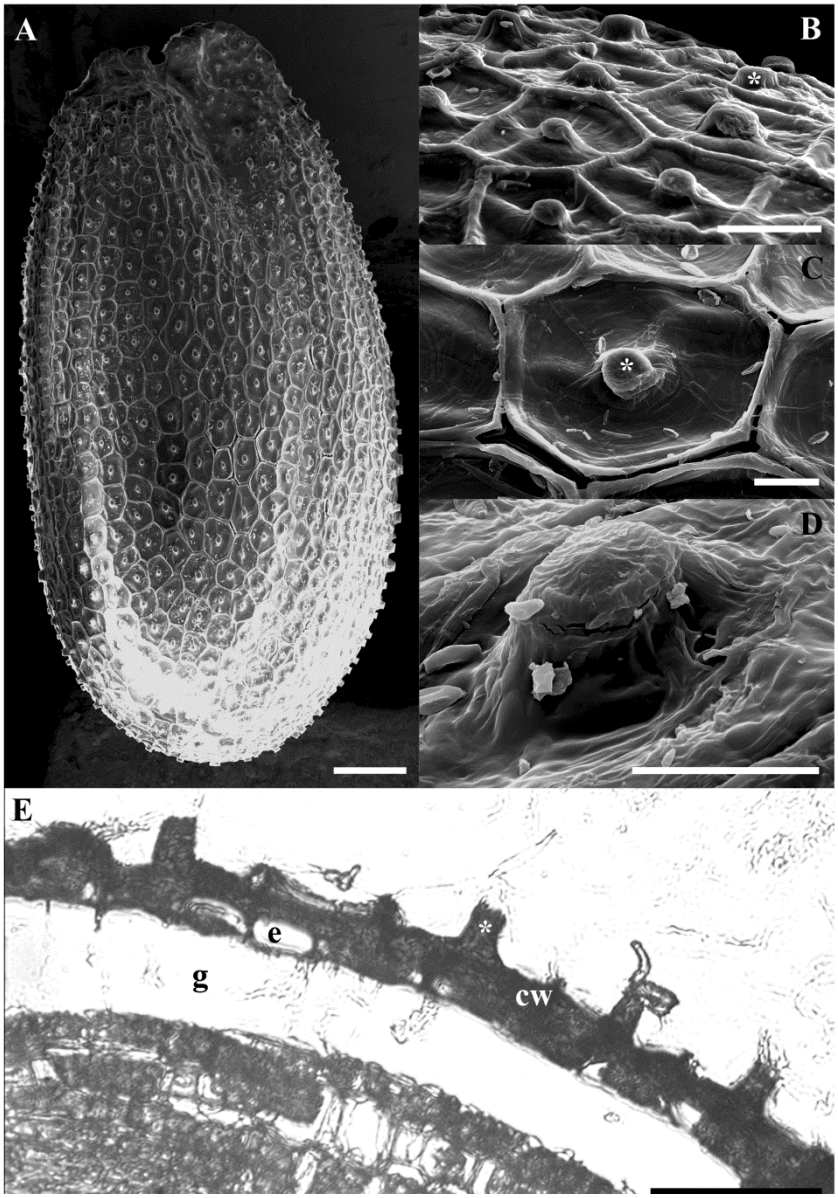

Figure 3.1 *Capsella bursa-pastoris* L. Medik (shepherd's purse) seed coat structure shown using scanning electron (A-D) and light (E) micrographs. A, a whole shepherd's purse seed (scale bars = 100 µm). B to D, the testa cells which form the surface of shepherd's purse seed under increasing magnification. The central columella is identified (*) in B and C while D shows the columnella under highest magnification (scale bars: B = 40 µm; C and D = 10 µm). E, section taken from a paraffin-wax embedded seed, showing a sectional view of the columella (*) which is an outgrowth of the testa (thickened secondary seed coat cell walls; cw; scale bar = 40 µm). This micrograph also shows a gap (g), which is an artefact caused by the embryo dissociating from the seed coat and subtending endosperm cells (e; the lumen of an endosperm cell).

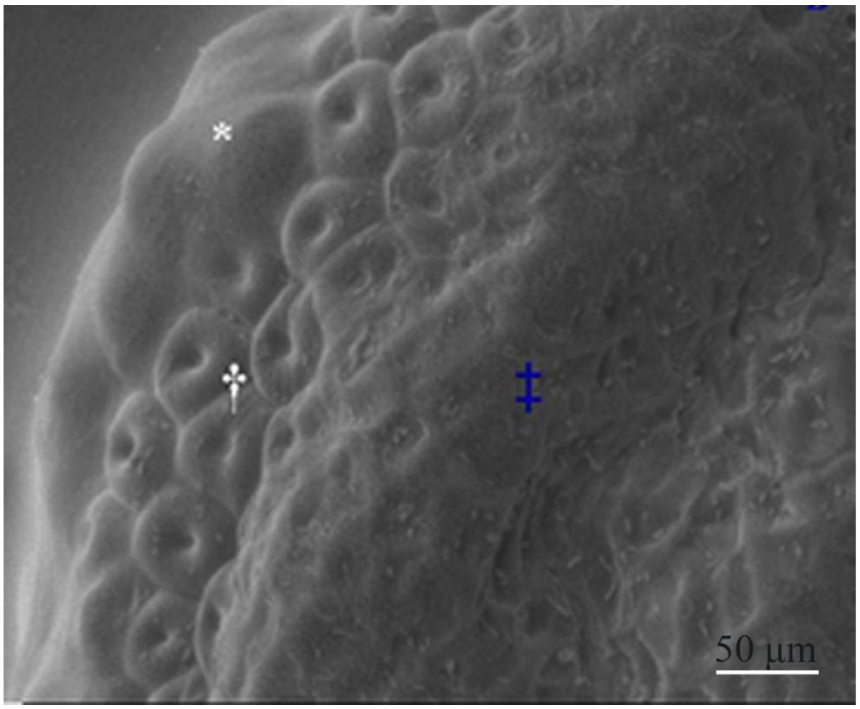

Figure 3.2 The SEM micrograph of a partially hydrated shepherd's purse seed showing: unswollen cells in the foreground (‡*); cells at swelling with stretched 'skin' attached to central columella and edges of each testa cell which was at donut shape (†); and, cells at fully swollen state with 'skin' raised (*).

3.3.2 Mathematic model

(a) Governing equation

The mass transfer of water into a testa cell is governed by a diffusion model:

$$\frac{\partial C}{\partial t} + \nabla \cdot \left(-D \nabla C \right) = 0 \tag{3.1}$$

where C is water content of mucilage, t is time, D is a diffusion coefficient and ∇ denotes the vector differential operator.

(b) Boundary and initial conditions

Figure 3.3B shows a diagrammatic representation of the testa cells and mucilage swelling. The flux at boundary 3 (upper-most wall, Figure 3.3B) is determined by:

$$-\mathbf{n} \cdot \left(-D \nabla C \right) = k_m \left(C - C_m \right) \tag{3.2}$$

where **n** is the outward unit normal vector on the boundary and k_m is the mass transfer coefficient (m/s).

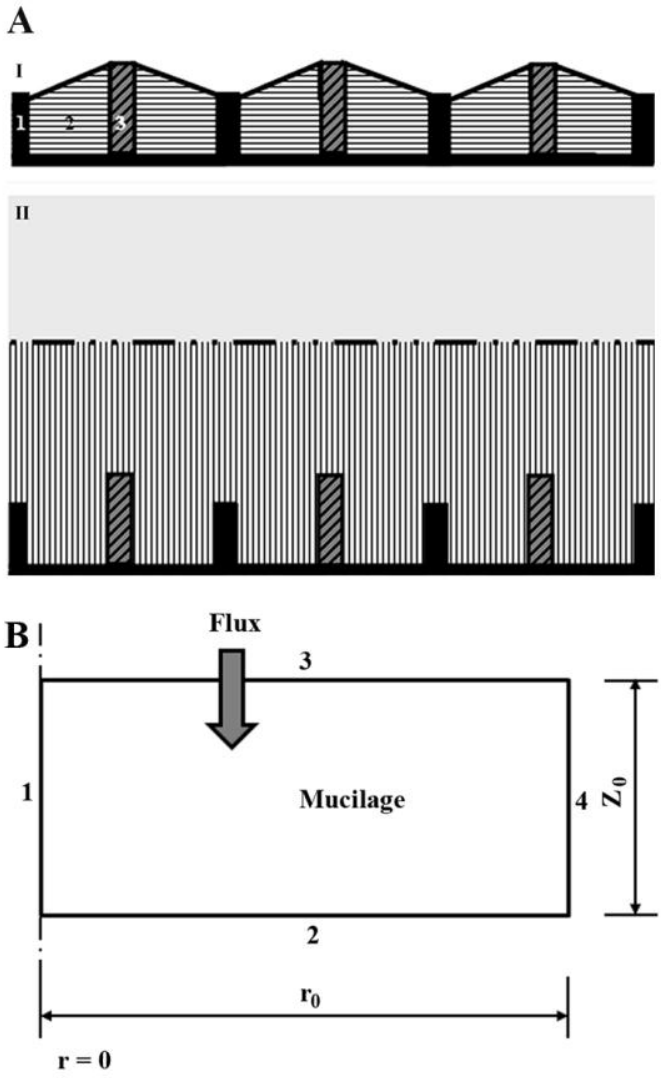

Figure 3.3 Schematic representations of seed mucilage swollen in *Capsella bursa-pastoris* (L.) Medik. (shepherd's purse). A, the testa cells and internal dry mucilage in a dry state (I), and a fully hydrated state (II). For I and II, light-grey shading denotes the pectinaceous component, and hatching the orientation of cellulose fibres (Iannetta *et al*., The James Hutton Institute, UK, unpubl. res.). The thick black lines show the periclinal secondary thickened cell walls at the base and sides of each cell. The uppermost diagonal black line at the top of each cell denotes the uppermost (primary) periclinal cell wall. The central columella has internal diagonal hatching and a dark-grey infill. B, shows the dimensions of the mucilage filled void situated between columella and outer wall, simplified as a rectangle and shown in sectional half-cell view.

Table 3.1 The parameter values (definitions and sources) which were used and applied to the proposed mathematical model for myxospermous seed mucilage swelling.

Parameter	Values	Description	Reference
r_0	20 μm	Radius of single testa cell	Measured
z_0	10 μm	Initial mucilage (or testa cell) height	Measured
D	$1.9\times10^{-10}\ m^2\ s^{-1}$	Diffusion coefficient of water	Hough *et al*. 1993
μ_w	10^{-3} Pa•s	The viscosity of water	Crowe 2001
C_0	0. 1g g^{-1}	Initial water content	Assumed
k_m	2.3×10^{-5}	Mass transfer coefficient	Spiazzi and Mascheroni,1997

The water holding capacity or equilibrium water content C_{eq} is a function of the osmotic pressure of the external solute and it is obtained from the experimental data of PEG solution given by:

$$C_{eq} = \frac{17.3e^{4.1p}}{1+17.3e^{4.1p}} \tag{3.3}$$

where p is osmotic pressure of PEG solution, MPa.

For boundary 1 (the columella, Figure 3.3B), the axial symmetry boundary condition is applied,

$$-\mathbf{n}\cdot\left(-D\nabla C\right)\Big|_{r=0}=0;\;\; t>0 \tag{3.4}$$

The other two boundaries (2 and 4, lower-most wall and right hand side wall; Figure 3.3B) are insulating boundaries, *i.e.* no water transfers through them:

$$-\mathbf{n}\cdot\left(-D\nabla C\right)\Big|_{r=0}=0;\;\; t>0 \tag{3.5}$$

Then the initial condition is given:

$$C=C_0=\text{const};\;\; \text{t=0} \tag{3.6}$$

(c) The measurement of mucilage swelling

The volume of mucilage after swelling is given by:

$$V=V_0+\alpha V_w \tag{3.7}$$

where V is the total volume after swelling, V_0 is the initial volume of mucilage and V_w is the volume of water, the sum of water moving through the boundary. The coefficient α is used to describe the effect of polymer chain change during mucilage swelling, $\alpha \geq 1$. If α = 1, there is no change, and the volume of water absorption is equal to the volume increase. The experimental measurements and calculations (below) showed that mucilage volume changed in relation to the amount of water absorbed and that swelling was due to a combination of water uptake and polymer chain relaxation. Of the total swelling (x75) on a *per* testa cell basis the contribution is apportioned as 1:3.7, respectively. α is therefore attributed a value of 4.7. The degree of mucilage swelling is characterised by Q, which is formed as:

$$Q=\frac{V-V_0}{V_0}=\alpha V_w \tag{3.8}$$

The absorption of water will reach equilibrium when the swelling pressure reaches zero,

and the equilibrium depends on the interaction of osmotic pressures of mucilage and water. The swelling degree at equilibrium is noted as Q_{eq}.

(d) Model parameters

The parameters of transport are dominant in this model. The diffusion coefficient has the most important effect on the volume change of mucilage. The diffusion of water into mucilage may be influenced by the composition and microstructures of the cell wall. For simple molecules in plant tissue, the order of the diffusion coefficient is 10^{-10} m^2 s^{-1}. In this chapter, the coefficient of water diffusion through an apple slice from Hough *et al*. (1993) was applied as 1.9 $\times 10^{-10}$ m^2 s^{-1}, which was determined by the best fit of their model. For a dry seed, the initial water content of mucilage is very low. In this model, C_0 is assumed to be 0.1 g g^{-1}, and is assumed to be close to the water content of seeds stored at room temperature and room humidity (ISTA).

The cell walls comprising the shepherd's purse seed testa form a structure consisting of hexagonal units that collectively are similar in appearance to the structure of bee honey-comb (Figure 3.1). Here, the mathematical geometry of each testa cell is simplified in two dimensions as two cylinders; the inner and outer cylinders represent the columella and cell walls, respectively. The mucilage is situated in the void between the two cylinders. Due to the symmetry of the cylindrical geometry, the void (and swelling processes therein), is modelled in two dimensions as a 'half-cell' (Figure 3.3B). The convection and diffusion equations with boundary- and initial- conditions were solved using the software Multiphysics COMSOL (http://www.comsol.com), using the parameters and expressions defined in Table 3.1.

3.4 Results and discussion

3.4.1 Seed size and weight change during mucilage hydration and swelling

Mucilage swelling may take place through the uptake of water and increased polymer chain relaxation. Therefore, to assess the contribution of these two processes, mucilage volume changes were assessed as a result of hydration in water and in relation to the weight or volume of water absorbed. If the proportional volume change was similar to weight gain, then swelling was predicted to be only a function of water uptake. However, if the proportional volume change was greater than that predicted by weight gain, then polysaccharide relaxation had also occurred. Furthermore, weight of mucilage contained in each seed was measured relative to the mucilage dry weight to assess the hydrogel capacity of the mucilage.

Towards this end, measurements from light micrographs showed that the average size of a dry shepherd's purse seed was 0.92 ± 0.07 x 0.51 ± 0.05 mm^2 (length x width, respectively: n = 40), the volume 0.134 ± 0.005 mm^3 and the weight 114 ± 3 µg (n = 500). After hydration in water, the length increased by 0.52 ± 0.01 mm, the width by 0.60 ± 0.01 mm and the volume to 0.93 ± 0.03 mm^3, which was a *ca.* 6 fold increased over that of the dry seed. The average weight of a single seed after hydration was 573 ± 20 µg, an increase of 460 µg or 4 fold. The quantity of mucilage (as proportion of the dry seed weight) was estimated by extraction, and the extraction distinguished the relative contribution (by weight) of the two mucilage layers. Specifically, the soluble outer layer of mucilage accounted for 3.7 ± 0.2 % of seed weight, while the enzyme extraction process, which removed all the seed mucilage, accounted for 25.2 ± 0.5 % of seed weight (*ca.* 28.7 µg). The inner layer mucilage weight therefore accounted for 21.5 ± 0.1 % of the dry seed weight. Consequently, after hydration and on the *per* seed basis, the mucilage increased its weight by *ca.* 16 fold. For the volume increase, only the inner

layer mucilage was considered as the outer layer was diffused and the volume was difficult to measure. The initial inner layer mucilage volume was calculated by measuring the epidermal cells and the volume increase was estimated to be 75 fold. The volume increase was therefore greater than the weight increase, which indicated that mucilage swelling was not only due to water uptake but also the polymer chain relaxation. Also, the scale of increase (16 fold) indicated that the shepherd's purse seed mucilage may be characterised as a 'superabsorbent hydrogel' (that is capable of absorbing water in the range 10-1000 g g^{-1} dry mucilage; *c.f.* Zohuriaan-Mehr and Kabiri, 2008).

3.4.2 Mucilage swelling kinetics in different concentrations of PEG solution

For the purposes of modelling the mucilage swelling process, it was important to know the osmotic pressure of the seed mucilage. Mucilage swelling was found to decrease as the osmotic pressure of the hydration solution increased (Figure 3.4 A – C). The volume and surface area of hydrated seeds were also measured to find out their relationship with the osmotic pressure of the hydration medium (Figure 3.4 D, E). Seed mucilage volume decreased from 0.93 ± 0.03 mm^3 in water to a recordable minimum of 0.134 ± 0.022 mm^3 at -1.15 MPa (representing a decline in seed surface area from 4.635 ± 0.093 to 1.35 ± 0.043 mm^2, respectively). Both the volume and surface area of hydrated seeds were expressed as exponential functions of osmotic pressure (Figure 3.4D, E). Seed plus mucilage volume and surface area did not change significantly in solutions of osmotic pressures lower than -0.54 MPa. To give this data an environmental context, specifically an indication of the ability of the mucilage to compete for soil moisture, the osmotic pressure of the mucilage (-0.54 MPa) was equivalent to a salt (sodium chloride) concentrations of 0.11 M (6.6 g L^{-1}; *c.f.* Van't Hoff, 1887). In germination studies of Arabidopsis at the same PEG concentration (20% [w/v] PEG, or -0.54 MPa), wild type

seed germination was 30% of total germination in water, whereas seed mucilage deficient *MYB61* mutants failed to germinate (Penfield *et al*., 2001). Similarly, seed of *A. sphaerocephala* failed to germinate when imbibed in aqueous solutions at -0.87 MPa (equivalent to 0.2 M NaCl) or lower (Yang *et al*., 2010). Myxospermous seeds may therefore benefit from the capacity of the mucilage to compete effectively for water within the soil environment, and enhance seed germination and plant establishment.

3.4.3 Model simulations of mucilage swelling

Using those parameters determined in the previous sections, or gathered from the literature, simulations were run on mucilage swelling at equilibrium Q_{eq}, in response to different osmotic pressures (Figure 3.5). Q_{eq} data generated from model simulations (closed circles, Figure 3.5), compared favourably with the experimental measures (section 3.4.2). The Q_{eq} decreased as the osmotic pressure increased and the theoretical findings were therefore in close agreement with the observed data. Shepherd's purse mucilage swelling was halted at -1.15 MPa, and above this value mucilage volume increased greatly (75 fold) as already demonstrated (Figure 3.5).

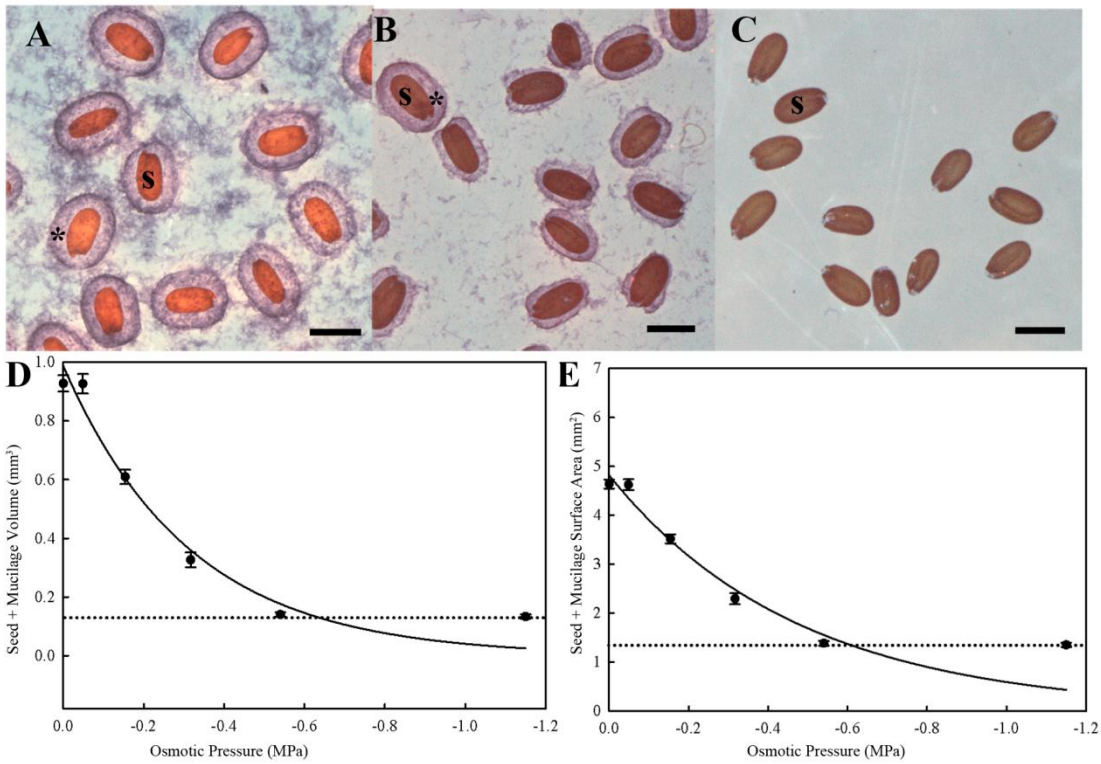

Figure 3.4 The swelling of *Capsella bursa-pastoris* (L.) Medik (shepherd's purse) seed coat mucilage in polyethylene glycol 6000 solutions of concentrations on increasing osmotic pressure assessed with light microscopy where: A, shows seeds hydrated in water, and B and C show seeds immersed in PEG6000 at 15% and 30% [w/v] solutions (representing osmotic pressures of -0.32 and -1.15 MPa, respectively). Seeds are indicated (s) and seed mucilage (*). Scale bars = 1 mm. Changes in physical parameters of shepherd's purse whole seeds (seed plus mucilage) are also shown as they responded to hydration in different osmotic pressure (PEG6000) environments, where: D, shows volume responses, and; E, surface area responses. The responses are fitted to exponential decay models (solid lines), where volume = $0.9749e^{2.9574p}$ (R^2=0.9821) and surface area = $4.6847e^{1.7757p}$, R^2=0.9594, for figures 3 D and E, respectively. Seed-only volume and surface area changes are shown (dotted line).

Other simulations were also carried out which simulated the values for Q over time in response to four different aqueous environments of increasing osmotic pressure (Figure 3.6), and different mucilage depths (Figure 3.7). These indicated that mucilage swelling required more time to reach equilibrium in water (5s; and in agreement with experimental observations), than in a solution of lower osmotic pressure (for example; 2.2 s in -0.54 MPa PEG, Figure 3.6). In addition, while mucilage depth (or cell height) did not alter Q_{eq}, swelling time to reach Q_{eq} increased as mucilage depth increased (Figure 3.7). At a depth of 10 µm (as measured in dry seeds) the time for swelling to Step II was about 5s, similar to that estimated from confocal time lapse microscopy

(Iannetta *et al*., The James Hutton Institute, UK, unpubl. res.), while at double this depth swelling time had increased to 12 s.

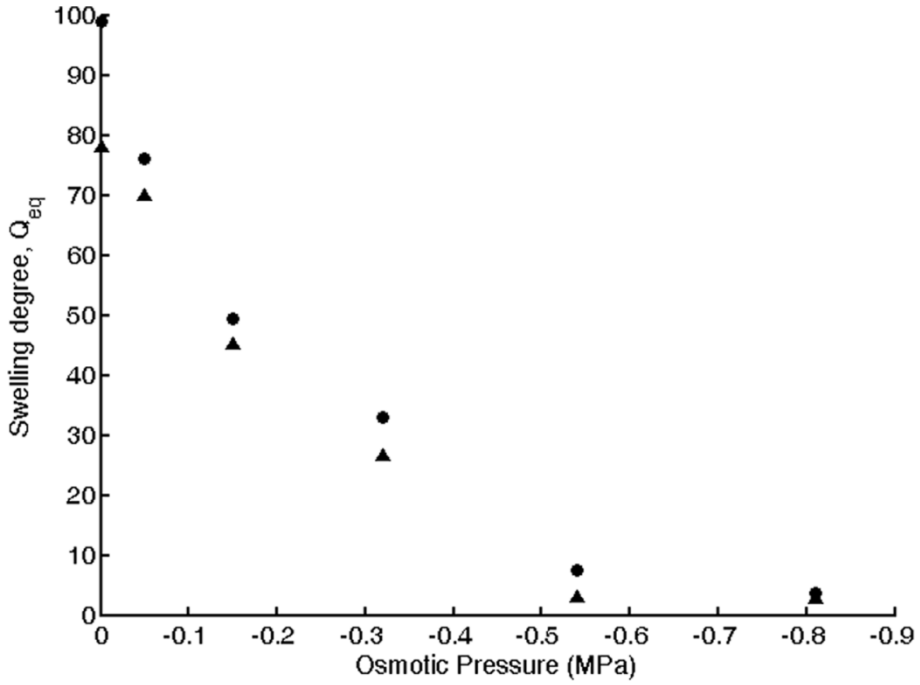

Figure 3.5 Mucilage swelling degree (Q_{eq}) at equilibrium from mathematical model simulations in response to polyethylene glycol osmotic pressure. ●: the modelled data and ▲: experimental data.

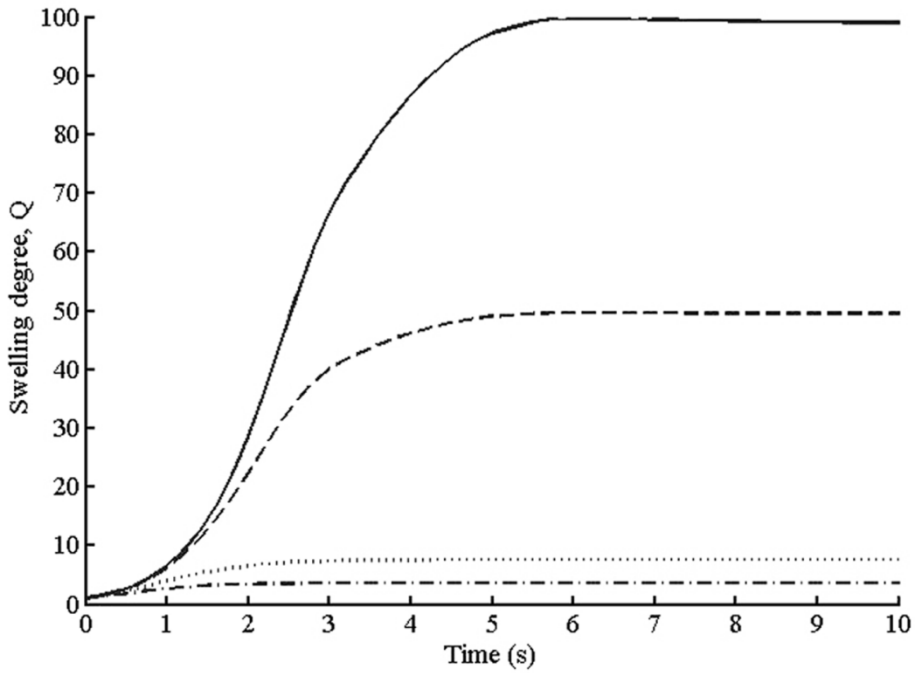

Figure 3.6 Mucilage swelling degree from mathematical model simulations in response to polyethylene glycol osmotic pressure at different times. The solid, dashed, dotted and dot-dashed lines indicate osmotic pressure of 0, -0.15, -0.54, -and 0.81 MPa, respectively.

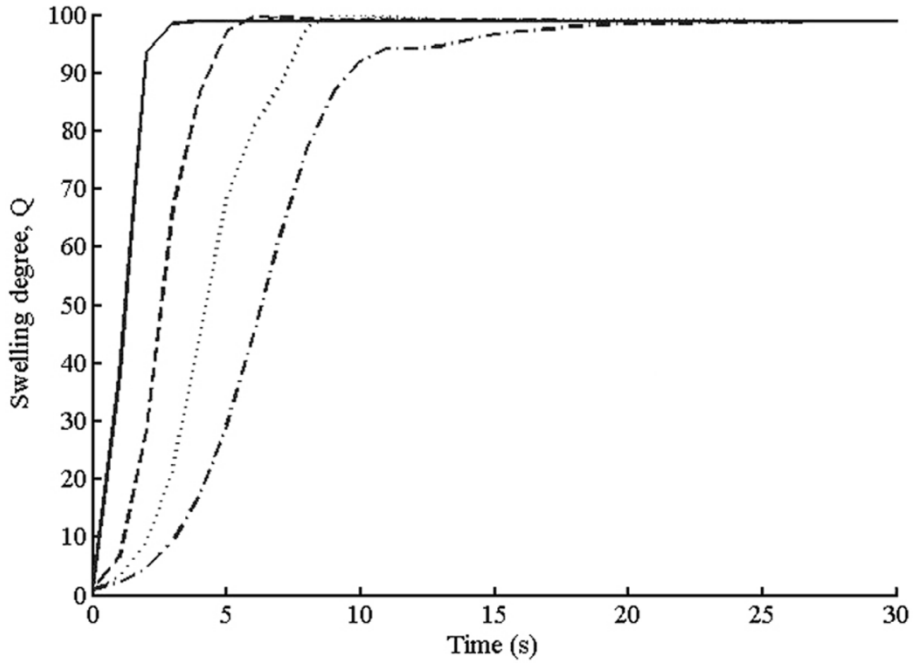

Figure 3.7 Mucilage swelling degree (Q_{eq}) at equilibrium from mathematical model simulations in response to mucilage depth (*z*; see Figure 3.3B) at different times. The solid, dashed, dotted and dot-dashed lines indicate mucilage depths of 10, 15, 20 and 25 μm, respectively.

3.5 Summary

Myxospermous seed mucilage swelling in shepherd's purse occurs as a function of water uptake and polymer chain relaxation. The mucilage has a low osmotic pressure (to -0.54 MPa), and may be described as superabsorbent hydrogel capable of absorbing 16 g water *per* g dry mucilage. Experimental observations of mucilage swelling were used to provide theoretical and empirical data which enabled the creation of a mathematical model that uses diffusion equations to predict seed mucilage swelling in relation to varying biological and environmental conditions. The mathematical model takes into account the contribution of polymer relaxation and is the first mathematical model to simulate the swelling of myxospermous seed mucilage. The model will be developed to assess interactions between myxospermous seed mucilage and soil. For example, myxospermous seeds within the soil seed bank will expand upon hydration and thereby possibly affect soil stability and hydraulic conductivity *via* a reduction in pore space. Such effects of myxospermous seeds may be related to soil type, and simulations could

identify those parameters for seed-soil combinations which optimise both stability and water-retention.

Chapter 4 **The rheological properties of the seed coat mucilage**

4.1 Introduction

In the last Chapter, it was demonstrated that when hydrated, the seed mucilage absorbs water and swells to contain the seed within a mucilaginous sheath. The whole seed coat mucilage of shepherd's purse seeds can absorb relatively large amounts of water (16 g of water g^{-1} dry weight), increasing seed volume by 7 fold, and dry mucilage volume by 75 fold (Deng *et al.*, 2012). The seed coat mucilage is composed mainly of a matrix of the plant cell wall polysaccharide pectin, which is held within a scaffold of cellulose fibres which are in turn anchored to the testa surface (Western *et al.*, 2000; Windsor *et al.*, 2000). The myxospermous seed mucilage of Arabidopsis (and shepherd's purse; Iannetta, personal communication) possesses two distinct layers after hydration and staining with the pectin specific stain ruthenium red: an inner layer which is composed of cellulose and pectin, and the outer layer which is composed of mainly pectin. The outer layer may be removed in an aqueous dispersion by agitation; the cellulose component is anchored to the testa and may be removed by enzyme digestion (Western *et al.*, 2000; Windsor *et al.*, 2000; Willats *et al.*, 2001; Western, 2006; Deng *et al.*, 2012). The seed mucilage has been shown to enhance water absorption by the seed (Young and Evans, 1973), improving the contact surface area and adhesion between the seed and the soil (Grubert, 1974; Grubert, 1981; Uren, 1993; Gutterman and Shem-Tov, 1997). Also, the seed mucilage has been shown to affect seed germination (Yang *et al.*, 2010; Toorop *et al.*, 2012). However, the fact that the outer layer of seed mucilage may be easily removed means the mucilage may be dispersed within the soil. Mucilage dispersed in this way may influence soil physical properties, such as soil aggregate stability for example. This possibility, become more tenable if one considers that a single shepherd's purse plant may yield up to 90,000 seeds (Hurka and Haase, 1982).

However, the potential function of myxospermous seed mucilage as a ‘soil conditioner’ is untested. Particularly since the mucilage may also be a nutritional source for microbes, and facilitate rhizosphere forming microbes to support seedling establishment (Yang *et al.*, 2012).

However, ahead of assessing the soil-seed mucilage interaction, the rheological or ‘flow behaviour’ properties of the seed mucilage itself should first be determined, and it is this perspective (as opposed to purely ecological considerations), which are reported here. If the viscosity of this mucilage is high for example, it is more likely to aid the formation of soil aggregates and maintain soil-seed contact.

Most information on the plant mucilage rheology comes from studies on drug delivery or food thickening (Traore *et al.*, 2000; Koocheki *et al.*, 2009), and from a wide range of plant species, including, *Linum usitatissimum* (linseed, Wannerberger *et al.*, 1991; Wu *et al.*, 2010), *Sinapis alba L.* (white mustard, Gerhards and Walker, 1997), *Opuntia ficus-indica* (barbary fig, Medina-Torres *et al.*, 2000), *Alyssum homolocarpum* (alyssum, Koocheki *et al.*, 2009) and *Plantago ovata* Forsk. (psyllium, Farahnaky *et al.*, 2010). Both steady and dynamic state rheological parameters, measured using a strain controlled rheometer, indicated that these plants mucilages were generally shear thinning and temperature and concentration dependent. Dynamic rheology has shown that seed mucilage demonstrate viscoelastic properties, which allow them to be characterised as ‘weak gels’ (Medina-Torres *et al.*, 2000, for barbary fig; Farahnaky *et al.*, 2010, for psyllium). Furthermore, the viscoelastic attributes of seed mucilage may be a function of their composition as ‘polyelectrolytes’ (Hietala *et al.*, 2009). Polyelectrolytes are polymers which have electrolyte group, and their viscosity and shear modulus are therefore also (in addition to other general factors), ion-strength dependent. However, in general functional or ecological terms, rheological properties

enable these seed mucilages to be stable under a range of external (physical) forces, and therefore may act to stabilise the soil-seed composite. In this context, and as the cellulose component of mucilage is rather difficult to remove, the present study therefore attempts to define the rheological properties of the outer mucilage layer of shepherd's purse seeds, which is easily removed and disperses as an aqueous extract. As a precursor to experiments upon soil-seed mucilage interactions, I present the first description of the rheological characteristics of water extractable myxospermous mucilage fraction from the seeds of the model in-field (arable) wild plant shepherd's purse. I present quantitative measures of the viscoelastic properties of the water extractable seed mucilage under deformation at different concentrations, and using range of oscillatory amplitudes, frequencies and temperatures. Rheology parameters, including dynamic viscosity(η^*), storage modulus (G'), loss modulus (G''), loss factor (tan δ), flow stress (τ_f) and yield stress (τ_y), were measured to obtain a detailed assessment of the seed mucilage.

4.2 Materials and methods

4.2.1 Mucilage extraction and dispersion preparation

Dry shepherd's purse seeds were mixed with distilled water (1:10 [w/w]), and stirred continuously overnight at room temperature (21 ^{o}C) before centrifugation (5000 rpm, 20 min.). After centrifugation of the seeds, three layers can be seen, which are: seeds, a narrow viscous layer and a less viscous supernatant from the bottom of the centrifuge tube to the top, respectively. The test seed mucilage comprised both the supernatant and viscous layer. Since the extracted mucilage can be concentrated by centrifugation at moderate speeds (in a bench top centrifuge), the extracts are not a simple solution but a dispersion. The extractable seed mucilage dispersion was collected into glass Petri dishes (90 mm diameter), each dish containing about 40 mL of liquid and was frozen to

-80 ℃ before freeze-drying for 7 d. The freeze dried mucilage is shown in Figure 4.1. Different mucilage dispersion concentrations (1 – 7 and 10 % [w/w]) were prepared in distilled water by agitation. All samples were then stored overnight at 4 ℃ to normalise before testing.

Figure 4.1 Freeze dried shepherd's purse seed mucilage collected in Petri dish.

4.2.2 Oscillatory rheological measurement theory

Oscillatory rheological measurements are more appropriate than steady measurements for characterising the gelling or viscoelastic behaviour of a mucilage dispersion (Mezger, 2006). Using oscillatory rheology, it is possible to quantify the solid-like or fluid-like properties of the mucilage from the storage modulus (G') and loss modulus (G'') in the linear viscoelastic range. In shear stress controlled measurements, the shear stresses are applied to the sample and the resultant shear strains are recorded. The G'

value is an index of the deformation energy stored in the sample during shear, representing the elastic behaviour of a sample, whereas the *G''* value is a measure of the deformation energy used up in the sample during shear and lost to the sample afterwards (Mezger, 2006). If *G'* is much greater than *G''*, the material will behave more like a solid; that is, the deformations will be essentially elastic and recoverable. However, if *G''* is much greater than *G'*, the energy used to deform the material is dissipated viscously and the material behaves more like a liquid (Rao, 1999). This property is characterized by the loss factor $\tan\delta = G''/G'$. For a gel, $\tan\delta$ is less than 1. Another important rheological parameter is the complex viscosity η, which reflects the shear resistance to flow. Yield stress (τ_y) indicated the extreme high end of the linear viscoelastic range, after which the material is failed under the applied stresses or strains and the point where *G'=G''* is defined as the flow point, the relate shear stress is τ_f. However, in some literatures, they defined the flow point shear stress as yield stresses.

4.2.3 Rheological measurements

The dynamic shear rheological properties were measured using a rotational rheometer (Haake, Rheowin Mars II, Germany, see Figure 4.2). According to the recommendation given by Mezger (2006) for measuring the rheology of dispersions and gels, the rheometer was fitted with 35 mm diameter parallel plates with a gap spacing of 1mm. The temperature was controlled by a Peltier cooling unit (MARS II, Universal Temperature Controller; ±0.3 ℃). The oscillation sweep tests assessed a range of amplitudes, temperatures and frequencies, as described below. Tests assessing the influence of temperature and frequency were carried out on only 6 % and 7 % [w/w] mucilage, as these concentrations were closest to the mucilage concentration as it existed hydrated on the seed coat (Deng *et al.*, 2012). All rheological measurements were performed in triplicate for each mucilage concentration using separate samples.

Results presented in the following section are the means of the three measurements unless stated otherwise.

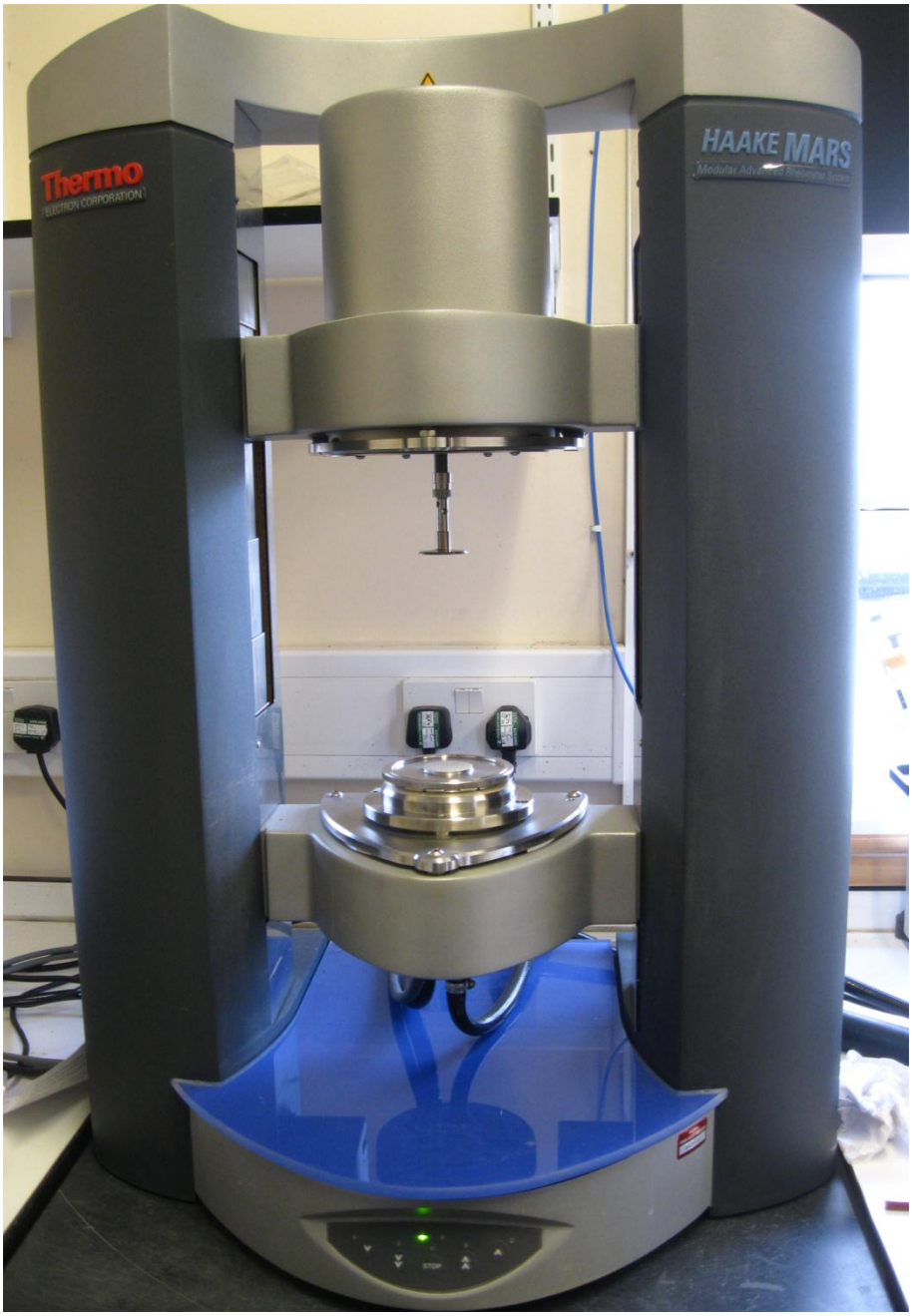

Figure 4.2 The Haake, Rheowin Mars II rotational rheometer for measuring mucilage rheology.

4.2.4 Amplitude stress sweeps

In the amplitude stress sweeps, the stresses were increased from 0.1 to 1000 Pa at a constant frequency of 0.5 Hz and temperature of 20 ℃. The linear viscoelastic range referred to the region where an increase in applied shear stress did not influence

rheological behaviour. The stresses applied in temperature and frequency sweep tests were within the linear viscoelastic range, in which a small level of deformation applied prevents structural damage to the mucilage during measurement. The mucilage samples were loaded onto the rheometer plate and then left for 3 min. to equilibrate.

4.2.5 Temperature sweeps

In temperature sweeps, temperature dependence properties were measured by heating the sample from 0 – 80 ℃. The frequency and the amplitude remained at a constant value, 0.5 Hz and 0.2 Pa, respectively. Temperature increased 8 ℃ every minute. The samples (6 % and 7 %) were loaded onto the precooled plate. The viscosity (η), storage modulus (G'), and loss modulus (G'') were measured as a function of temperature.

4.2.6 Frequency sweeps

Frequency sweeps were performed from 0.1 to 100 rad s^{-1} at 20 ℃. The stress applied in the latter two tests was 0.2 Pa, which was within the linear viscoelastic region.

4.2.7 Data analysis

The relationship between rheological parameters (η, G', G'', τ_y, τ_f) and mucilage concentration (C) was fitted by a power law regression:

$$y = a_1 C^b \tag{4.1}$$

where a_1, b are fitted parameters and y is different rheological parameter.

In the frequency sweeps, the magnitudes of log (η, G', G'') *versus* log (ω) were subjected to linear regression using the following equations:

$$\eta = k_1 \omega^{n_1} \tag{4.2}$$

$$G' = k_2 \omega^{n_2} \tag{4.3}$$

$$G'' = k_3 \omega^{n_3} \tag{4.4}$$

where k_i and n_i (i=1, 2, 3) are fitted parameters.

4.3 Results

4.3.1 Amplitude stress sweep tests

Typical results for amplitude sweep tests on the extracted shepherd's purse seed mucilage at a concentration of 4 % [w/w] are presented in Fig.1. At low shear-stress levels, neither *G'*, *G''* nor η changed significantly, indicating they were within the linear viscoelastic range. A shear stress of 0.2 Pa (Figure 4.3), which lay within the linear viscoelastic range, was therefore applied in temperature and frequency sweep tests for 6 % and 7 % [w/w] mucilage. As higher shear stresses were applied, *G'* and *G''* began to decrease, indicating that the mucilage was shear-thinning or becoming pseudo-plastic. In addition, the seed mucilage behaved as a gel, since the storage modulus (*G'*) was greater than the loss modulus (*G''*) before the flow point (*i.e.* $\tan\delta < 1$). This suggested that the polymers which comprised the mucilage were cross-linked (Mezger, 2006).

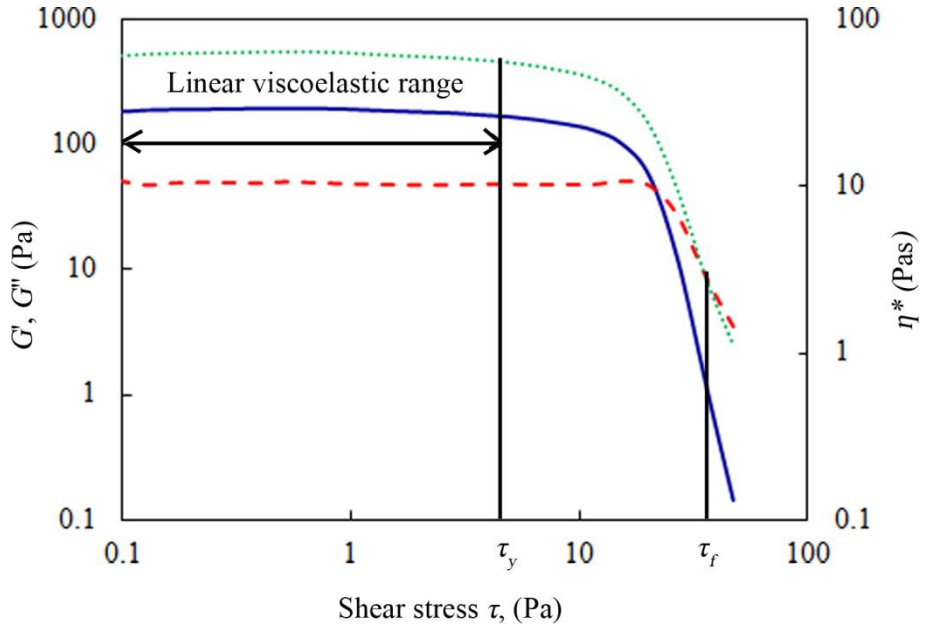

Figure 4.3 A typical oscillatory flow curve achieved for *Capsella bursa pastoris* (L.) Medik. (shepherd's purse) seed mucilage. Plotted on log-log scale and where η, G' and G'' are denoted by dotted, solid and dashed lines, respectively.

4.3.2 Effect of concentration

The rheological parameters (η, G', G'' and tanδ) of the mucilage dispersion as a function of concentration are shown in Figure 4.4 – Figure 4.7. The viscosity η increased substantially with increasing mucilage concentration, from 10 Pa s (2 % [w/w]), to 360 Pa s (10 % [w/w]; Figure 4.4), a 36 fold increase in viscosity for a 5 fold increase in concentration. Similar increases were seen for the storage (G') and loss modulus (G''; Figure 4.5), while G' was larger than G'' at all the concentrations tested. This characteristic also reinforced the fact that the seed mucilage behaved as a gel, even at the lowest mucilage concentration used (1 % [w/v]). At high concentrations the mucilage behaved more like a solid material as G' was much greater than G'' (4.5 fold at 10 % [w/w], Figure 4.5). τ_y and τ_f also increased as the mucilage concentration increased (Figure 4.6 and Figure 4.7). The relation between the rheological parameters (η, G', G'', τ_y, and τ_f) and mucilage concentration C was fitted by Eq. (1) and the parameters are listed in

Table 4.1. tan δ ranged from 0.22 to 0.47, as would be expected for a gel-like material (

Figure 4.8). After the concentration increased to 5 % [w/w], tan δ remained almost the same.

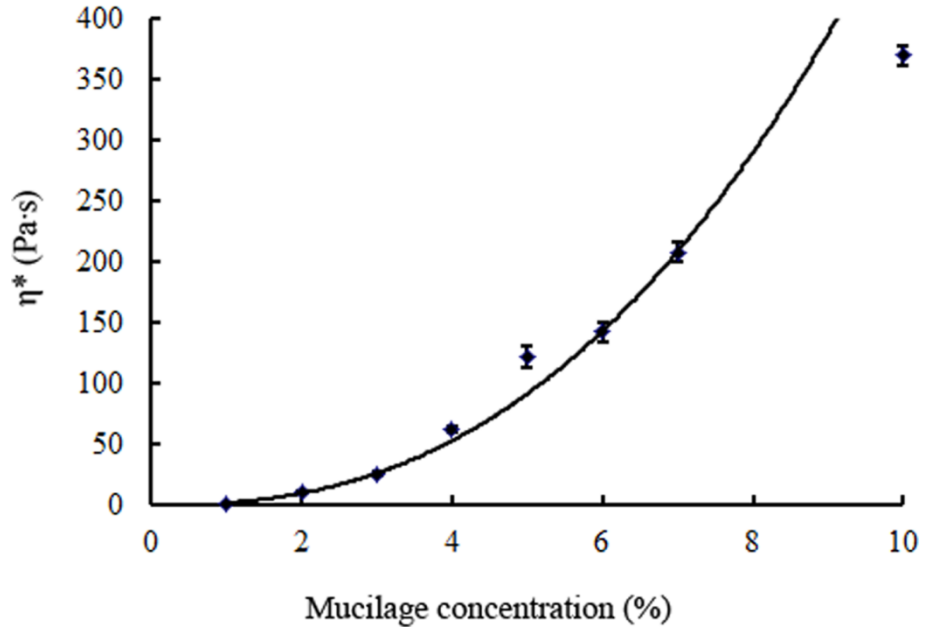

Figure 4.4 The viscosity (η) of *Capsella bursa pastoris* (L.) Medik. (shepherd's purse), seed mucilage dispersions at different concentrations (1 – 10 % [w/w]). Bars show standard error of the mean, n = 3. The lines are power curve fits.

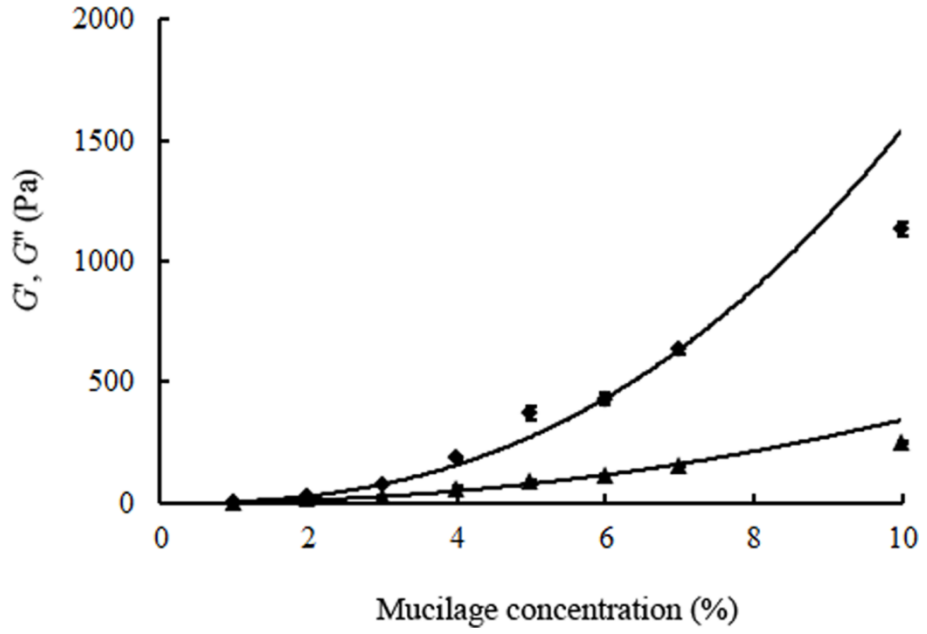

Figure 4.5 The storage modulus (*G'*, ♦) and loss modulus (*G''*, ▲) of *Capsella bursa pastoris* (L.) Medik. (shepherd's purse), seed mucilage dispersions at different concentrations (1 – 10 % [w/w]). Bars show standard error of the mean, n = 3. The lines are power curve fits.

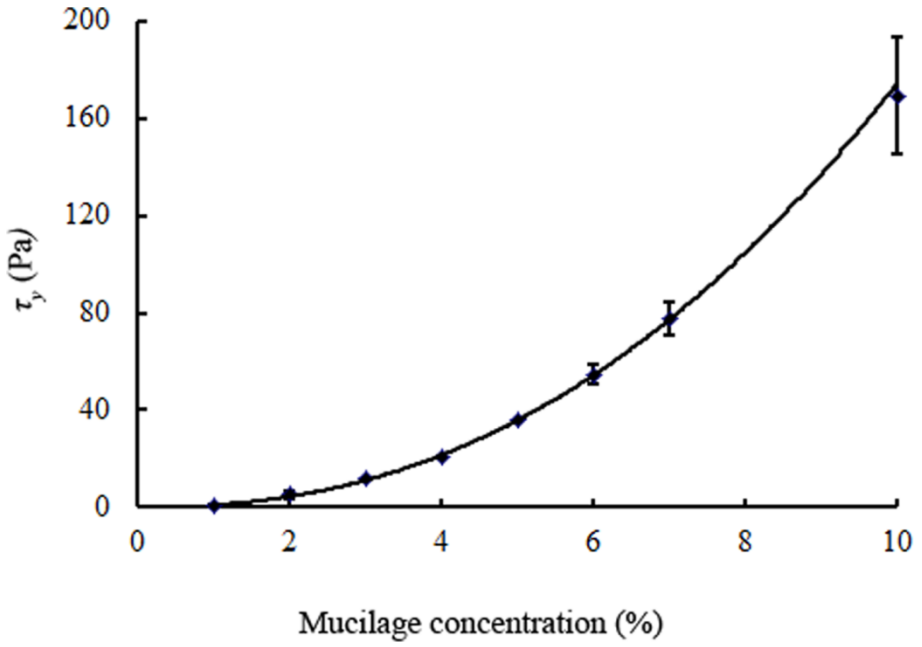

Figure 4.6 The yield stress (τ_y) of *Capsella bursa pastoris* (L.) Medik. (shepherd's purse), seed mucilage dispersions at different concentrations (1 – 10 % [w/w]). Bars show standard error of the mean, n = 3. The lines are power curve fits.

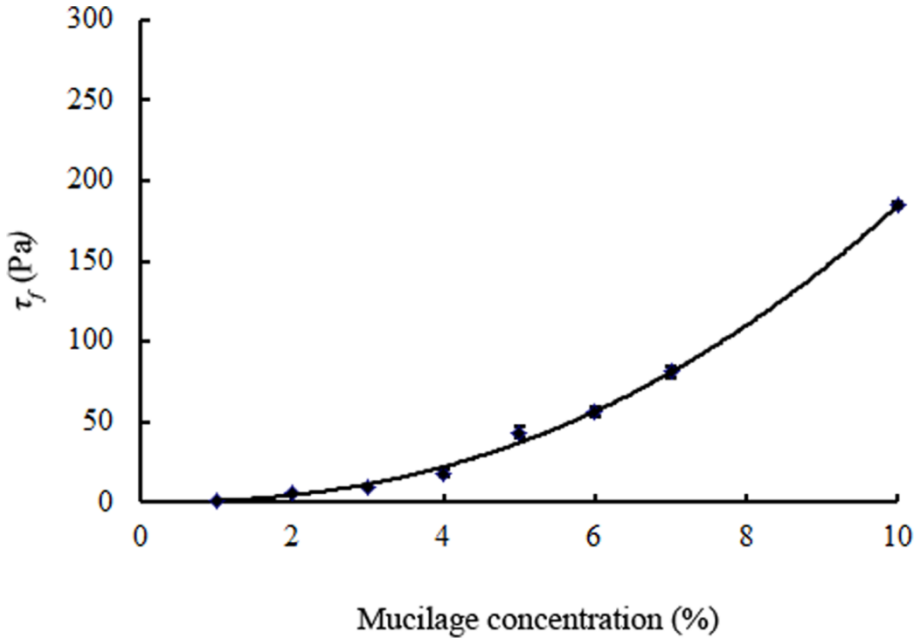

Figure 4.7 The flow point stress (τ_f) of *Capsella bursa pastoris* (L.) Medik. (shepherd's purse), seed mucilage dispersions at different concentrations (1 – 10 % [w/w]). Bars show standard error of the mean, n = 3. The lines are power curve fits.

Table 4.1 The power model parameters of rheological properties for mucilage as function of concentration.

parameters	a_1	b	R^2
η^*	1.753	2.453	0.988
G'	4.968	2.49	0.989
G''	2.551	2.12	0.979
τ_y	0.901	2.289	0.997
τ_f	0.883	2.323	0.994

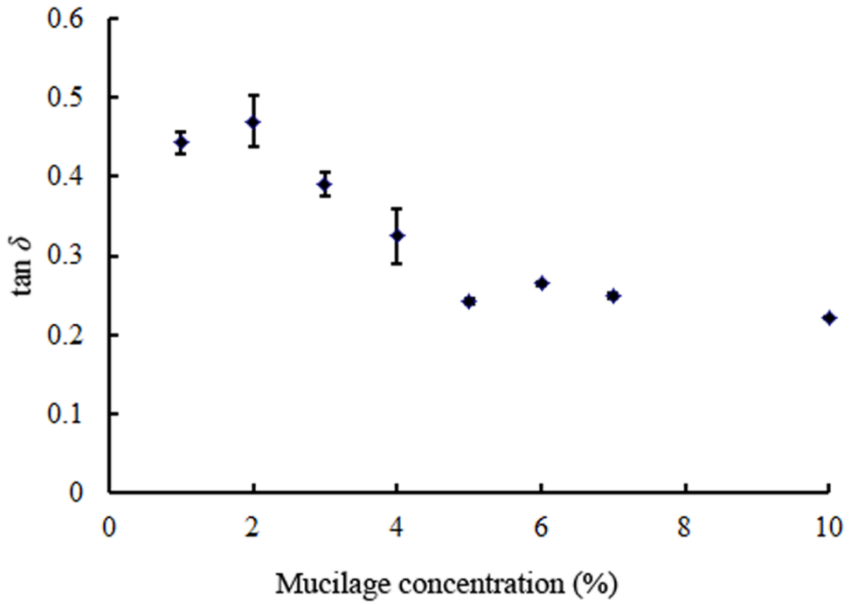

Figure 4.8 Loss factor (tan δ) variation for *Capsella bursa pastoris* (L.) Medik. (shepherd's purse) seed mucilage concentration [w/w]. Bars indicate standard errors.

4.3.3 Effect of shear frequency

Figure 4.10 illustrates the effect of shear frequency on η, G' and G'' of shepherd's purse mucilage at 6 and 7 % [w/w]. As shown in the figure, η decreased as frequency increased, thus demonstrating frequency dependency under different rates of oscillating shear stress. G' and G'' increased slightly with increasing frequency, with G' being

greater than *G''* for all the frequencies measured. These data highlighted that the seed mucilage was predominantly elastic in character.

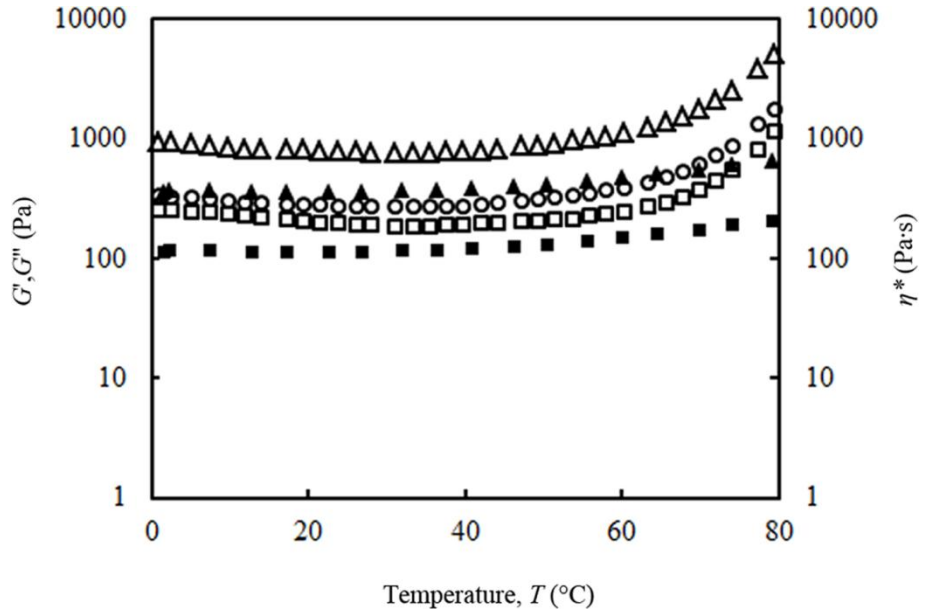

Figure 4.9 Temperature sweep test data for *Capsella bursa pastoris* (L.) Medik. (shepherd's purse), seed mucilage at concentrations of 6 % (open symbol) and 7 % (closed symbol) [w/w] for viscosity (η, ●), storage modulus (G', ▲) and loss modulus (G'', ■) plotted on a log scale.

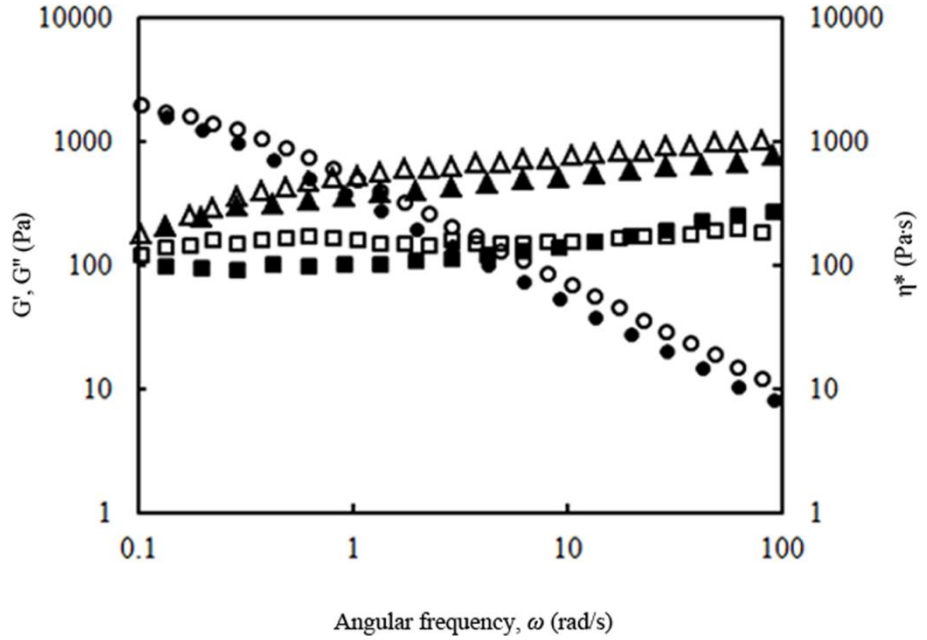

Figure 4.10 Frequency sweep test data for *bursa pastoris* L. Medik. (shepherd's purse), seed mucilage at concentrations of 6 (open symbol) and 7 % (closed symbol) [w/w]. Viscosity (η, ●), storage modulus (G', ▲) and loss modulus (G'', ■) *versus* temperature (T) are plotted at a log scale.

The fitted parameters (n_i, k_i; i=1, 2, 3) for Eqs. (2) – (4) and coefficient R^2 are given in Table 4.2. The values of k_1 and k_2 increased as mucilage concentration increased. In addition, the slope n_2 was greater than n_3, and indicated that the largely elastic properties of mucilage increased as concentration increased.

Table 4.2 The power model parameters of 6 % and 7 % (w/w) mucilage at different frequency.

Concentration	η			G'			G''		
	k_1	n_1	R^2	k_2	n_2	R^2	k_3	n_3	R^2
6%	344.8	-0.83	0.999	108.7	0.176	0.974	338.8	0.16	0.886
7%	442.5	-0.80	0.995	153.2	0.228	0.903	447.6	0.034	0.441

4.4 Discussion

The results have demonstrated that the water extractable (the outer-layer) of the shepherd's purse seed mucilage has a high viscosity and is shear-thinning. The rheological properties of mucilage were also concentration dependent. The power law parameter 'b' for the relationship between viscosity and mucilage concentration was 2.453, which was a little higher than that value which is classically obtained for hydrocolloid gels and cellulose suspensions (2.25: de Gennes, 1979). That *G'* was greater than *G''* at all the frequencies shows that the seed mucilage behaves as a gel-like material. The differences between the viscosities of extracted seed mucilage and plant root mucilage or between different types of myxospermous seeds may be ecologically relevant. For example, at their natural (fully hydrated state), the aqueous seed mucilage extracts (at 6 % [w/w]), have much higher viscosity compared to root cap mucilage (0.1 % [w/w]; Guinel and McCully, 1986a; McCully and Boyer, 1997). The viscosity of the entire maize root mucilage 0.145 Pa·s (at a low oscillation rate; Read *et al.*, 1999). For shepherd's purse seed mucilage, the viscosity is *ca.* 100 Pa·s at 6 % [w/w] mucilage

concentration (1000x greater). This difference in viscosity may highlight the different ecological roles of root and seed mucilages; one role of root mucilage is to act as a lubricant and help root penetration. For seed mucilage, the main physical role may be to enhance seed-soil contact and forming seed-soil aggregates and to attract and hold greater volumes of water (*per* unit weight).

Table 4.3 summarises the viscosities of shepherd's purse seed mucilage with those from myxospermous seeds and fruits for other species, and also in comparison to root mucilages. As the seed mucilages are non-Newtonian fluids, their viscosities vary depending on environmental conditions. Therefore, the viscosities were compared at the same conditions (2 % [w/w], 0.01 s^{-1} and 20 ^{o}C), with exception of the root mucilage, as such high concentrations have not been reported in the peer-reviewed literature. This shows that (under the defined conditions stated), that seed mucilage viscosity is greater than that of the mucilages from fruit (and roots). For example, the viscosity of mucilage from the fruit of Barbary fig was 0.1-1 Pa·s at 2 % [w/w], and 10 for shepherd's purse seed mucilage. Such functional properties indicate that the structural properties of the seed mucilage are also distinct from that of fruit mucilages. Fruit mucilage generally contains predominantly pectic polysaccharides and some proteins. In contrast, the seed mucilage is a complex structure which may be considered in engineering terms as a matrix of cellulose fibres (the continuous phase), which is embedded in a dispersed phase (the pectin). However, the viscosity of shepherd's purse seed mucilage is less than that of mucilage from the seeds of psyllium, which has been exploited by food technologists as a therapeutic dietary fibre, able to absorb large volumes of water to alleviate both diarrhoea and constipation (Singh, 2007). This study is focused on the water extractable part of mucilage, it should be noted that *in situ*, this capability may be a concerted function as the mucilage is a complex of cellulose fibres that are embedded within the pectinaceous component: and the cellulose fibres are stronger than the pectins. Therefore, once the outer layer has dissociated from the seed and the cellulose fibres are exposed, these fibres may also interact with soil components to help anchor the seed. The adhesive quality of myxospermous seeds from a wide variety of species has been reported (Grubert *et al.,* 1974). If the seeds were dispersed in the soil, they could

increase stability of soil aggregates which was also implied by the increase of τ_y which may reflect the ability of a soil to withstand mechanical forces.

Table 4.3 The viscosity of 2 % [w/w] mucilages from different of plant species and different plant parts at 20 ^{o}C and a 0.01 s^{-1} shear rate except the root mucilage which was measured at 0.1 % [w/w].

Mucilages	Viscosity (Pa s)	Plant parts	Test methods	Reference
shepherd's purse	10	seed	dynamic	this study
alyssum	1	seed	steady	Koocheki *et al.*, 2009
basil seed	1000	seed	steady	Hosseini-Parvar *et al.*, 2010
psyllium	250	seed	dynamic	Farahnaky *et al*., 2010
fenugreek	200	seed	steady	Chang and Cui, 2011
Barbary fig	0.1–1	fruit	steady	Medina-Torres *et al*., 2000
okra	1	fruit	steady	Woolfe *et al.*, 1977
maize	0.145	root	dynamic	Read *et al.*, 1999

Temperature is an important factor for seed germination and plant growth. According to Vandebroek (2006), shepherd's purse seeds can germinate at 5 – 30 ^{o}C. This study shows that the mucilage is stable within a wide range of ambient temperatures (0 – 40 ^{o}C), the stability of mucilage-soil adhesion might also be important in relation to stabilising the physical conditions within the temperatures ranges normally experienced by soil (sub-surface), and those conditions required for seed germination. As

temperatures elevates above this range, the interactions between polysaccharides molecules are likely to increase (*i.e.* seed mucilage viscosity would increase; as shown in Fig. 4), and while the physical consequences of this remain to be tested, this finding conflicts with reports for the seed mucilage of the barbary fig, (Medina-Torres *et al.*, 2000), and *Alyssum homolocarpum* (Alyssum, Koocheki *et al*., 2009), whose viscosity decreased as temperature increased. The greater viscosity of shepherd's purse seed mucilage at high temperature may have occurred due to water evaporation, although tests were sealed and done in a hydrated chamber to minimise this impact. The mucilage also tested positive with Lugol (iodine) solution (data not shown), which suggests the presence of starch (or xyloglucan), and raises the possibility that thickening may also be due to gelatinisation at high temperatures. It is also possible that xyloglucan may interact with starch to maintain mechanical stability during heating (gelatinisation; Temsiripong *et al.*, 2005).

From a structural perspective, biopolymer dispersions are usually classified into one of four types: strong gels, weak gels, an entanglement network system or a dilute solution (Clark and Ross-Murphy, 1987). For strong gels, *G'* is far much larger than *G"* and both moduli are frequency independent; for weak gels, *G'* is lightly larger than *G"* and both are slightly frequency dependent; for entanglement network system, *G'* is smaller than *G"* at low frequencies and larger than *G"* at high frequency; for dilute solutions, *G'* is far smaller than *G"* at all frequencies and both are strongly frequency dependent. Consequently, for strong gels, log (*G'*, *G"*) *versus* log ω plots should have a slope of zero, while for weak gels and highly concentrated dispersions such plots should have positive slopes and *G'* should have a higher magnitude than *G"* and be slightly frequency dependant. Therefore, the seed mucilage of shepherd's purse was more similar to a weak gel according to standard rheological descriptions (Table 4.2), and suggests that the macromolecular structure was as ordered chain segments forming a

weak three-dimensional network. The slope for η (-0.83 and -0.8, for 6 and 7 % [w/w]) was close to that reported for psyllium of -0.77 (at a mucilage concentration of 2.5 % [w/w]; Farahnaky *et al.*, 2010).

That the seed mucilage of shepherd's purse displayed weak-gel behaviour suggested that it can enhance adhesion to soil particles and therefore soil stability around the seed. Soil polysaccharides including those of microbial origin, fungal and plant mucilage can play an important role in binding soil particles to increase the soil aggregation stability (Caesar-Tonthat, 2002). As our data show that the water dispersible component of the shepherd's purse seed mucilage exhibits high viscosity and yield stress, the potential of the seed mucilage to aggregate and stabilise soil is highlighted.

From the above analysis, and that in Deng *et al.* (2012), the ecological advantage of mucilage may be as follows. On imbibition, the mucilage concentration when fully hydrated is around 6 % [w/w]: the mucilage is highly viscous and dense, acting antitelechoric by allowing adhesion of the seed to the soil and by preventing the seeds from being easily dispersed under moist conditions (Ellner and Shmida, 1981). The original role of the mucilage may therefore also serve to ensure that progeny remain close to their maternal source (environment), increasing the chance of accessibility to water in a landscape that may be usually dry. Whether, in mass, seed mucilage is able to alter the properties of soil now needs to be tested. Weeds can shed many seeds and arable soil seedbank densities may be tens of thousands of seeds m^{-2} of soil (Squire *et al.*, 2000; Heard *et al.*, 2003). Even if these propagules are incapable of germination or are dead, the soil chemical and physical properties may still be affected by the presence of seed, and /or seed mucilage. For example, Terpstra (1995) reported that shepherd's purse seed dormancy may be determined by a function of soil moisture content and soil pore size: dormancy (non-germination) increasing when soil-pore spaces is sufficiently

large to allow large volumes of water loss by gravitation. It is possible that the water extractable mucilage may disperse in soil to reduce soil pore space, and improve water retention and aggregate stability.

4.5 Summary

The dynamic rheological properties of mucilage extracted from the myxospermous seeds of *Capsella bursa-pastoris* (L.) Medik. (shepherd's purse) was assessed as a function of mucilage concentration (1–10 % [w/w]), temperature (0–80 ℃) and shear frequency (0.1–100 rad s^{-1}) is quantified. The seed mucilage was shear thinning and it was classified as a highly viscous "weak gel" as the storage modulus (G') was greater than loss modulus (G'') at all frequencies. The relationship between the viscoelastic parameters (η^*, G', G'', τ_y and τ_f) and mucilage concentration were well fitted by power models. The values for η, G', and G'' increased (the mucilage becoming more viscous), as temperature increased above 40 ℃ and were also slightly frequency dependent. The extracted shepherd's purse seed mucilage is more viscose than that from other plant parts, such as fruits and roots. These properties highlight the possibility that myxospermous seed mucilage may affect soil conditions and therefore present an additional facilitative ecological role (beyond that role already reported, which directly affects seed biology; and this is discussed in the next chapter about affecting the physical properties of soils.

Chapter 5 **Effect of seed and seed mucilage on soil physical properties**

5.1 Introduction

Myxospermy is a term which describes a trait of plant seeds to become bound by mucilage sheath upon exposure to water. The trait is ecologically important and ancient: myxospermous seeds (or seed pods) are produced by species spanning many different plant and phylogenetically diverse plant families (Grubert, 1974; Grubert, 1981; Yang *et al.*, 2012). Myxospermous seed mucilage does not simply absorb water, but may compete for it, and especially in low osmotic potential environments (containing polyethylene glycol or saline; Penfield *et al.*, 2001; Yang *et al.*, 2010; for *Arabidopsis thaliana* (Arabidopsis) and *Artemisia sphaerocephala* Krasch (Asteraceae), respectively). This capacity is a function of the seed mucilages low osmotic potential (-0.54 MPa), which enables it is able to absorb a weight of water that is up to 16x the mucilage dry weight (Deng *et al.*, 2012; for *Capsella bursa-pastoris* L. Medik. (shepherd's purse)). In this way, it has also been shown that the myxospermous capability can influence (for example), seed germination and dormancy (Grubert, 1981; Gutterman, 1993; Toorop *et al.*, 2012).

Clearly, the mucilage is very important ecologically and its role and potential functions have been recently reviewed (Yang *et al.*, 2012). However, the myxospermous seed coat mucilage has not yet been considered or assessed in relation to its potential effect on the physical structure of soil, nor to regulate soil-water interactions. This capacity remains to be tested and particularly in relation to sandy-type soils: since plants producing seeds (or seed pods) of a myxospermous capacity may represent up to 40 % of the species which are found in the sandy (low organic matter containing) soils in arid environments (van Rheede van Oudtshoorn and Van Rooyen, 1999).

In contrast, the mucilage exuded by plant roots or fungal hyphae has been studied extensively and is reported to improve soil stability and reduce water transport (see review by Morel *et al.*, 1991). For example, Caesar-Tonthat (2002), showed that the mucilage produced by a Basidiomycete fungus can enhance soil aggregation (in artificial soil), and Barré and Hallett (2009), showed that root and fungal exudates stabilised a range of soil types. Other synthetic polyacrylamide- or polyacrylate-based hydrophilic polymers referred to collectively as 'hydrogels', are commonly used in horticulture to increase soil-water holding capacity and improve soil stability and structure (Al-Darby, 1996; Akhter *et al.*, 2004; Andry *et al.*, 2009). However, these synthetic acrylamide-based polymers may pose environmental risks as they are toxic, environmental pollution and not easy to degrade (Jani *et al.*, 2009). Therefore, there is a growing interest in the use of renewable natural polymers (such as gums and mucilage, Jani *et al.*, 2009), as they are environmental friendly and may to deliver multiple ecosystem services, including the growth of soil microorganisms.

The capacity of seeds and/or seed coat mucilage to affect the functional behaviour of soils may also have particular implications for the seedbank of food (that is arable farmed), production systems. Since arable wild flower diversity is in serious decline it has been suggested that this loss would compromise those ecological services normally offered by soil (Hawes *et al.*, 2005). However, no test has yet identified a causal link, nor quantified the relationship, between the density of seeds in the soil seedbank density and delivery of specific ecosystem services. Therefore, this chapter report on the use of myxospermous seeds of the model plant of shepherd's purse (Iannetta *et al.*, 2007; Begg *et al.*, 2011; Deng *et al.*, 2012; Toorop *et al.*, 2012), to assess their role on soil-water relations. Shepherd's purse is a species which is particularly persistent, abundant and widespread (Iannetta *et al.*, 2010), and it yields myxospermous seeds, the mucilage of which is highly viscose (100 Pa s at fully hydrated state, from Chapter 4), as the

mucilage represents a significant resource investment, accounting for 25 % of the dry seed weight (Deng *et al.*, 2012). Furthermore, that one sixth of the seed mucilage (by weight), is easily dispersed in water and therefore the soil environment.

Furthermore, the consideration of seed-soil-water relations should not be made with exclusive reference to myxospermous seeds, but also the seed mucilage (alone) and non-myxospermous seeds. Therefore, the relative capacity of these three factors to affect the ecosystems services to sandy-loam and clay soil is tested. Specifically, 'regulating services', defined by soil water retention and hydraulic conductivity, and 'provisioning services' such as soil stability, as defined by the rheological parameters of shear modulus, viscosity and yield stress.

5.2 Materials and methods

5.2.1 Seed test soil, extracted-mucilage and seed amendments

The sandy-loam test soil (organic matter content 8 % [w/w]) was collected from the James Hutton Institute woodland (GPS location: 334183, 730690), and a clay-type (Ca-montmorillonite) soil was purchased from local store. The sandy-loam soil was broke down to 2 mm for water retention curve and hydraulic conductivity tests and 0.4 mm for rheology tests. All soils were amended with either: extracted mucilage only (MO; 0.5 and 1 % w/w]); myxospermous seeds (MS), or; demucilaged seeds (DS). The seed amendment being applied at two densities: 5 and 10 % [w/w], except in soil hydraulic conductivity test where 2 % [w/w] was also measured. All treatment concentrations/densities are described relative to soil dry weight; and each treatment was assessed relative to non-amended (control), soil samples. For all amendments soil-water retention was recorded. Hydraulic conductivity was measured for only seed amendments in sandy-loam soil. Hydraulic conductivity data was not gathered as the

quantity of extracted mucilage required was too large. Similarly, rheology data was gathered only for the MO amendment, as the presence of seeds present a physical structure that is so large as to preclude the recording of stable measurements on the scale required for the instrument which was used.

5.2.2 Seed mucilage extraction and preparation of demucilaged seeds

The MO material was obtained by the same method described in Section 4.3. For preparation of myxospermous and demucilaged seeds, the following processes were applied. All the seeds used for soil amendment were killed by dry-autoclaving at 105 ℃ to ensure that they did not germinate during the experiment. Furthermore, autoclaving did not appear to affect the mucilage behaviour: expansion and loss during imbibition and was verified by microscopic observation of samples stained with ruthenium red (data not shown). DM seeds were obtained using the enzyme Cellic^{TM} CTec (Density 1.15 g ml^{-1}, Novozymes A/S, Denmark; *c.f.* Deng *et al.*, 2012). The seeds were first mixed with distilled water (1:10 [w/v]), and then mixed with Cellic^{TM} CTec (12 % [w/w]), and stirred for 48 h at 50 ℃. The enzyme treated seeds were washed x3 to remove the dissolved mucilage and then dried at 37 ℃ for 5 d. They were then stored at room temperature.

5.2.3 Water retention curve

The water retention curve was measured for matric potentials (Ψ) that ranged from 0 to -250 kPa. The water retention of $\Psi > -5$ kPa were measured using ceramic plate collecting with water column (Figure 5.1A). For $\Psi < -5$ kPa, a pressure plate extractor was used with different pressure plate cell (1.0 bar, 5.0 bar), according to the Ψ value (Figure 5.1B).

The treated (or control/non-amended), soils were packed into a cylindrical container of 3.8 cm in diameter and 3 cm in height with porous bases made of nylon fabric. For all the treatments, the same amount of soil mixture (50 g) was packed in the cylinder. The soil samples were first saturated for 2 d before applying any pressure. The soil samples were weighed after equilibrium at each pressure and the water content (θ) was derived. Data for all treatments (and control), samples were determined in triplicate.

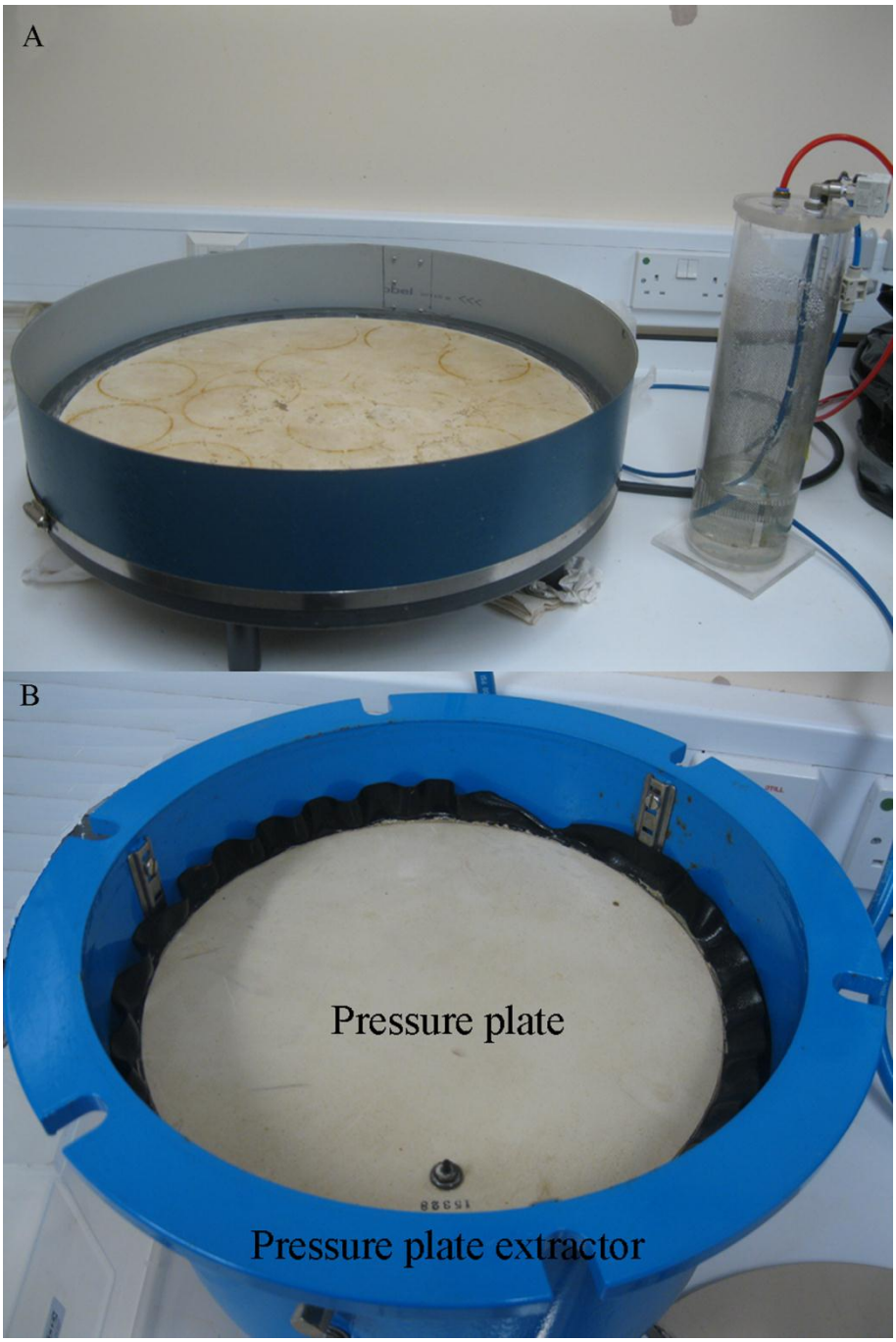

Figure 5.1 (A) The pressure plate for measuring soil water retention at water matric potential less than 5 kPa. (B) The Richards pressure plate for water matric potential more than 5 kPa and the pressure plate cell where the soil cores are placed on.

5.2.4 Soil hydraulic conductivity

Changes in the hydraulic-conductivity of soils in response to seed amendment was assessed using methodology developed by Leeds-Harrison *et al.*(1994), and as modified by Hallett and Young (1999). In order to reduce water evaporation during the tests, the water reservoir was changed to a sealed-container. The water loss during the tests was

recorded digitally using a PC interfaced balance with software Ohaus Balance Talk. All the soil columns were packed into a 4 cm cylinder with a bulk density of 1200 kg m^{-3} and then saturated for 3 d.

The steady water flow rate Q was used to evaluated hydraulic-conductivity K using the following equation

$$Q = \frac{4brS_0^2}{f} + 4rKp \quad (1)$$

where b is a parameter that depends on the soil-water diffusivity function, r is the radius of the infiltrometer tip, f is the fillable air porosity, and p is the pressure head (Leeds-Harrison and Youngs, 1997). The value of b can be in the range $0.55 \leq b \leq \pi/4$ with 0.55 being an average value (White and Sully, 1987). The hydraulic-conductivity K is evaluated as the slope of a plot of Q against p. In this study, the water head pressure h was measured at -0.5, -2 and -5 cm. Each seed soil combination was measured in three replicate samples.

5.2.5 Soil rheology tests

Rheology was only determined for the MO amendment. Mucilage/clay (Ca – montmorillonite; Surrey Finest, WRB Minerals, UK), solutions were prepared at a soil-water concentration from 140 – 200% [w/w]. While the mucilage/sand-loam solutions were provided at a soil-water concentration of 55 and 70 % [w/w] only. Prepared samples were stored for 24 h at 4 ℃ prior to assessment to ensure they were fully equilibrated.

An oscillating amplitude stress sweep test was used to apply stress ranging from 0.1 to 10 kPa and the frequency of vibration was kept constant at 0.5 Hz. The oscillatory rheological parameters were used to compare the visco-elastic properties: storage

modulus (G'), loss modulus (G''), viscosity (η) and yield stress (τ_y). The sample was loaded onto the rheometer plate with great care and allowed to equilibrate for 5 min. to recover from shearing during set-up. All rheological determinations are made using extracts which were prepared in triplicate. The rheological properties were measured using a rotational rheometer (Haake, Rheowin Mar II, Germany), and data were analysed with Rheowin software. The parallel plate PP 35 Ti (35 mm in diameter) with a gap of 2 mm was used. The temperature of the lower test-sample plate is controlled using constant water flow from a water bath (MARS II, Universal Temperature Controller) at 20 ±0.3 ℃.

5.2.6 Statistics analysis

All the statistical analyses were carried out using Excel. Statistical test were performed using a one-way ANOVA in Excel and all statistically significant differences discussed are in relation to P values < 0.05.

The soil moisture characters were fitted to van Genuchten (1980) model.

$$\theta = \theta_r + (\theta_s - \theta_r)\left[\frac{1}{1+(\alpha|\psi|)^n}\right]^m \tag{5.2}$$

$$m = 1 - \frac{1}{n} \tag{5.3}$$

where α, n, m are fitted parameters. ψ, θ_s, θ_r are the matric potential (cm), saturated water content and residual water content, respectively.

The relationship between rheological parameters (G', η, τ_y) and water content (θ) was fit by a power law regression:

$$y = c\theta^d \tag{5.4}$$

where c, d are fitted parameters and y is different rheological parameter.

5.3 Results

5.3.1 Soil water retention

Sandy-loam soil water retention, as affected by seed mucilage, was determined as a function of soil matric potential (Ψ) in Figure 5.2. The figure showed that the soil-mucilage mixtures retained more water than the soil-only control. The water retained by saturated sandy-loam soil increased by 10% with the addition of 1 % [w/w] mucilage. The mucilage almost had no great influence on clay soil water retention (Figure 5.3). Therefore, I did not carry out more experiments on seeds amended clay soil. As Ψ decreases, the differences in soil-water retention among the various treatments declined. There is no significant difference between 0.5 % and 1 % MS (p >0.05). Figure 5.4A shows that at saturation, soil containing DS increased soil Ψ by 12 % and 14 % more water for 5 and 10 % [w/w] respectively. MS-soil mixtures also increased soil Ψ and at saturate state, retained 15 % and 21 % more water for 5 and 10 % [w/w], respectively (Figure 5.4B). Again, there was no significant difference in soil water retention between soil containing added MS and DS at 5 % and 10 % [w/w] (p>0.05). But at field capacity approximate – 10 kPa, the increase in water content reduced in each treatment. In all, the water retention increase was greatest between 0 and 5 % MS.

All the data were fitted by van Genuchten model, and the fitted parameters and R^2 are listed in

Table 5.1 for sandy-loam soil.

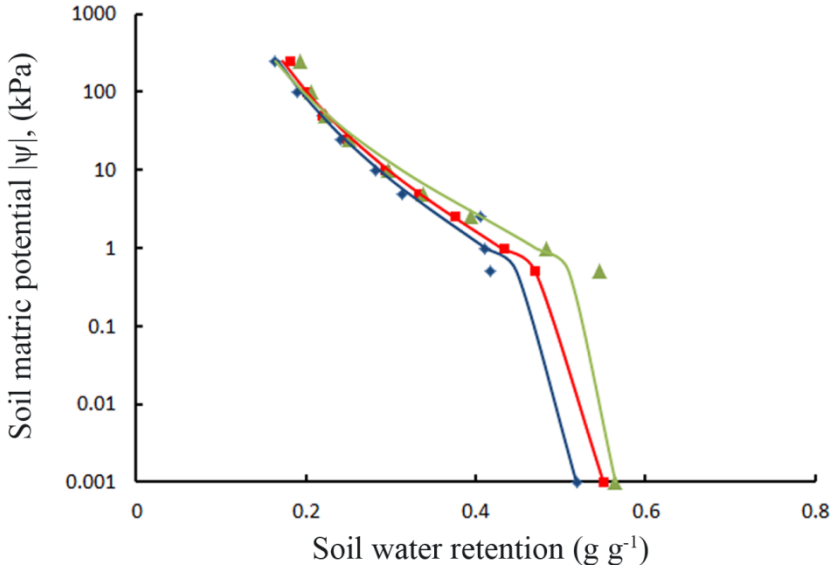

Figure 5.2 The water retention curve of mucilage amended sandy soil at different mucilage concentration. Experimental data: □ : 0 % mucilage; ○: 0.5 % mucilage; Δ: 1 % mucilage and solid line: van Genuchten model.

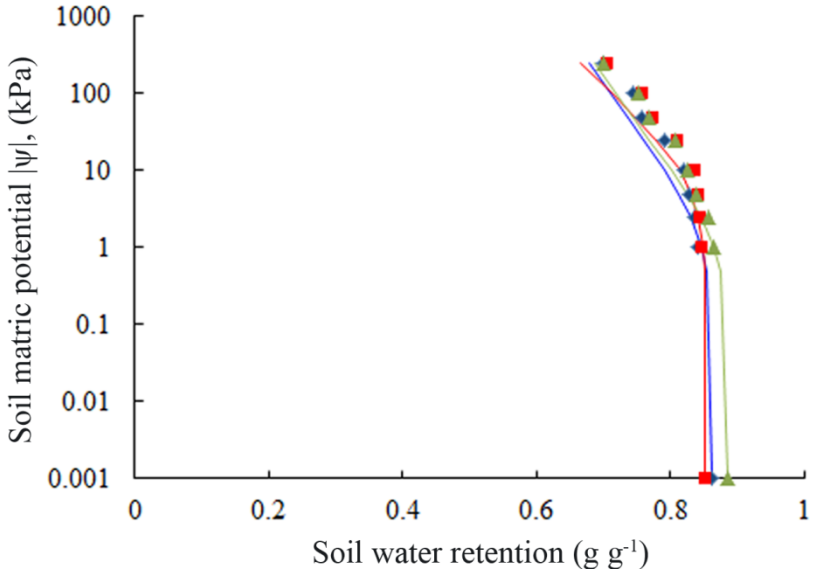

Figure 5.3 The water retention curve of mucilage amended clay soil at different mucilage concentration. Experimental data: □ : 0 % mucilage; ○: 0.5 % mucilage; Δ: 1 % mucilage and solid line: van Genuchten model.

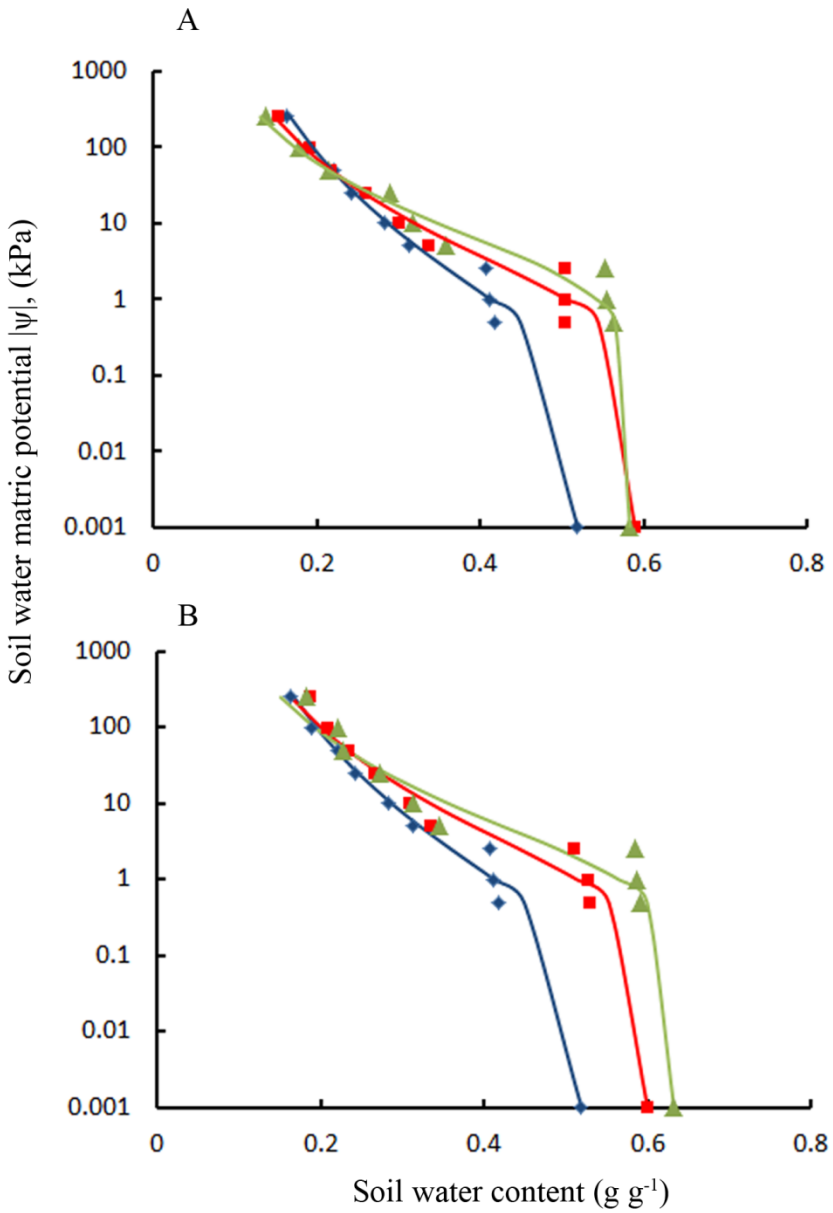

Figure 5.4 The water retention curve of seed amended sandy-loam soil at different seed densities. (A) sandy-loam soil + myxospermous seeds (MS), (B) sandy-loam soil + demucilaged seeds (DS). Where □ = control (0 % seed mucilage); ○ = 5 % [w/w]; Δ = 10 % [w/w]. Solid lines show the data fitted using the van Genuchten model.

Table 5.1 Fitted parameters for van Genuchten model as described in Eq. 5.2 for sandy-loam soil.

Amendment	**SO**	**DM**	**DM**	**MS**	**MS**	**MO**	**MO**
Density %[w/w]	**-**	**5**	**10**	**5**	**10**	**0.5**	**1**
$\alpha(m^{-1})$	31.6	11.4	4.5	12.4	7.4	34.5	16.9
n	1.18	1.25	1.33	1.24	1.29	1.70	1.21
R^2	0.99	0.98	0.98	0.98	0.97	1.00	1.00

5.3.2 Hydraulic conductivity

Figure 5.4 shows the flow rate of water into a test soil-seed mixture (sandy-loam soil with 10 % [w/w] MS), and plotted against the water pressure head. The slope of the straight line given in the graph quantifies the hydraulic conductivity of the test material. The hydraulic conductivity of sandy-loam soil is reduced significantly by the addition of MS and DS (Figure 5.5). The values of hydraulic conductivity are 0.14, 0.03 and 0.01 m d^{-1} for the corresponding concentrations of MS and 0.14, 0.08 and 0.02 m d^{-1} for DS at 0, 5 and 10 %, respectively. There is significantly difference in hydraulic conductivity values between MS and DS treatment ($p<0.05$).

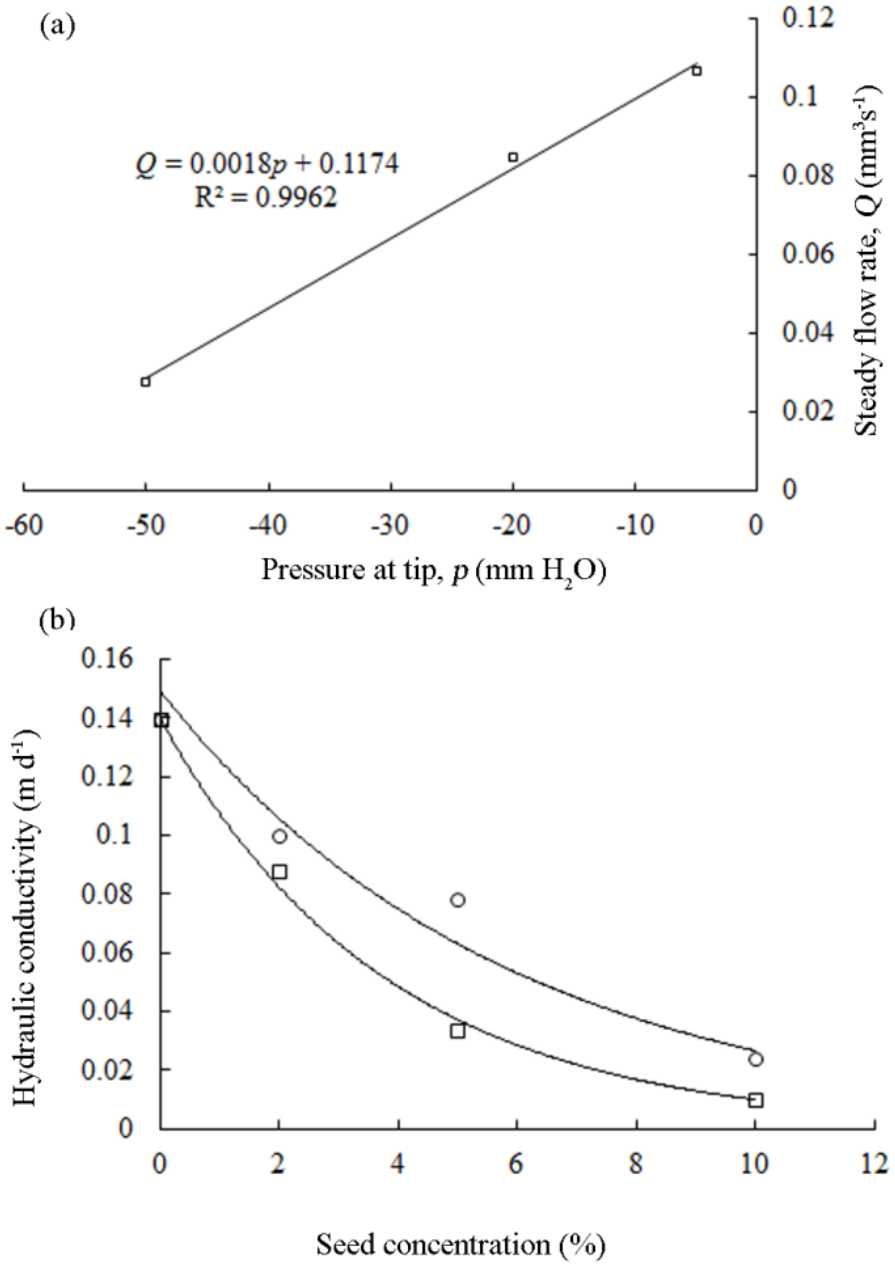

Figure 5.5 (A) The steady flow rate Q plotted against the water pressure head p for an infiltration tip of 4 mm diameter on the surface of a sandy-loam column. (B) The water hydraulic conductivity of sandy-loam soil at different seed concentrations. Experimental data: □ : MS; ○: DS, solid line: curve fitted line.

5.3.3 Rheological properties of clay-type soil and extracted seed-mucilage mixtures

General results from stress sweep tests

Figure 5.6 – Figure 5.9 presented the soil dispersions rheology behaviour with vary mucilage concentrations and water content under dynamic oscillation stress ramping.

The linear viscoelastic region (LVR) is the stress range over which the G' is independent of the applied stress. If the applied stresses are over the LVR, the soil structure will breakdown and the shear modulus decrease. The stability of soil can be indicated by the shear stress at the end of LVR, the storage modulus G' and the loss modulus G''. As shown in the Figure 5.6 – Figure 5.8, the 0.5 % and 1 % [w/w] mucilage had higher G', G'', η and longer linear viscoelastic regions compared to pure clay dispersion. As the water content of soil increased, the soil stability reduced significantly and the addition of mucilage improve soil stability better. The loss factor tan δ , which is the ratio of loss modulus G'' and storage modulus G', was shown in Figure 5.9. At lower shear stress range, it remained constant and there was no significant difference between samples with and without mucilage, especially when soil water content was low. tan δ of mucilage free soil dispersion reached 1 first (flow point), that was the soil dispersion transit to mainly viscous or flow behaviour (Figure 5.9). The difference between samples with and without mucilage increased after the flow point.

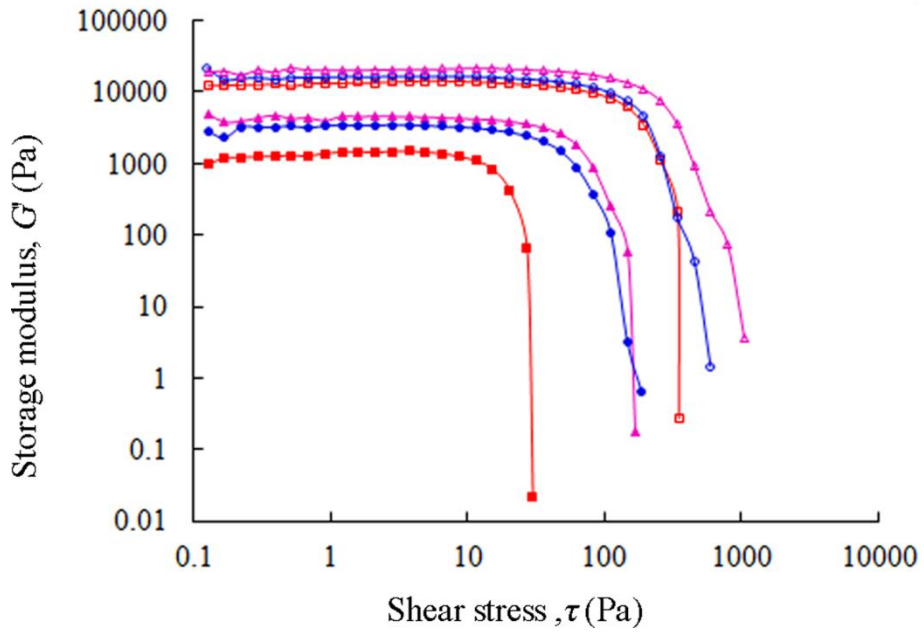

Figure 5.6 Storage modulus (*G'*) of clay soil in stress sweep tests at different mucilage concentrations and different water content. Where: □ = soil-only control (0 % mucilage); ○ = 0.5 % [w/w] mucilage; Δ = 1 % [w/w] mucilage, open marker is for 140 % water content and solid marker is for 200 % water content.

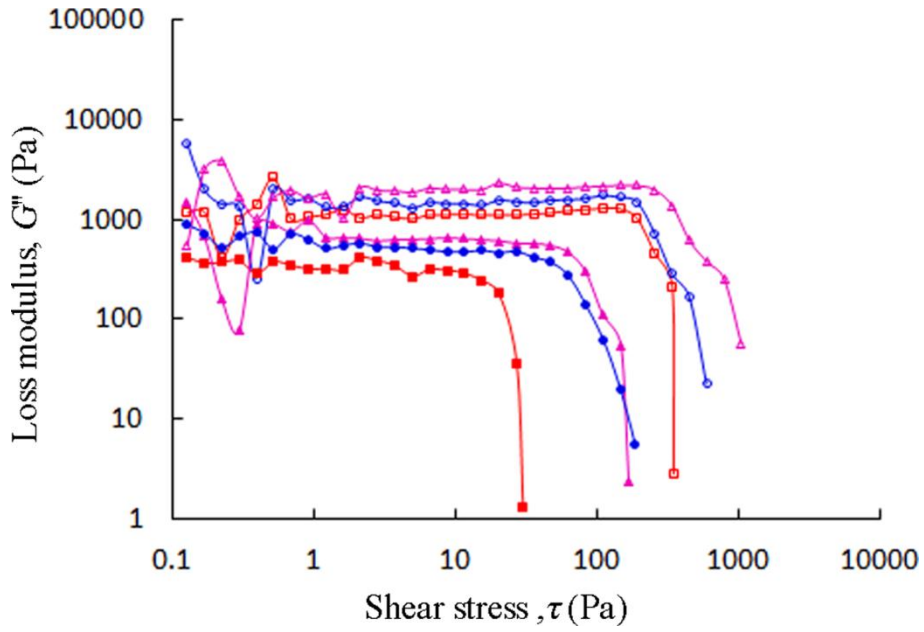

Figure 5.7 Loss modulus (*G''*) of clay soil in stress sweep tests at different mucilage concentrations and different water content. Where: □ = soil-only control (0 % mucilage); ○ = 0.5 % [w/w] mucilage; Δ = 1 % [w/w] mucilage, open marker is for 140 % water content and solid marker is for 200 % water content.

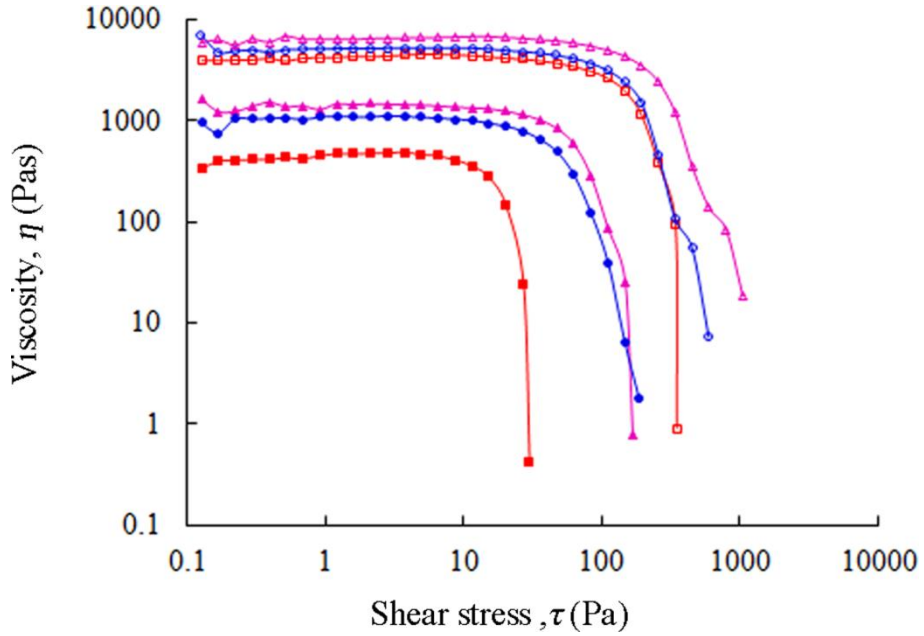

Figure 5.8 Viscosity (η) of clay soil in stress sweep tests at different mucilage concentrations and different water content. Where: □ = soil-only control (0 % mucilage); ○ = 0.5 % [w/w] mucilage; Δ = 1 % [w/w] mucilage, open marker is for 140 % water content and solid marker is for 200 % water content.

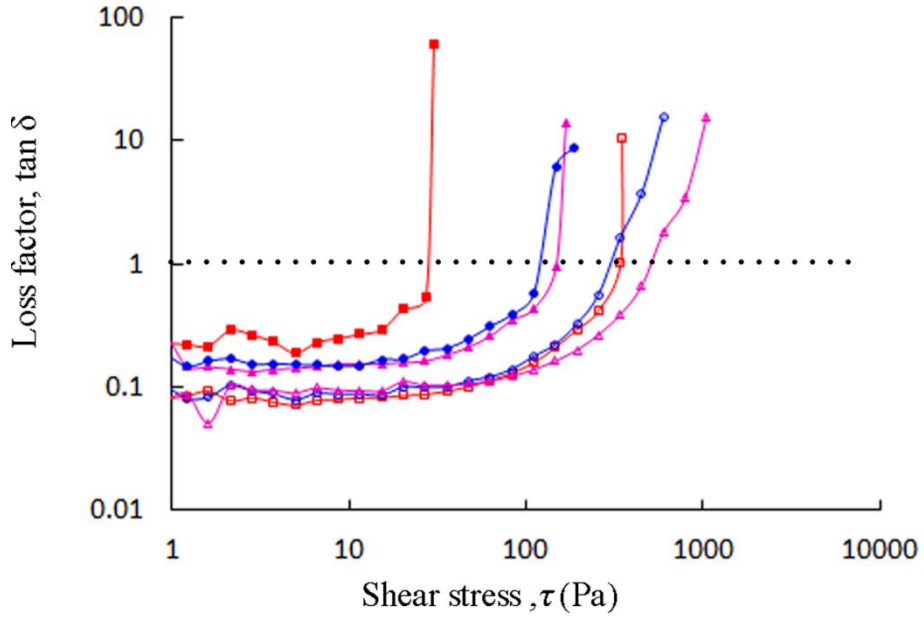

Figure 5.9 Loss factor (tanδ) of clay soil in stress sweep tests at different mucilage concentrations and different water content. Where: □ = soil-only control (0 % mucilage); ○ = 0.5 % [w/w] mucilage; Δ = 1 % [w/w] mucilage, open marker is for 140 % water content and solid marker is for 200 % water content.

Soil storage modulus and viscosity

To compare the rheology parameters of soil-mucilage mixture at different water content, the soil storage modulus and viscosity were derived from the LVR range. The storage

modulus G' was plotted against soil-water content at different mucilage concentrations (Figure 5.10). For all treatments, a decrease in water content was accompanied by an increase in G'. The storage modulus G' decreased from 21404 Pa at 140 % water content to 3182 Pa at 200 % water content with 1 % [w/w] mucilage. However, there is no significant difference between 0.5 % and 1 % [w/w] mucilage ($p > 0.05$).

Soil viscosity was highly affected by water content and mucilage concentration too (Figure 5.11). The trend of soil viscosity is quite similar to that of storage modulus. It decreases as the water content increases. The viscosity of 1% [w/w] mucilage soil dropped from 6843 Pa to 1026 Pa when water content increased from 140 % to 200 %. Both 0.5 % and 1 % [w/w] mucilage increased soil viscosity, especially at higher water content: and in this context the two mucilage concentrations were equally effective.

Soil yield stress and flow point

Figure 5.12 and Figure 5.13 shows the yield stress and flow point stress against water content at different mucilage concentrations respectively. The yield stress is the stress at which the LVR region ends and the soil structure is disturbed. While the flow point stress is the stress when tan $\delta = 1$ which indicates the soil transits from mainly elastic to mainly viscos behavior and begins to flow. The figure showed that the soil had higher stability with higher mucilage concentration and therefore can resist higher external forces. However, the yield stress of 0.5 % [w/w] is close to that of 1 % [w/w] mucilage at higher water content especially over 180 %.

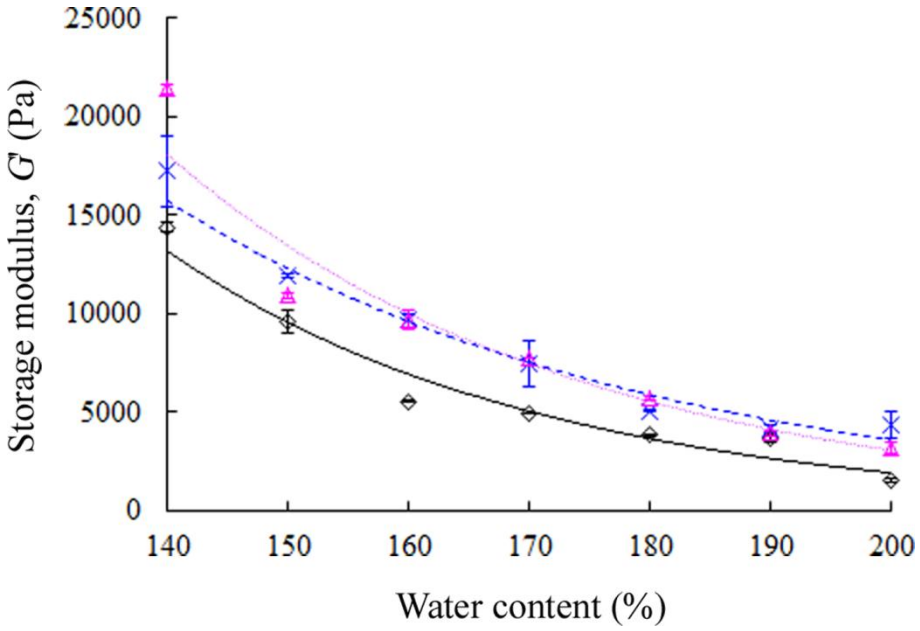

Figure 5.10 Storage modulus (*G'*) of clay soil as function of water content at different mucilage concentrations. Where: □ = soil-only control (0 % mucilage); ○ = 0.5 % [w/w] mucilage; Δ = 1 % [w/w] mucilage. Data fits using a power law curve are shown with lines: solid = control (no mucilage); dashed, 0.5 % [w/w], and; dotted 1 %, [w/w].

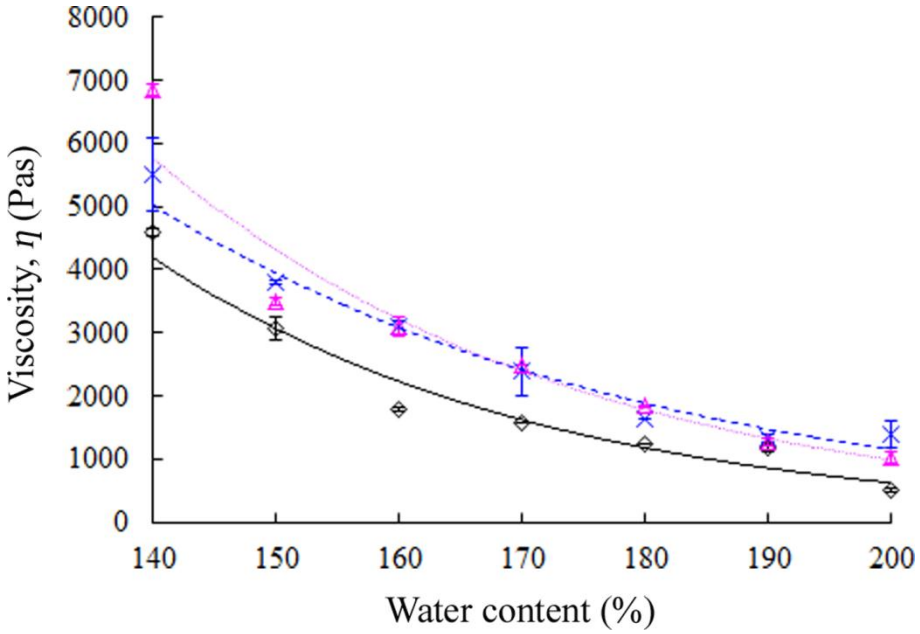

Figure 5.11 Viscosity (η) of clay soil as function of water content at different mucilage concentrations. Where: □ = soil-only control (0 % mucilage); ○ = 0.5 % [w/w] mucilage; Δ = 1 % [w/w] mucilage. Data fits using a power law curve are shown with lines: solid = control (no mucilage); dashed, 0.5 % [w/w], and; dotted 1 %, [w/w].

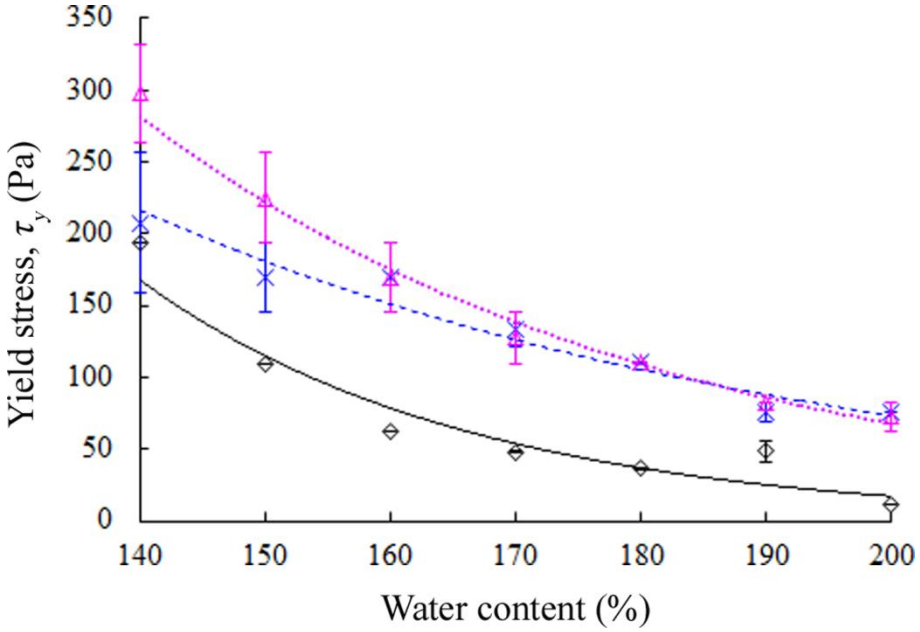

Figure 5.12 Yield stress (τ_y) of clay soil as function of water content at different mucilage concentrations. Where: □ = soil-only control (0 % mucilage); ○ = 0.5 % [w/w] mucilage; Δ = 1 % [w/w] mucilage. Data fits using a power law curve are shown with lines: solid = control (no mucilage); dashed, 0.5 % [w/w], and; dotted 1 %, [w/w].

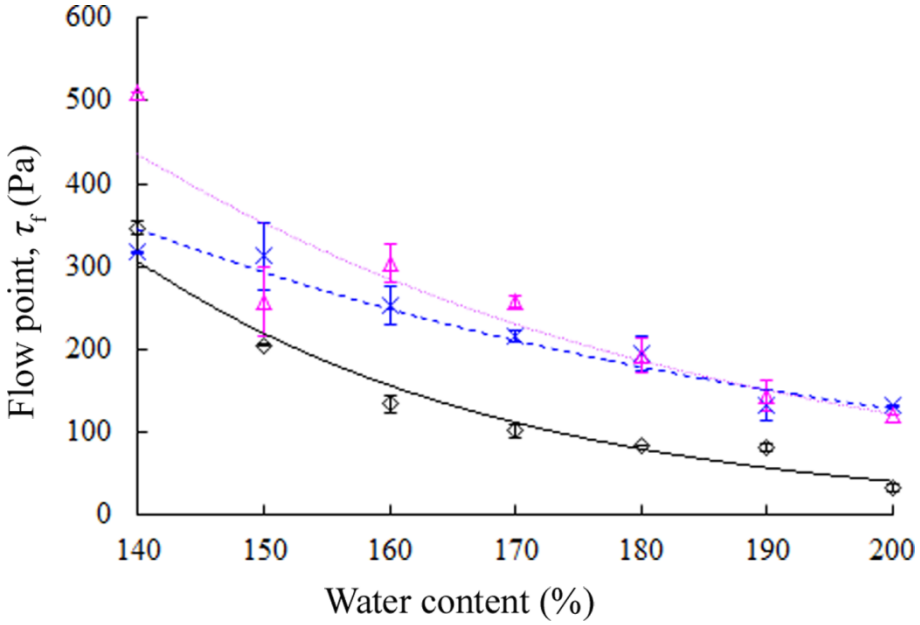

Figure 5.13 Flow point (τ_f) of clay soil as function of water content at different mucilage concentrations. Where: □ = soil-only control (0 % mucilage); ○ = 0.5 % [w/w] mucilage; Δ = 1 % [w/w] mucilage. Data fits using a power law curve are shown with lines: solid = control (no mucilage); dashed, 0.5 % [w/w], and; dotted 1 %, [w/w].

Soil loss factor

The loss factor tan δ is less than 1 for all the samples at all the water content (Figure 5.14). Soil with more mucilage shows higher tan δ values with more water, which is the viscose behaviour is dominant over the elastic behaviour and therefore, the soil is less stable.

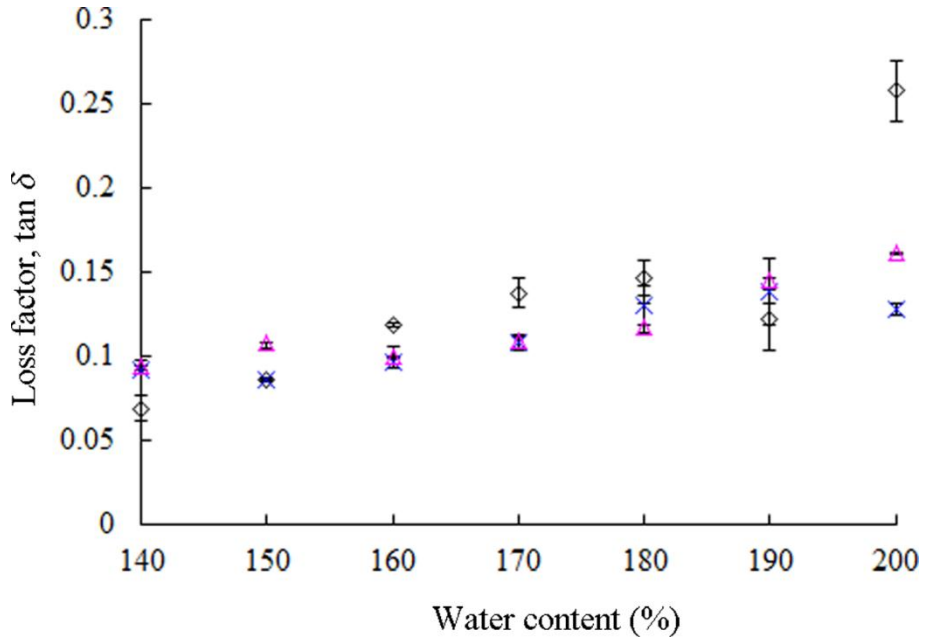

Figure 5.14 Loss factor of clay soil as function of water content at different mucilage concentrations. Where: □ = soil-only control (0 % mucilage); ○ = 0.5 % [w/w] mucilage; Δ = 1 % [w/w] mucilage.

5.3.4 Rheological properties of sandy-loam soil and extracted seed-mucilage mixtures

Similar analysis was carried out on sady loam soil. Figure 5.15 – Figure 5.18 showed the sandy soil rheology behaviour under shear stress sweeping tests. Most of the trend found in sandy-loam was similar to that in clay soil. Only the different phenominon was reported here. It is noted that unlike the behaviour of clay type soil, the storage modulus *G'* of sandy-loam first dropped after the LVR region (p_1) and then became constant for a while before further decreasing. This second constant area was defined as p_2 here and it last longer as the mucilage concentration increased.

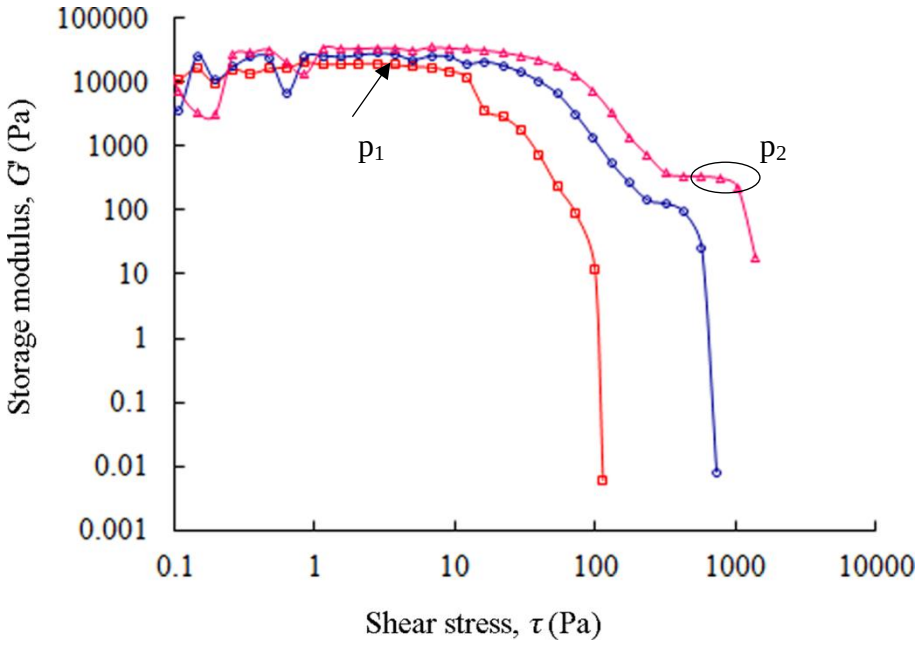

Figure 5.15 Storage modulus (*G'*) of sandy-loam soil in stress sweep tests at different mucilage concentrations at 55 % water content. p_1 is the first LVR region and p_2 is the second LVR region. Where: □ = soil-only control (0 % mucilage); ○ = 0.5 % [w/w] mucilage; Δ = 1 % [w/w] mucilage.

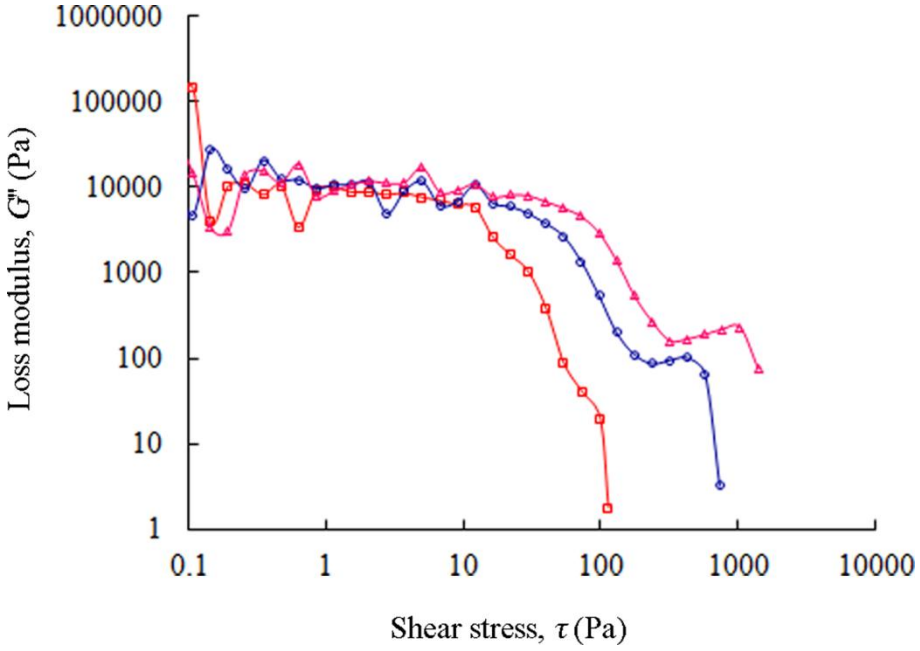

Figure 5.16 Loss modulus (*G''*) of sandy-loam soil in stress sweep tests at different mucilage concentrations at 55 % water content. Where: □ = soil-only control (0 % mucilage); ○ = 0.5 % [w/w] mucilage; Δ = 1 % [w/w] mucilage.

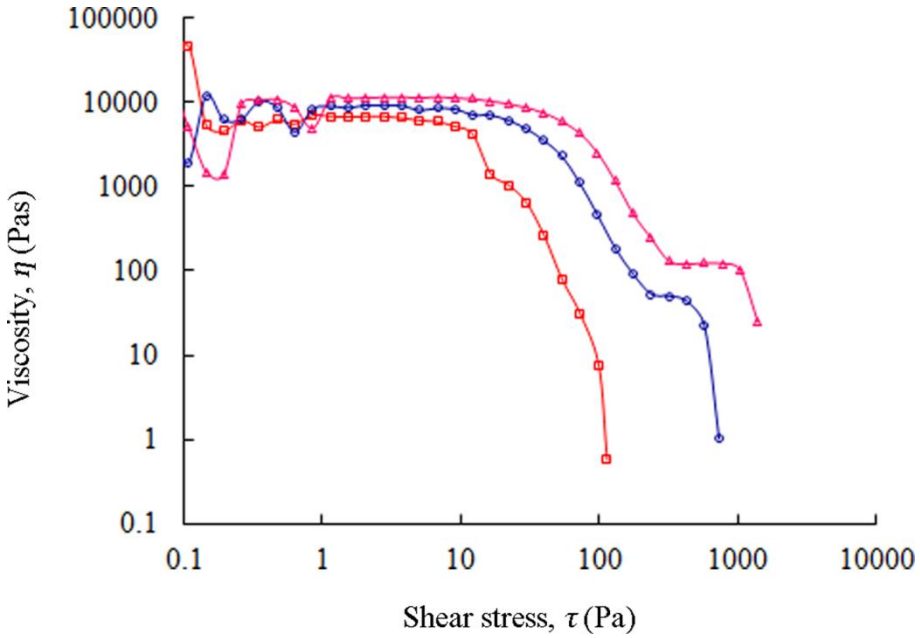

Figure 5.17 Viscosity (η) of sandy-loam soil in stress sweep tests at different mucilage concentrations at 55 % water content. Where: □ = soil-only control (0 % mucilage); ○ = 0.5 % [w/w] mucilage; Δ = 1 % [w/w] mucilage.

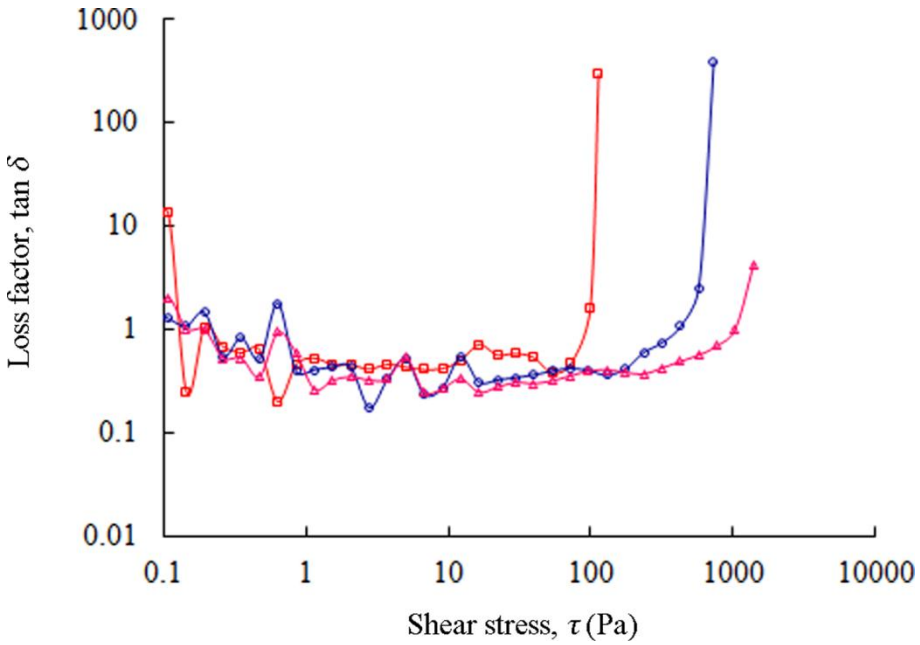

Figure 5.18 Loss factor (tanδ) of sandy-loam soil in stress sweep tests at different mucilage concentrations at 55 % water content. Where: □ = soil-only control (0 % mucilage); ○ = 0.5 % [w/w] mucilage; Δ = 1 % [w/w] mucilage.

In Figure 5.19 – Figure 5.22, the sandy-loam soil rheology parameters were ploted against the mucilage concentration at diffent water content. The sandy-loam stability was improved by the addtion of seed mucilage. The effect was more significant in 55 %

than in 70 % water content. The increase in yield stress and flow point stress was more significant than in shear modulus and viscosity.

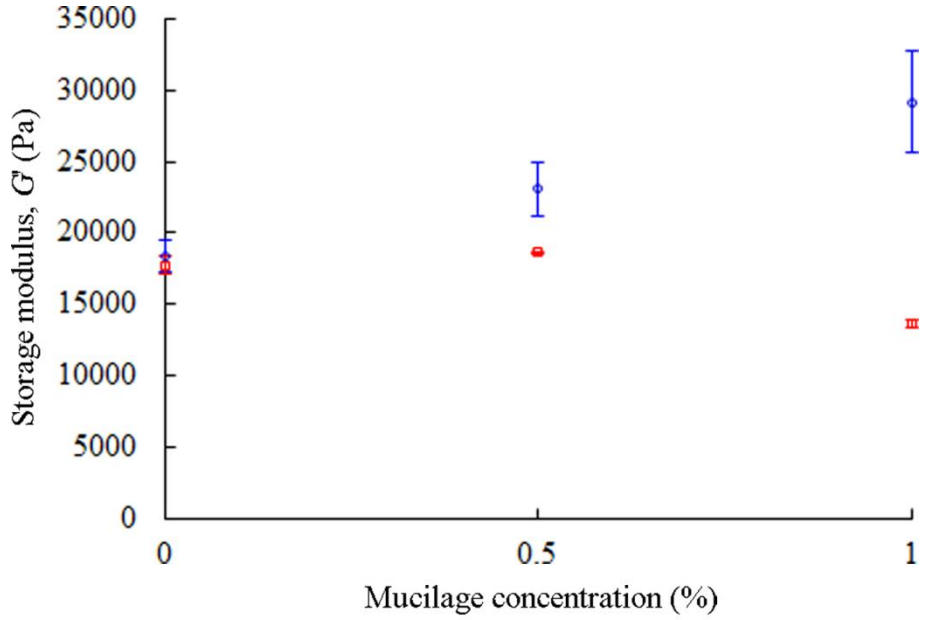

Figure 5.19 Storage modulus (G') of sandy-loam soil as function of mucilage concentrations at different water content. Where: □ = 70 % water content; ○ = 55 % water content.

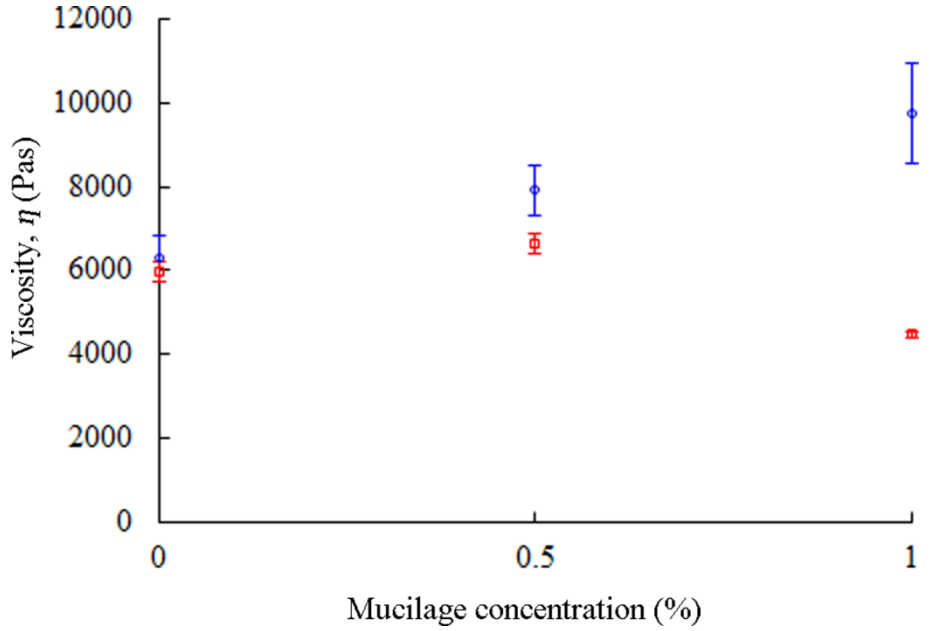

Figure 5.20 Viscosity (η) of sandy-loam soil as function of mucilage concentrations at different water content. Where: □ = 70 % water content; ○ = 55 % water content.

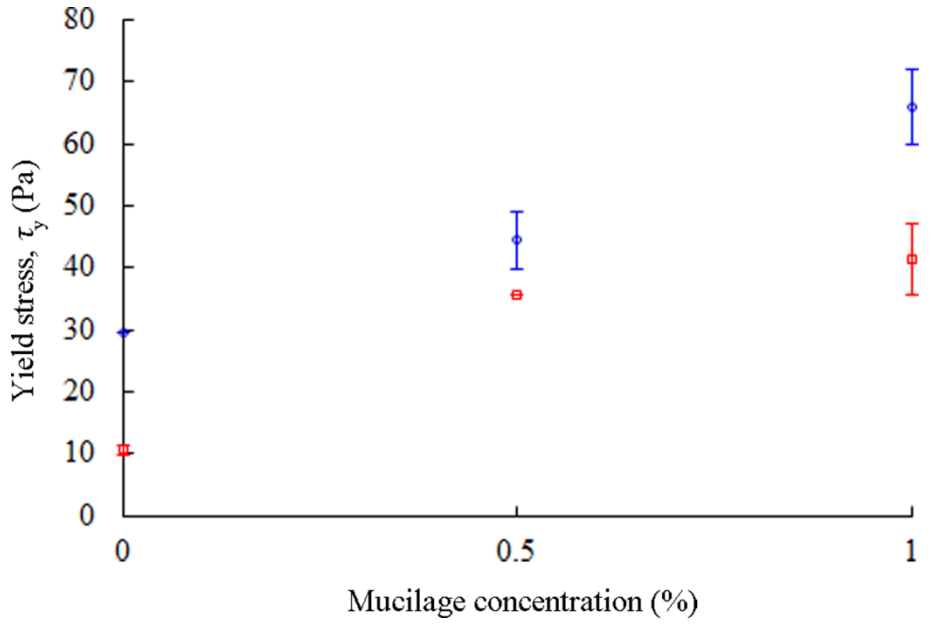

Figure 5.21 Yield stress (τ_y) of sandy-loam soil as function of mucilage concentrations at different water content. Where: □ = 70 % water content; ○ = 55 % water content.

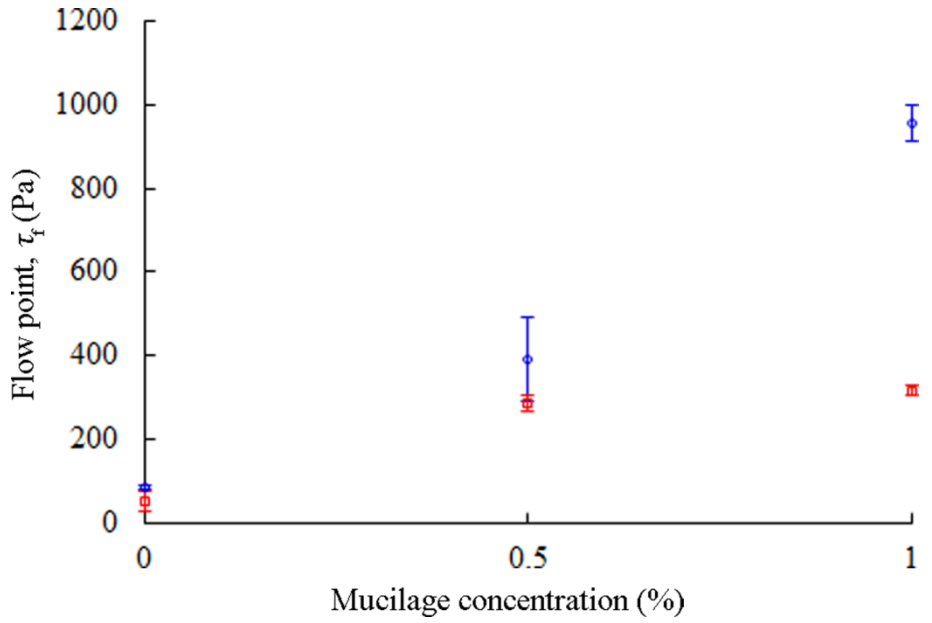

Figure 5.22 Flow point (τ_f) of sandy-loam soil as function of mucilage concentrations at different water content. Where: □ = 70 % water content; ○ = 55 % water content.

5.4 Discussion

5.4.1 Water retention

Soil water retention is a most important soil property that affects plant growth and showed that MO, MS, DS can all improve the soil water retention. However the ability of the improvement are in the order: MS > DS > MO. This indicates that even the seeds only (without mucilage) can alter the soil physical properties. It may due to that the seeds can change the pore structures in the soil and thus hold more water under matric potentials and seed themselves can absorb water. The mucilage may have least effect because its swelling capacity could be reduced when confined within soil matrix, and therefore has less impact on soil pore structure. This possibility is raised from reports that some acrylamide or acrylic acid based commercial superabsorbent hydrogels (Alcosorb, Stockosorb 500 Medium, Stockosorb 500 Micro, and Stockosorb HCMG) when hydrated *ex situ* retain water in the range 200 – 500 kg kg^{-1} (d wt). However, in sand their effectiveness was reduced to 40 – 140 kg kg^{-1} (Bhardwaj *et al.*, 2007). Also, it is also possible that the mucilage may be degraded during the water retention tests which take about 1 – 2 months. The finding also suggests that within certain limits, the bigger the seeds and the more the seeds, the more water retained by soil.

5.4.2 Hydraulic conductivity

If compare the values of hydraulic conductivity to the permeability classes for agriculture and conservation proposed by (O'Neal, 1952), it was found that the addition of 5 % seeds to sandy-loam soils change the permeability from moderately slow (0.12 – 0.48 m d^{-1})to slow (0.03 – 0.12 m d^{-1}). The addition of 10 % converted the permeability from moderately slow to very slow (less than 0.03 m d^{-1}).

The reduction in hydraulic conductivity of sandy-loam soil by myxospermous seed amendment is likely to be a consequence of two main effects: (1) the swelling of mucilage changes the pore size and pore distribution in the soil; (2) the kinetics of water diffusion into the mucilage regulates water molecules absorption by, and through, it because the water is tightly confined in a very viscose gel. Consequently, the steady flow rate under infiltration is reduced as the soil pore spaces have been restricted and/or blocked, as well as being retained, by the seed mucilage. Various studies have shown that soil hydraulic conductivity can be reduced by clogging pores caused by microorganisms ('bioclogging'; Thullner *et al.*, 2004; Engesgaard *et al.*, 2006; Boult *et al.*, 2008; Mostafa, 2009). Myxospermous seed mucilage may therefore operate in the similar way. However, compared with other biopolymers which have been studied to have a plugging effect in soil and found that the mucilage have a rather efficient reduction in hydraulic conductivity. Khachatoorian *et al.*(2003) carried out a serious of experimental work to identify the plugging effect of each biopolymer and their results showed that 1 g L^{-1} of PHB had the most efficient effect on reducing soil permeability, which reducing the permeability by a billion-fold which the chitosan and PGA reduced by a million-fold while only 30 for guar gum and 8 for xanthan. The effects of plugging depend on the structure of biopolymers. However, the high reduction caused by PHB and PGA may also because of the growth of bacteria which was not considered by the author.

5.4.3 Mucilage and water content on rheology

The soil stability under shear stresses is determined by the soil particle connections. In clay soil, the particle bond will break and rebuild under stresses (Chen, 1990). During the shear stress testing, the clay platelet will rearrange the structure from randomly organised scaffolding to parallel orientated particles (Holthusen *et al.*, 2010). At lower

stresses, the clay platelet can recover from the rearrangement. However, at higher stresses, it is difficult to recover from the change and also the number of particle bonds reduced. It is reported that the yield stress and shear stress resistance is related to the connection between the soil particles (Torrance, 1999). Therefore, at shear stress resistance of soil is reduced. But in sandy type soil, the connection between soil particles is weaker than that of clay. The sandy soil resists stresses by particle interface friction, especially when soil is of low water content. With increasing seed mucilage in soil, the rheology parameters were increased. As stated above, the mucilage can enhance the connection between soil particles and may improve sandy soil to behave like clay soil. This can be proved by the fact that mucilage is a high viscose and sticky material and it can prevent seeds from being washed off by rain (Grubert, 1974; van Rheede van Oudtshoorn and Van Rooyen, 1999; Caesar-Tonthat, 2002).

In sandy-loam soil, the mucilage has contributed to a second elastic range of storage modulus G' at increasing shear stress. It is suggested that at low shear stresses, soils containing larger particles (silt, sand) only breakdown the bonds between small particles (Ghezzehei and Or, 2001). At larger shear forces, the larger particles are reoriented and take into effect to resist the force and result in a second elastic range. The present study shows that the second maximum is more pronounced for the samples with more mucilage (Figure 5.15). Without the mucilage, the rebuild bond between the larger particles is weak and is easily broken under stresses. Compare with the effect of mucilage role on clay rheology, it has more profound role in sandy-loam. Among all the rheology parameters, the seed mucilage increased the yield stress of soil significantly and it only caused moderate or low increases to soil storage modulus and viscosity. This indicated that soil with mucilage can under through more deformation before the soil particles linkage breakdown and the structure destroyed and is not brittle. It should be also noted that in this experiment, only the extracted mucilage were applied in the soil,

which represents the outer pectinaceous layer of seed mucilage (Deng *et al.*, 2012). The inner layer mucilage which contains cellulose and pectin may provide more significant role in soil rheology if the whole myxospermous seeds are applied.

It was explained that the increased water content decreased soil rheology with the most change at low water content. The decreasing trend is in agreement with Ghezzehei and Or (2001) and Karmakar and Kushwaha (2007). The reason for this phenomenon is that water molecules may flow freely between soil particles and thus reduce the friction between solid-solid particles (Karmakar and Kushwaha, 2007). The presence of myxospermous seed mucilage in soil will result in the soil pore size redistribution. It also has a high water holding capacity, imbibe relatively large volume of free water and increase the friction between the soil particles. However, the impact of mucilage concentration in soil is not large beyond 0.5 % [w/w] at high water contents. The impact of mucilage was therefore greater for the drier soils. The most significant role of mucilage is to increase soil yield stress at lower water contents.

The mucilage concentrations and seed densities used to discern these *in vitro* observations should be appraised relative to those levels which may be found *in field*. Therefore, if we consider only the average yield of a single shepherd's purse plant (and for only a single reproductive cycle/season), which is reported as *ca*. 90,000 seeds per plant (to a maximum of *ca.* 500,000 seeds plant^{-1}:Hurka and Haase, 1982; Iannetta *et al.*, 2010; respectively). Therefore, also assuming these (90,000), seeds are dispersed within a 0.5 m diameter area (r = 0.25m), around the mother plant, and are scattered throughout the typical plough depth of an arable field (d = 0.2 m): the volume containing these seeds may be calculated using the formula for a cylinder (π r^2 d) and the weight of sandy loam soil (at a density of 1400 kg m^{-3}). Thus, and taking account of the average single seed weight for shepherd's purse (0.12 mg), the total seed and soil weights may

be estimated to show a soil seed bank density of *ca.* 0.03 %. Furthermore, considering that weight of mucilage which is easily dispersed in water and lost to the soil (*ca*. 4% of the dry seed weight; Deng *et al*., 2012), and using the measures defined the mucilage concentrations is 0.001 % [w/w]. Thus, given that many shepherd's purse plants may be found where they occur, and co-existing with other wild plant species, the seedbank seed densities and seed mucilage concentrations tested here may just a little higher than the levels found naturally. What is more, the experiment established the levels required to make a difference as a soil amendment. Therefore, the test seed densities and mucilage amount were acceptable for applying as soil amendment. Further studies should perhaps focus on the optimal concentration of seeds/mucilage in soil to engineer and control soil water conductivity, soil stability and ultimately plant growth: especially where these are applied as novel amendments to eroded soils and/or of poor agronomic potential.

To summarise: individually, the roles of the MO and seed (MS and/or DS) upon soil physical properties and soil-water relations are complex. However, it is clear that the seed and mucilage-only components have a synergistic effect, and their relative role in soil-water content, -flow and -stability may have a greater, or reduced affect, depending on the amount of available water, and in all likelihood soil type too. Myxospermous seed mucilage can increase the water retention, reduce the hydraulic conductivity of soil, and increase the rheology. In addition the wild plant seeds, whether myxospermous or not, can affect the physical structure of soils and highlight that the simple presence of seed in a soil seedbank will influence the nature soils to deliver certain ecosystem services.

Further studies should focus on modelling seed-soil interactions to identify the optimal concentration of seeds (and seed-mucilage), for various soil types. In this way it may be

possible to engineer novel soil amendments and control soil water conductivity, soil stability and should be ultimately tested upon their ability to improve of sustain plant, and especially crop plant, growth. This focus would be especially pertinent should they be effective in soils limited agronomic potential.

5.5 Summary

Three different experiments were carried out to test the effect of myxospermous and non-myxospermous seeds and the extracted myxospermous seed mucilage on the physical properties of soil. Although the seed densities and mucilage concentrations used are higher than that found in nature, it was discerned that shepherd's purse seeds, whether myxospermous or not, increase soil water retention and rheology, and reduce soil hydraulic conductivity.

1. The additions of 0.5 % and 1 % MO to sandy-loam soil increased the saturated water retention by about 6 % and 10 % respectively. There is no significant difference between 0.5 % and 1 % MO in increasing the shear modulus and viscosity of clay soil, though they increased the rheology compared to control sample.

2. The additions of 5 % and 10 % MS seeds to sandy-loam soil increased the saturated water retention by about 15 % and 21 %. They reduced the hydraulic conductivity of sandy-loam soil by about 76 % and 93% respectively.

3. The additions of 5 % and 10 % DS seeds to sandy-loam soil increased the saturated water retention by about 12 % and 14 %. They reduced the hydraulic conductivity of sandy-loam soil by about 44 % and 83% respectively.

4. The mucilage has more effect on sandy-loam soil than clay soil rheology, with the most significant effect on yield stress. The mucilage increases rheology much more when soil water content is low. At higher water content, there is no significant

difference between 0.5 % and 1 % [w/w] mucilage. For sandy soil, the addition of mucilage contributes to a second elastic range during the stress sweep test.

In all, this study would suggest that 5 % MS addition to sandy-loam soil is the best, as it retained adequate water, slowed the water percolation losses rate and maintained the stability. The findings of this chapter will help understanding the ecological significant of myxospermy on soil physical properties when soil is wet.

Chapter 6 **Numerical modelling of water flow through soil amended with the myxospermous seeds of shepherd's purse**

6.1 Introduction

From the research findings described in previous chapters it was found that myxospermous seeds presented both water dispersible and immobile (seed anchored), mucilage (Deng *et al.*, 2012). These components act in concert to increase soil water retention and stability and reduce water hydraulic conductivity. *In situ*, the seed derived mucilage may reduce or completely block water-flow through porous media due to its swelling capacity. This functional characteristic of the mucilage (or gel) in porous media has (bio-)technological application in numerous engineering areas due to the plugging effect. For example, synthetic gels are widely used in oil and gas wells to block water flow, and enhance the oil recovery rate (Zitha *et al.*, 2002; Khachatoorian and Yen, 2005). Regarding the ability of localised gel deposition to regulate fluid flow: numerous experimental observations have noted that polymers or gels applied near the liquid-inlet to porous media, may reduce the infiltration rate of fluids significantly (*e.g.*). For example, the soil permeability of sandpacks reduced 35 – 60 %, as a result of the xanthan gum and Cr(III) gel (Eggert Jr. *et al.*, 1992): this reduction was due to the swelling properties of the gel, and syneresis, due to pH variations. Meanwhile biopolymers include xanthan, polyhydroxybutyrate (PHB), guar gum, polyglutamic acid (PGA) and chitosan were also investigated to decrease soil permeability. Khachatoorian *et al.*(2003) carried out a serious of experimental work to identify the plugging effect of each biopolymer and their results showed that 1 g L^{-1} of PHB had the most efficient effect on reducing soil permeability, which reducing the permeability by a billion-fold while the chitosan and PGA reduced by a million-fold while only 30 for guar gum and 8 for xanthan. The effects of plugging depend on the structure of biopolymers. However,

the high reduction caused by PHB and PGA may also because of the growth of bacteria which was not considered by the author. Gels can also help preserve water as an amendment in soils within arid regions across the globe, protecting the soil from loss or erosion due to wind, rain or ground water leaching. However, such tests have not yet extended to examine the role of such gels (or mucilages), as when bound to the surface of small solid particles: as exemplified by the myxospermous seeds of wild plants. In this regard, the observations and data gathered in the preceding chapters for the myxospermous seeds of shepherd's purse, may be applied in a theoretical approach as a first step towards increasing our understanding of how specific factors may inter-relate to regulate water flow and infiltration. Such factors, or variables, include: where the myxospermous seeds are localised in the soil, that is whether higher or lower in the soil profile, also; their quantity, that is the density of seeds in the seedbank, or; the height of the soil-seed bank layer. Such insight would empower ecological engineering approaches that aim to use myxospermous seeds, or synthetic mimics, to regulate water use, and perhaps plant water use efficiency in nature.

In order to simulate the flow in gel amended soil, there are a lot of studies carried out. These numerical models usually based on the flow and transport equations. For some cases, the reaction model is required to simulate the polymer reaction or gelatin process in porous media when the polymer mixture is injected with cross-linking agent. Khachatoorian and Yen (2005) proposed a numerical modes to simulate the *in situ* gelation of three cases: polyacrylamide/redox, canthan/Cr(III) and xanthan/borax. For these gels applied in porous media, the gels will react and cross-link with other polymers through the gelatin process. As the gelling process going on, the gel viscosity increases and the gel aggregates will grow in size and therefore the permeability and flow rate in porous media are reduced. Zitha *et al.* (2002) also modelled the reduction of fluid flow in porous media using polymer gel (co-polymer of acrylamide and *t*-butyl-

acrylate cross-linked using poly-ethylene-imine). In their model, they considered the deformation of gels and porous media, the microscopic flow and gel displacement. The gel was considered as immobile when the stress was lower than a critical value or yield stress. The flow model can be generally modelled by the following approaches: the continuum models, the bundle capillary models, pore-scale network model. However, it is much simpler to apply myxospermous seeds and/or seed-mucilage to soil compared with the synthetic polymers. For instance, the mucilage of myxospermous seeds hydrates and swells rapidly, while the synthetic polymers require a longer time-period which can extend to hours or days. Therefore, if myxospermous seed mucilage (only) was applied to a porous media, the time taken for the mucilage swelling may be ignored, as swelling is assumed to be complete very soon after application in fluid containing soil. Furthermore, if the whole myxospermous seeds are applied *in situ*, the whole effect is more complex, as the inner layer of mucilage is bound to seeds, and the outer layer will disperse in the aqueous carrier (Deng *et al.*, 2012). Mucilage swelling capacity and high viscosity will also have an important influence on the hydraulic properties of the soil.

Therefore, in this chapter an initial mathematical model is developed which is able to simulate the effects of myxospermous seed amendments upon soil water infiltration. Towards that end, we have shown that (myxospermous), seeds should be considered soil hydraulic conductivity reducers (from the experimental data presented in Chapter 5). Also, assumptions are accepted, include: (1) that the myxospermous seeds (at least), may be considered as immobile in the soil, and; (2) that Darcy's law may be used to simulate the flow in porous medium as the fundamental principle.

In this way, parametric studies were carried out to assess specific factors (or variables), affected water-flow. These factors are: myxospermous seed bank density (the weight of

seeds as a percentage of the soil weight, C_s); seed-amended soil-layer thickness (h_s), and; the distance of the seed-soil layer from the soil surface (d_s). The soil-water parameters estimated in the model simulations were soil water velocity and pressure.

6.2 Numerical model

There is no need to further consider the transport equation and the role of seeds on soil relative permeability as this was reflected by the experimental data. Therefore the water flow in porous media can be simulated by Darcy's law combined with continuity equations. The mass conservation in a porous media is governed by the mass balance equation:

$$\frac{\partial p}{\partial t} = \nabla \cdot \left[K \left(\nabla p + \rho g \nabla D_s \right) \right] \tag{6.1}$$

where ρ is the density of mucilage mixture, D_s is the coordinate and t is time. The Darcy velocity is given by:

$$\mathbf{u} = -K \left(\nabla p + \rho g \nabla D_s \right) \tag{6.2}$$

where K is the hydraulic conductivity, μ is the mucilage mixture viscosity, p is the pressure of mucilage mixture, g is gravitational acceleration.

The hydraulic conductivity is a function of the seeds density and is given as:

$$K = 0.14e^{-0.26C} \text{ for myxospermous seeds (MS)} \tag{6.3}$$

$$K = 0.16e^{-0.18C} \text{ for demucilaged seeds (DS)} \tag{6.4}$$

6.3 Numerical model establishment

6.3.1 Initial and boundary conditions

Figure 6.1 presents a schematic diagram of the conceptual model which is developed for the model establishment from the soil column used in the experimental work in Chapter 5. The soil column dimensions are 4 cm diameter and 3 cm deep. The water flow equations above are solved using Comsol Multiphysics 3.5 in 2D symmetry models. The domain contains 6208 triangle meshes and solved using UMFPACK methods. For the simulations, a continuous water head of -5 cm is applied to the soil column. For the flow model, the boundary and initial conditions are given as follows:

$$z = 0, \;\; p = -5 \; cm \; \mathrm{H_2O} \tag{6.5}$$

$$z = -H, \; p = 0 \tag{6.6}$$

$$r = 0, \; \text{symmetry} \tag{6.7}$$

$$r = R, \; \text{u=0} \tag{6.8}$$

$$t = 0, \; p = p_0 \tag{6.9}$$

The reference points at which data was recorded were denoted r_1 (0.5 cm below the soil surface) and r_2 (1 cm below the soil surface) (Figure 6.1). The effect of soil seedbank density was not discussed in relation to r_2.

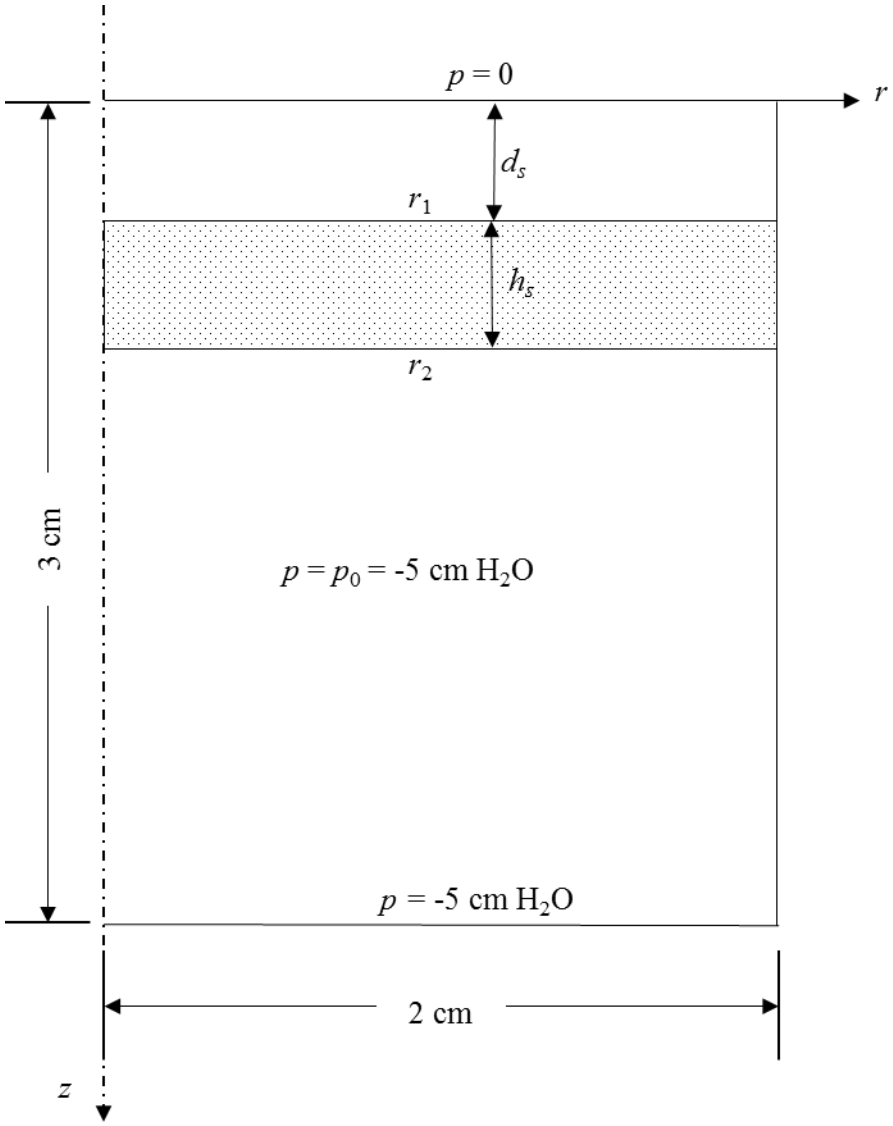

Figure 6.1 A schematic diagram which indicates the boundary and initial conditions for simulations of water infiltration through a two dimensional symmetry soil core of radius 2 cm and height 3 cm. The right-hand vertical line identifies the edge of an adjacent impermeable layer. h_s, denotes seed-soil layer depth (dotted/infilled area); d_s, denotes seed-soil layer distance from soil surface. The reference points at which data is recorded are denoted r_1 and r_2.

6.3.2 Validation of model

This numerical model is validated by the experimental data carried out in Chapter 5. The average water flow velocity $\bar{U}$ in soil was recorded. In the numerical models, the water flow velocity at average was given in the following equation:

$$\bar{U} = \frac{\int U d\Omega}{\int d\Omega} \tag{6.10}$$

where Ω is the area of the computational domain, U is the velocity of fluid. The comparison was made between 0, 5, 10 % [w/w] myxospermous and demucilaged seeds amendments.

6.3.3 Parametric studies

A series of parametric studies were therefore carried out to find the relative influence of the (myxospermous) seed related factors, to influence water flow rates in a soil seedbank. These are: seeds density and the position where the seeds are applied in the soil column. During the simulation, the amended seed-soil layer thickness (h_s), ranges from 0 – 1.5 cm (Figure 6.1: this is with the exception of the 'uniform distribution model' where the seeds are distributed evenly throughout the soil column). The distance from the amended layer to the surface of soil (d_s), also varies (from 0 – 1.5 cm), and the seed density (C_s), spans from 0 – 10 % [w/w]. The parameters for each case are listed in Table 6.1. This was carried out in the hope that the modelling may provide insight which indicates that (myxospermous) seeds may be effective as a novel soil amendment to improve soil qualities that enhance water retention, and perhaps even plant growth. When investigating one parameter, the others are fixed. All the simulations were carried out for moth DS- (demucilaged seed) and MS- (myxospermous seed) amended soil.

Table 6.1 Summary of parameter values and the range over which they were tested for the conceptual model described in the 2D schematic (Figure 6.1).

Case studies	Parameters and their range		
	Soil seedbank density, C_s (% [w/w])	Seed-soil layer height, h_s (cm)	Seed-soil layer depth, d_s (cm)
Group 1	0, 2, 4, 6, 8, 10	3	0.5
Group 2	4	0.5, 1, 1.5	0.5
Group 3	4	0.5	0, 0.5, 1, 1.5

6.4 Results

6.4.1 Validation of model

The numerical model was validated by the experimental data in terms of average water velocity (Figure 6.2). It showed that the experimental data was well fitted by the numerical data, especially for the myxospermous seeds amended soil. Although there was no experimental data for the velocity at each point, the Darcy's model was reasonable to simulate the water flow in seeds amended soil.

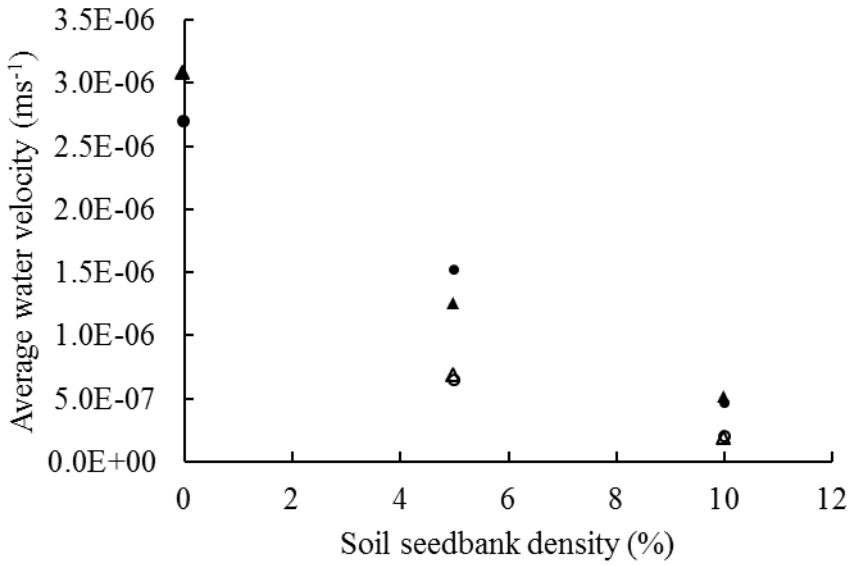

Figure 6.2 The average water velocity of experimental data and numerical data. Solid circle: demucilaged seeds experimental data, solid triangle: demucilaged seeds numerical data, open circle: myxospermous seeds experimental data, open triangle: myxospermous seeds numerical data.

6.4.2 The effect of soil seedbank density

Soil water pressure head and velocity at r_1 (0.5 cm below the soil surface) decreased in response to increasing DS and MS densities (Figure 6.3 – Figure 6.4). With the addition of seeds, the pressure head changed slower than the non-amended soil before they reached the final state. The MS amendments had greater effects on pressure head change than the DS amendments. For example, pressure head of 10 % [w/w] MS amendment did not reached the final state until 4000 s, while 10 % [w/w] DS almost reached the final state. The similar trend was found for soil velocity. In general, and at the same seedbank densities, the MS amendment reduced soil water velocity more significantly than the DS amendment. There was more reduction in soil water velocity for soil seedbank densities amendments at the 2 or 4% [w/w] inclusion rates; that is, water velocity reduction showed a decline from soil seedbank densities of 6 % [w/w] or greater (Figure 6.4A). For DS seeds amendments, the water velocity dropped 0.5 $\times 10^{-6}$ m s^{-1} when the seedbank density increased from 6 – 10 % [w/w], but it reduced 1.5 $\times 10^{-}$

^{6} m s^{-1} when the seedbank density increased to 4 % [w/w]. However, considering these densities for MS seeds, soil water velocity was reduced more at the lower (2 and 4 % [w/w]) inclusion levels than DS seeds. For example, 4 % [w/w] MS reduced water velocity from 3×10^{-6} m s^{-1} (in non-amended soil), to 1 $\times 10^{-6}$ m s^{-1}; while DS only reduced water velocity to 1.5 $\times 10^{-6}$ m s^{-1}.

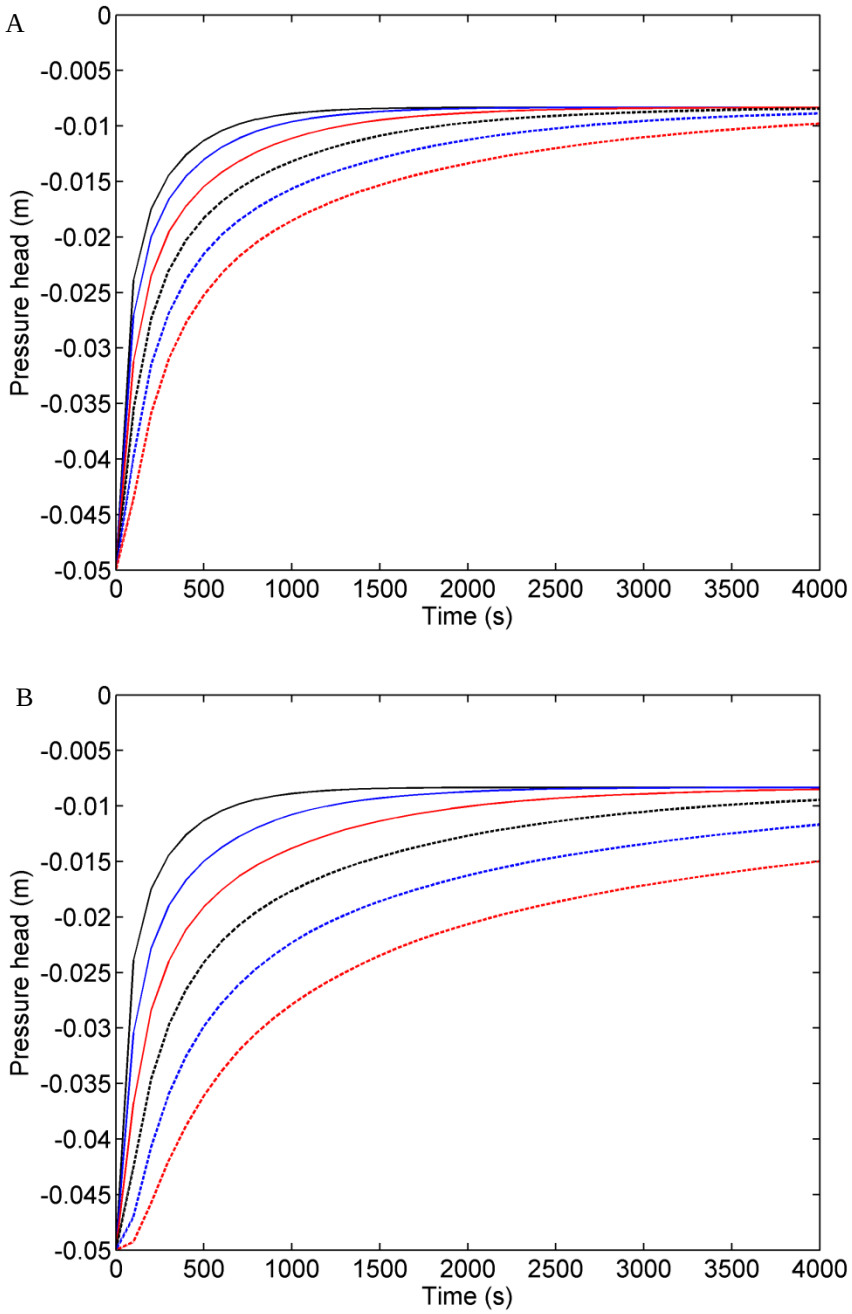

Figure 6.3 The water pressure head at r_1 (0.5 cm below soil surface) under different DS (A) and MS (B) density amendments. The solid black, blue, red and dashed black, blue and red lines show simulation results over time for soil seedbank densities of 0, 2, 4, 6, 8 and 10 % [w/w], respectively.

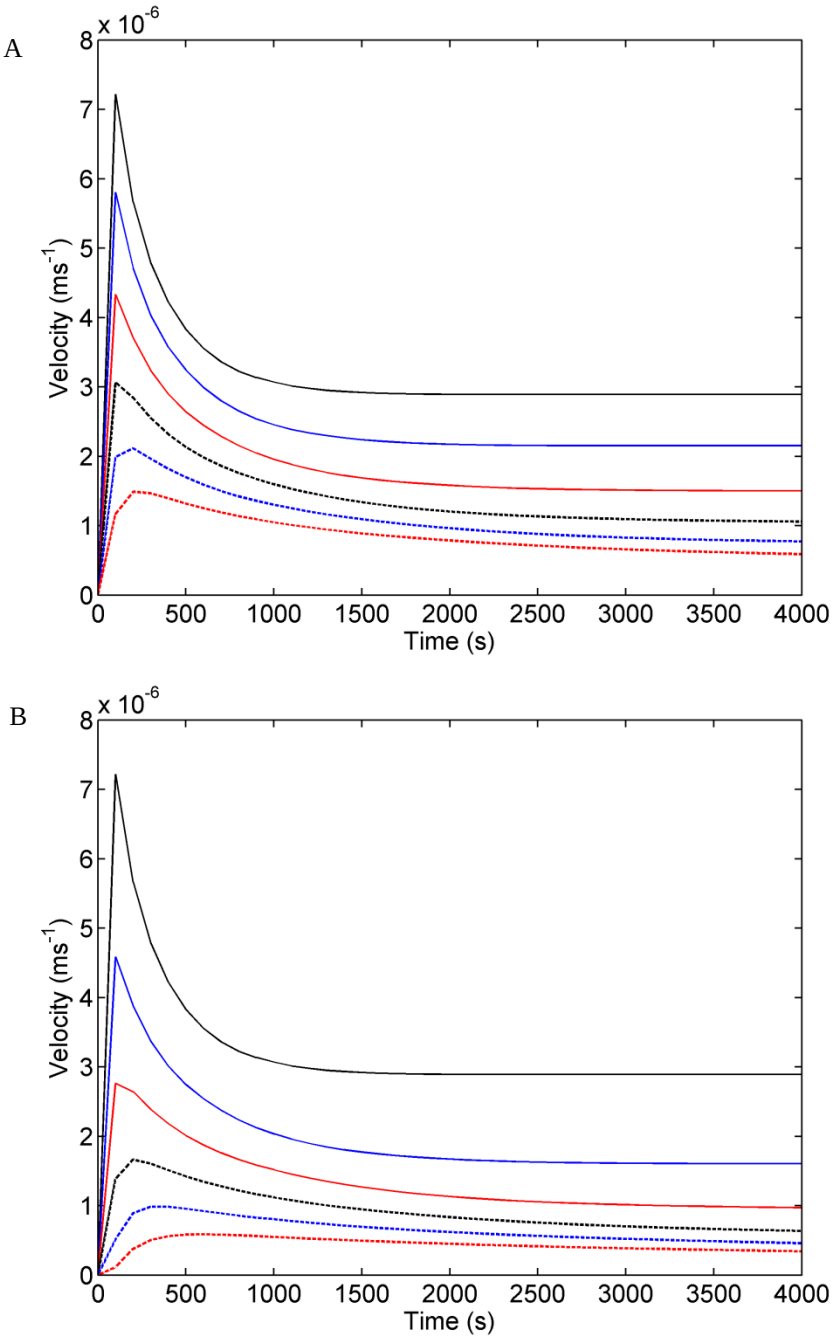

Figure 6.4 The water velocity at r_1 (0.5 cm below soil surface) under different DS (A) and MS (B) density amendments. The solid black, blue, red and dashed black, blue and red lines show simulation results over time for soil seedbank densities of 0, 2, 4, 6, 8 and 10 % [w/w], respectively.

6.4.3 **The effect of the height of seed-soil layer**

It showed from the last section that 4 % [w/w] seeds amendments had a relative higher influence on the water velocity and pressure head change in water flow in soil. In this part, the influence of the height of seed-soil layer was analysed at the fixed soil seedbank density (4 % [w/w]) for both MS and DS. In this section, two different points were chosen to analyse the water pressure and velocity. Figure 6.5 showed the pressure head at r_1, which was 0.5 cm below the soil surface and was the seed-soil layer and soil only interface. The water pressure head decreased as the seed-soil layer height increased, from -0.01 to -0.005 m and the profile was different from that of uniformly distributed seeds amendments. Water velocity at r_1 decreased as the seed-soil layer height increased (Figure 6.6). This effect was marked for the most narrow (0.5 cm) height for both seed types. However, the water velocity reduction was more marked for the addition of MS which showed at 50% reduction for 1.5 cm height of seeds, while 33 % reduction recorded for the DS amendment. The simulation was reassessed for seed-soil layers at r_2 (1 cm below soil surface) (Figure 6.7 and 6.8). Unlike the trend found for r_1, the pressure head at r_2 was lower than that of r_1 and the value was less than the non-amended soil. The water velocity at r_2 was less than r_1 at the beginning and as then reached the same velocity with r_1 with time increased.

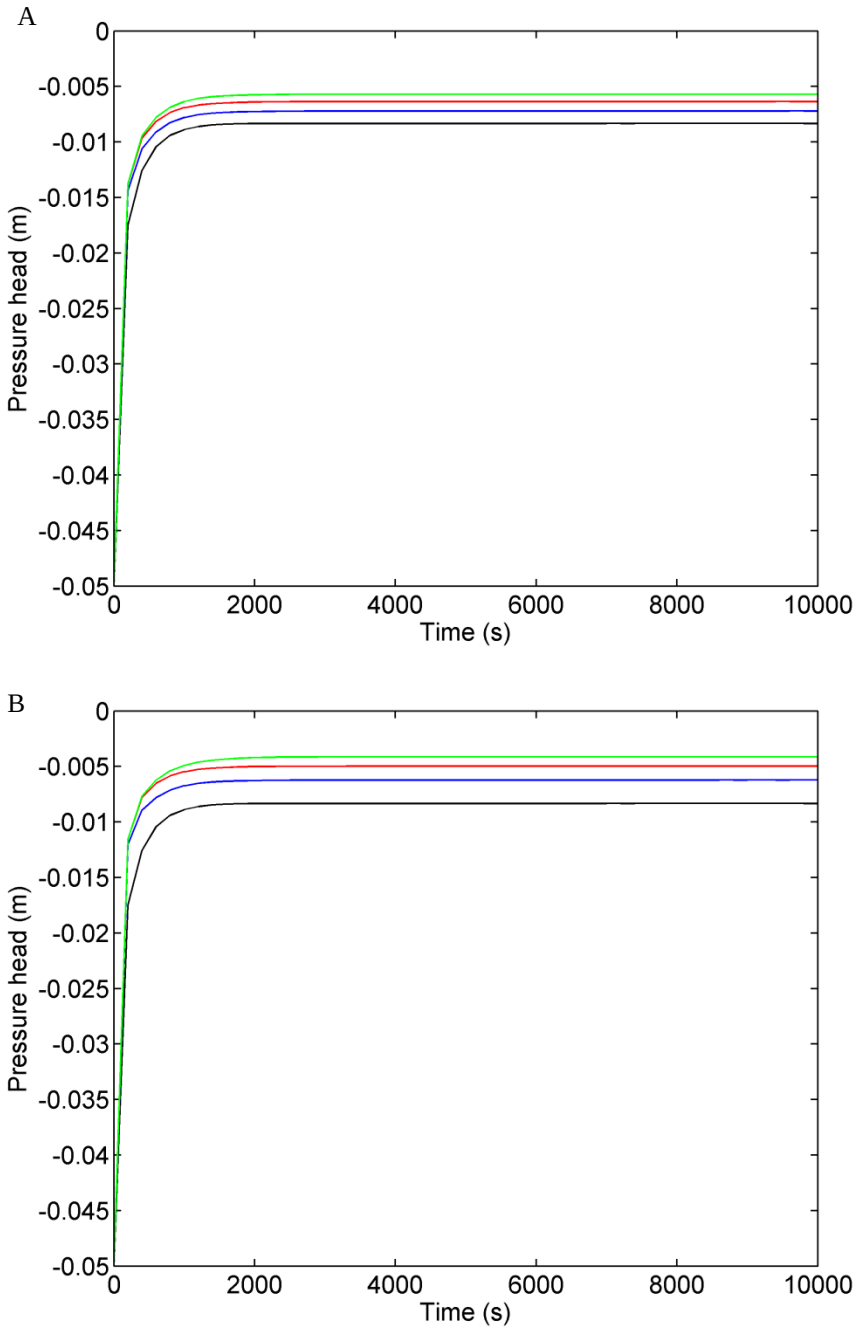

Figure 6.5 The water pressure head at r_1 (0.5 cm below soil surface) with different seed-soil height of DS (A) and MS (B) amended layer at a density of 4 % [w/w]. Black line, blue line, red line and green line represent amended seed-soil layer height of 0, 0.5, 1, 1.5 cm, respectively.

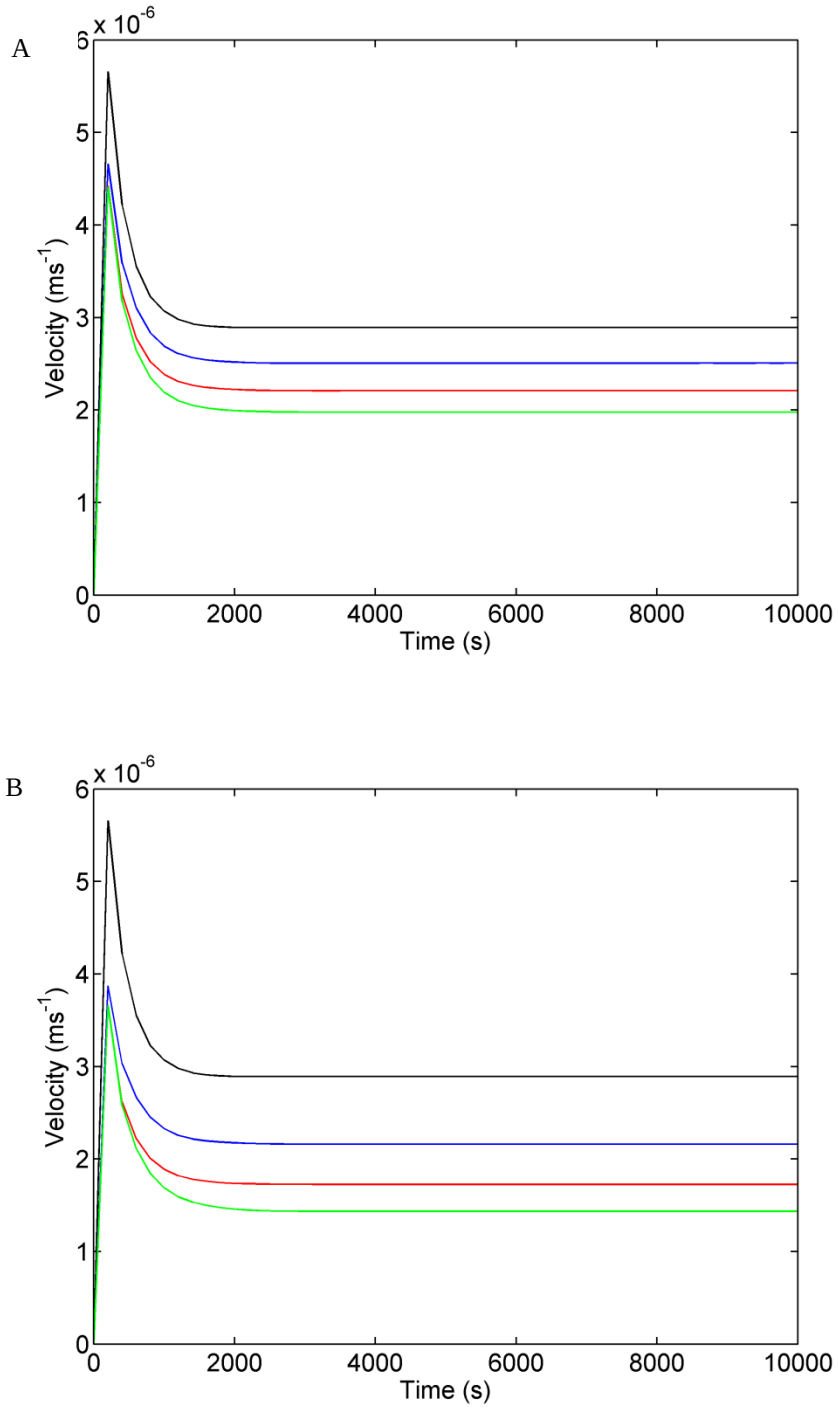

Figure 6.6 The water velocity at r_1 (0.5 cm below soil surface) with different seed-soil height of DS (A) and MS (B) amended layer at a density of 4 % [w/w]. Black line, blue line, red line and green line represent amended seed-soil layer height of 0, 0.5, 1, 1.5 cm, respectively.

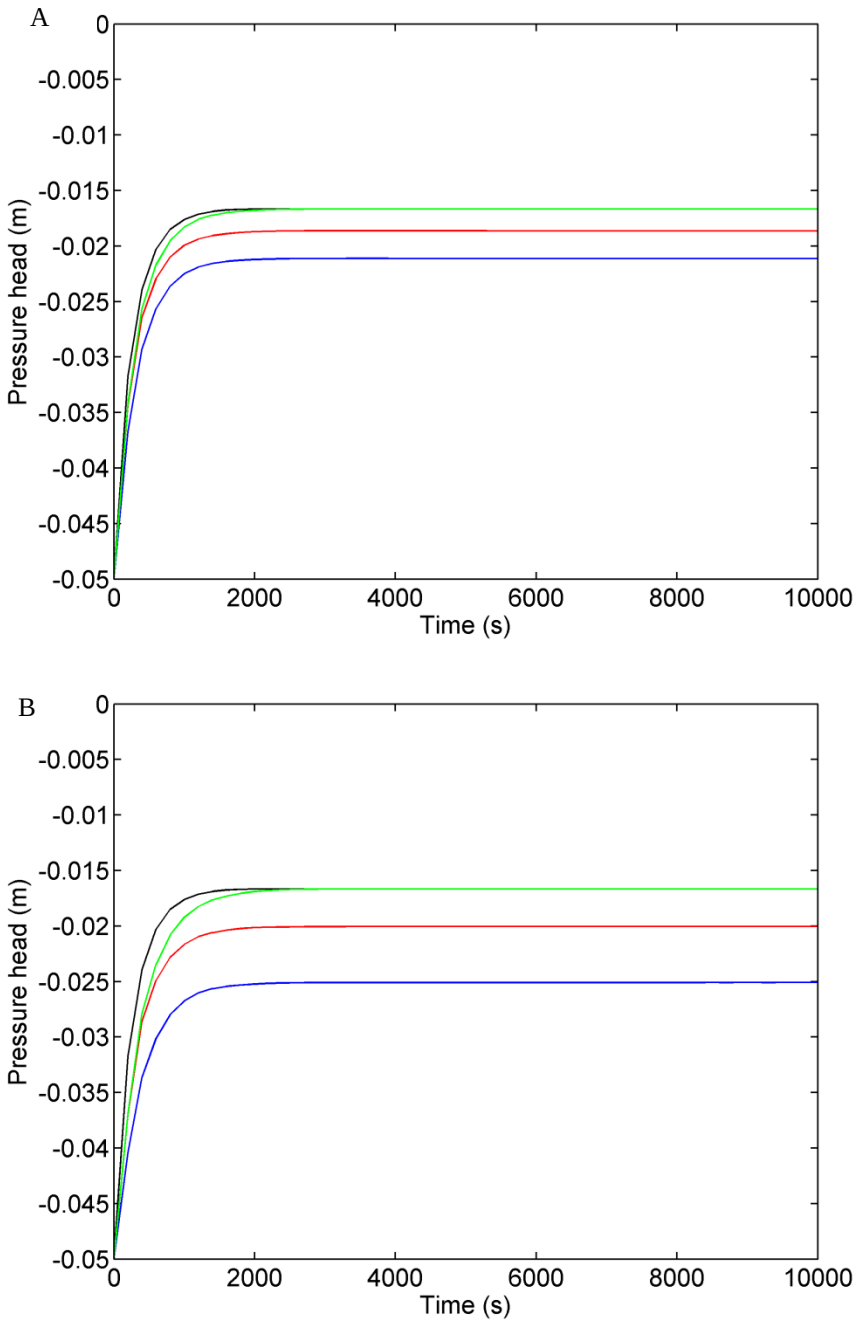

Figure 6.7 The water pressure head at r_2 (1 cm below soil surface) with different seed-soil height of DS (A) and MS (B) amended layer at a density of 4 % [w/w]. Black line, blue line, red line and green line represent amended seed-soil layer height of 0, 0.5, 1, 1.5 cm, respectively.

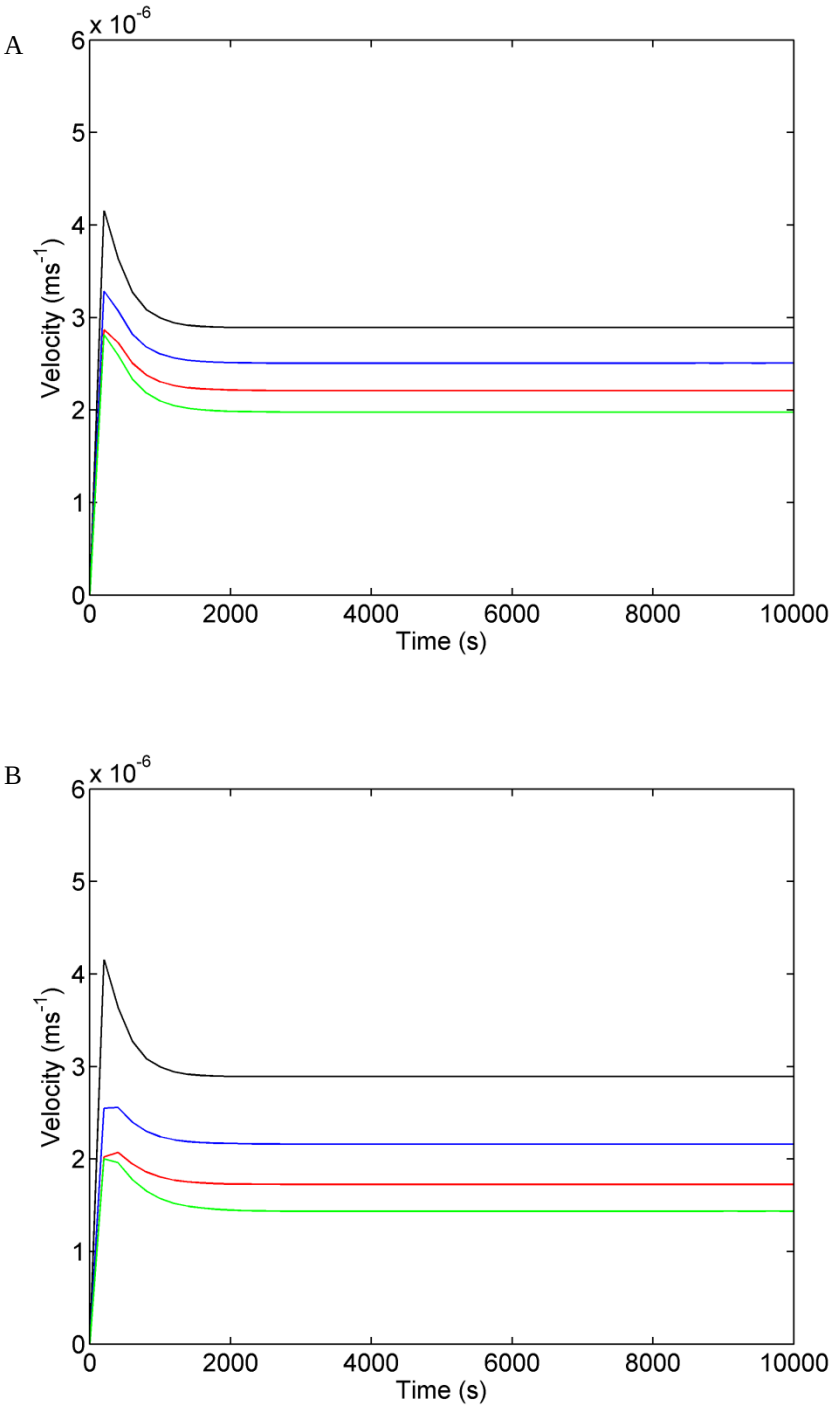

Figure 6.8 The water velocity at r_2 (1 cm below soil surface) with different seed-soil height of DS (A) and MS (B) amended layer at a density of 4 % [w/w]. Black line, blue line, red line and green line represent amended seed-soil layer height of 0, 0.5, 1, 1.5 cm, respectively.

6.4.4 The effect of seed-soil layer distance from the soil surface

Figure 6.9 – 6.10 illustrated the water pressure head and velocity of r_1 at different soil-seed layer distance from soil surface. The water pressure head of amended soil was a little greater than non-amended soil at all distance except from 0. If applying the seeds at the soil surface, the pressure was greatly reduced compared with soil only. Water velocity at r_1 of amended soil was less than that of non-amended soil; however, there was no difference for all the amendments after about 10 min. At the early stage, the water velocity increased as the distance of the seed-soil layer from soil surface increased (Figure 6.10). The most significant reductions to water velocity were caused by applying seeds in the soil surface (d_s = 0) at the beginning. Data gathered for r_2 shows a similar trend (Figure 6.11 – 12), though the extent of the water pressure head and velocity at the beginning decrease were significantly less. However, the final velocity at r_2 was the same as that of r_1. That was, seeds at the soil surface have greatest capacity to reduce the rate at which water entered the soil. Or, in other terms, the presence of seeds at the soil surface acted to increase the time period that they exposed to water, and therefore extend their imbibition time. Meanwhile, when the seeds were applied above the measuring point, the pressure head of amended soil was less than the non-amended soil, such as when d_s = 0, 0.5 cm for r_2.

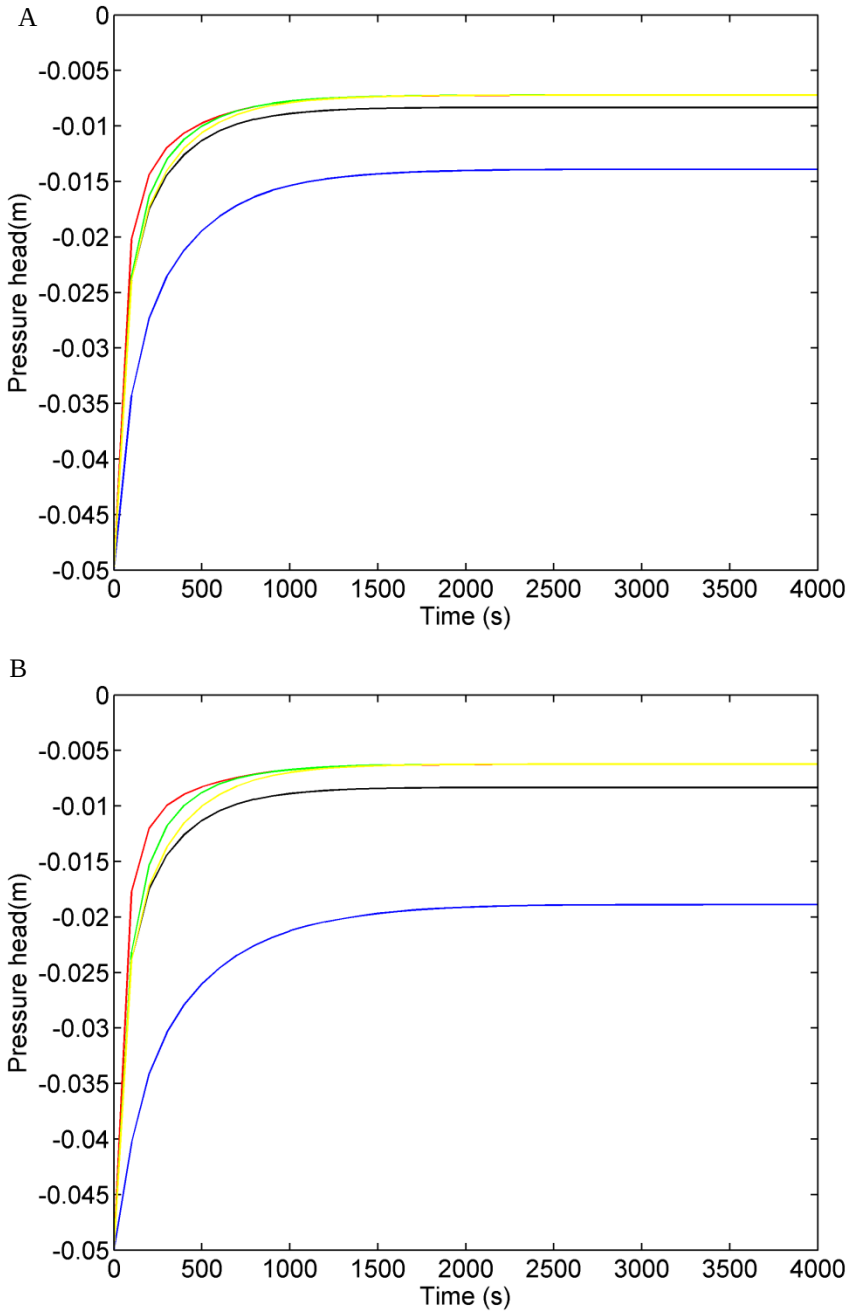

Figure 6.9 The water pressure at r_1 (0.5 cm below soil surface) with different distance of DS (A) and MS (B) amended layer to soil surface at 4 % [w/w]. Black line, blue line, red line, green line and yellow line represent amended soil layer distance from soil surface of soil only, 0, 0.5, 1, 1.5 cm, respectively.

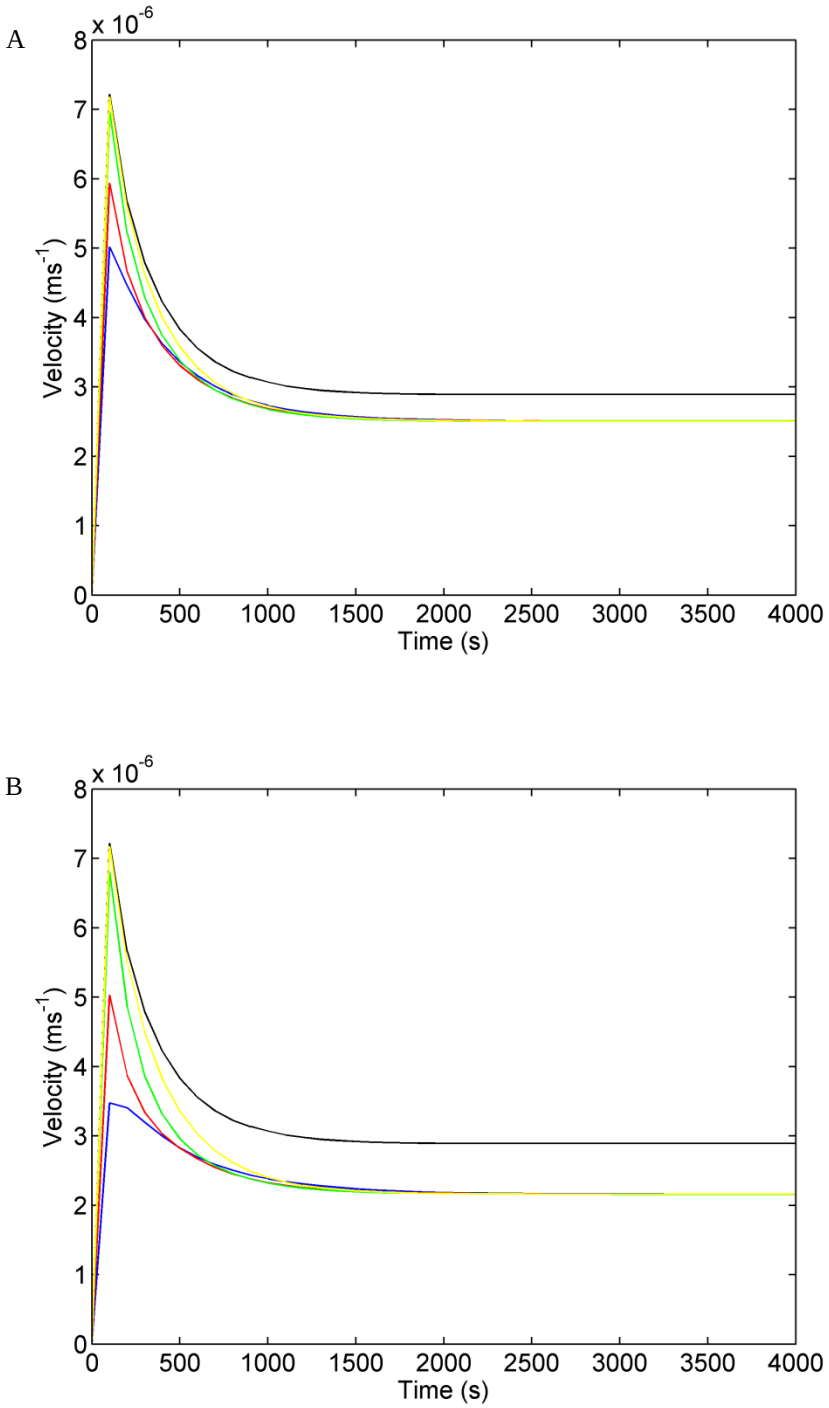

Figure 6.10 The water velocity at r_1 (0.5 cm below soil surface) with different distance of DS (A) and MS (B) amended layer to soil surface at 4 % [w/w]. Black line, blue line, red line, green line and yellow line represent amended soil layer distance from soil surface of soil only, 0, 0.5, 1, 1.5 cm, respectively.

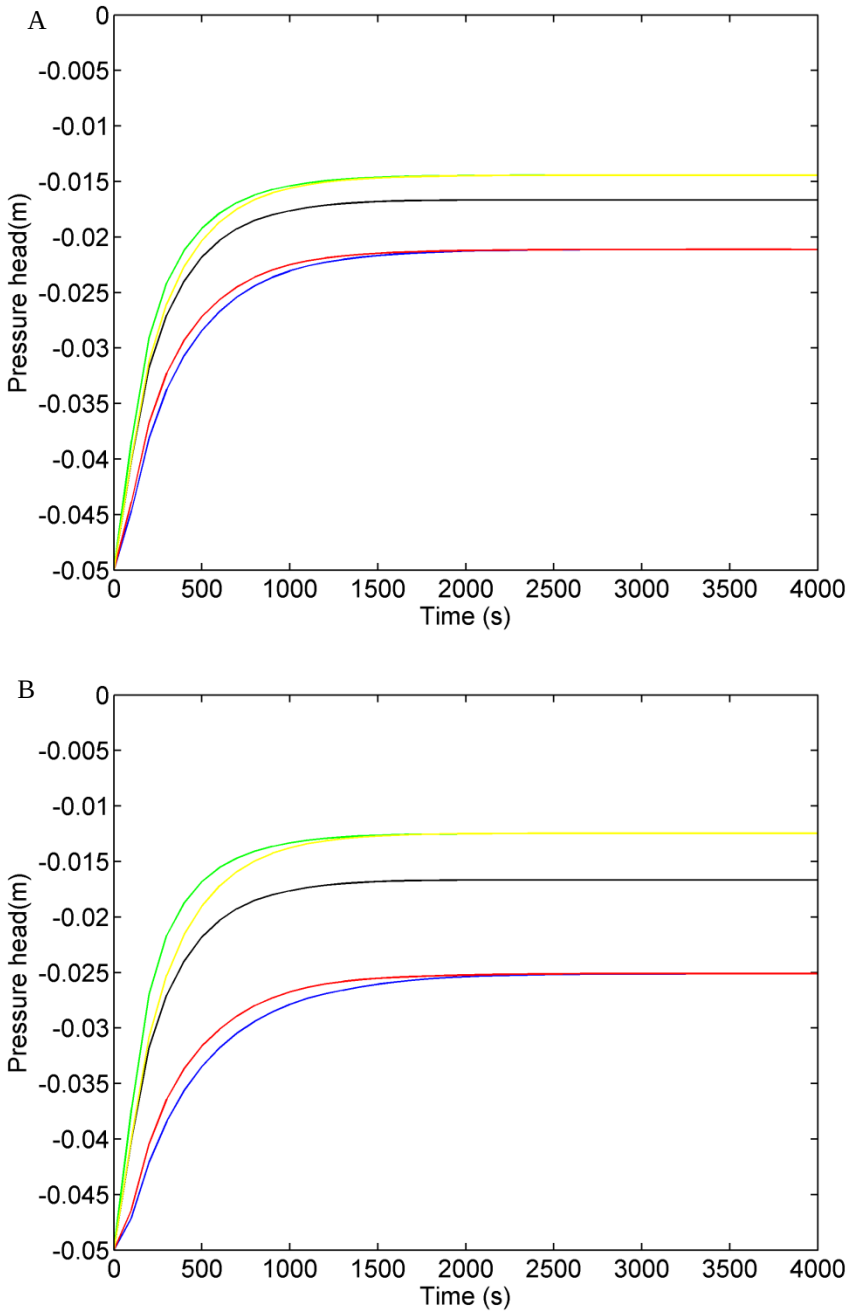

Figure 6.11 The water pressure at r_2 (1 cm below soil surface) with different distance of DS (A) and MS (B) amended layer to soil surface at 4 % [w/w]. Black line, blue line, red line, green line and yellow line represent amended soil layer distance from soil surface of soil only, 0, 0.5, 1, 1.5 cm, respectively.

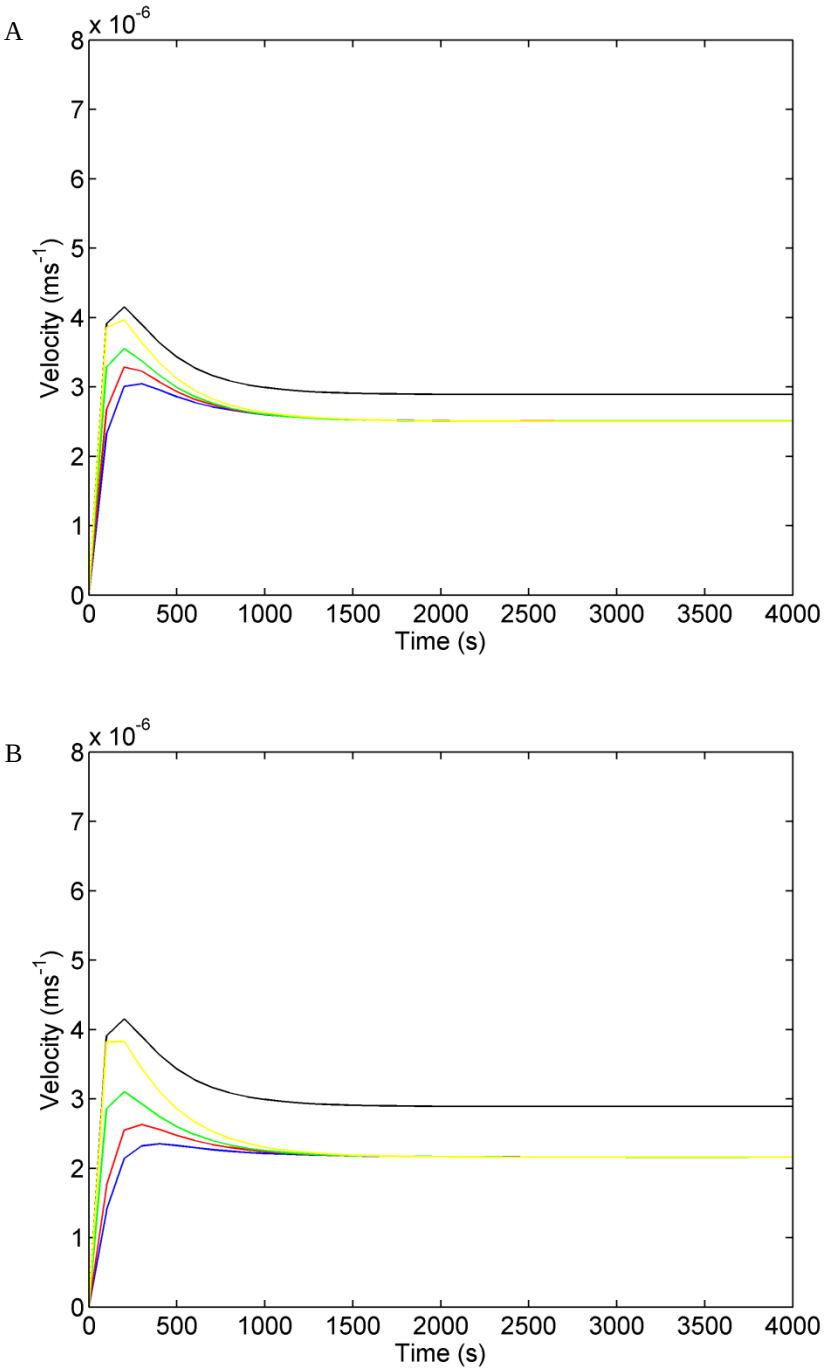

Figure 6.12 The water velocity at r_2 (1 cm below soil surface) with different distance of DS (A) and MS (B) amended layer to soil surface at 4 % [w/w]. Black line, blue line, red line, green line and yellow line represent amended soil layer distance from soil surface of soil only, 0, 0.5, 1, 1.5 cm, respectively.

6.5 Discussion

The numerical modelling data can well fit the experimental data in terms of the average velocity through the soil column. Therefore, this model can be further applied to carry out parametric studies and find out the general trend of the seed treatment. However, there was no data for the velocity at each point at different point which required further study with more advanced equipment.

The parametric studies showed that the myxospermous seeds of shepherd's purse when used as a soil amendment may significantly alter the soil-water flow. The density of seeds in the soil seedbank is an important feature that determines soil water velocity. The numerical simulations demonstrated that the optimal density of uniformly distributed seeds within a seedbank to reduce water velocity in sandy-loam soil is *ca.* 4 % [w/w]. It is clear that greater water velocity reduction was achieved using seed which are uniformly distributed in the soil seedbank, as opposed to deployment in either layers and at varying depths of heights (compare Figure 6.4, Figure 6.6 and Figure 6.10). It should however be also be noted that the 4 % [w/w] MS soil seedbank deployed uniformly reduced water velocity up to 66 % (Figure 6.10). This reduction was remarkable compared to that achieved by commercially available polymers: although the seed weight required is greater, (40x for the 4% [w/w] MS amendment) (Eggert Jr. *et al.*, 1992; Khachatoorian *et al.*, 2003). With a moderate increase to the MS seed density (6 % [w/w]), the mucilage swelling will block the soil-pore space and reduce the water flow velocity. However, as soil seedbank density increases the seed itself will increase soil pore-space which compensates the block of mucilage swelling and water flow rate is increased again. With the optimal soil seedbank density determined, it was considered how best to localise the soil-seed amendment along the soil profile (*i.e.* soil core depth). The numerical simulation showed that neither MS nor DS exert a

significant influence on the soil water flow for the amended soil layer distance from soil surface, especially over long time courses (Figure 6.12).

With a view towards those treatments which have greater capacity to slow the passage of water, it should also be highlighted that significance reductions in water velocity were achieved by deploying a seedbank uniformly in the soil (Figure 6.4). This reduces greatly, the rate at which water enters the soil and in functional terms beyond water transience, indicates that seeds at the soil surface would have more time to imbibe, and that the extent to which they are primed may be enhanced.

Although MS amendments proved more effective in reducing soil-water flow rates, the DS amendment also showed a similar and significant affect. This finding therefore supports the conclusion highlighted in Chapter 5: that is, shepherd's purse seeds, whether myxospermous or not, may provide ecosystem services.

The model developed was simple but based on experimental observations and data, though it does encompass several assumptions. Only the effect of MS seed amendment in soil hydraulic conductivity was considered and impact of mucilage dispersion within the soil was not considered. The mucilage viscosity and swelling capacity were also not taken into account as there was no data for these parameters *in situ*. It was reported that these parameters in soil were quite different from that measured *ex situ* and *in vitro* (Eggert Jr. *et al.*, 1992). Therefore, more experiments were required to acquire this data. However, the influence of parameters such as seeds density and the position where to apply seeds can be drawn from the modelling. Moreover, there was no experimental data by which the mathematical model may be validated and further is also still required. Similarly, and in terms of the functional and ecological significance of the suggested amendments to impact on plant growth, this was also still to be assessed.

6.6 Summary

In this chapter, a first and simple mathematical model is developed that simulates the flow rates and soil permeability of water in unsaturated sandy-loam soils that are amended to contain seeds (as part of a soil seedbank). The influence of the factors seedbank density and soil-seed layer depth were analysed in a series of parametric studies. The results showed that a soil seedbank density of 4 % [w/w] MS applied uniformly across the soil layer would have greatest capacity to reduce water flow rate. It should be noted that the effect is also true for non-myxospermous seed amendments, though it is reduced.

Chapter 7 **Conclusions and Future work**

7.1 Conclusions

In this project, the shepherd's purse was chosen as a model plant species due to the unique properties of its myxospermous seeds. Based on the literatures about the ecological role of seed mucilage, an initiate to discover the physical of myxospermous seeds will be important. This study is a joint project between engineering and biology and the aim is to find the potential application of natural resources in engineering. Varieties of studies relating to the seed mucilage and seed and their effect on soil physical properties and water flow in soil have been carried out experimentally and numerically.

In this work, I firstly characterised the seed mucilage general properties and measured the mucilage swelling ratio in solutions of different osmotic pressure. The results showed that the seed mucilage had a high water holding capacity and low osmotic potential. Its swelling ratio decreased as osmotic potential decreased. This trait enabled seeds with mucilage to adapt to water deficiency and salinity environment. A simple mathematical model based on diffusion and convection model was proposed to simulate the swelling process of seed mucilage.

Further studies about mucilage rheology were carried out to characterise the flow behaviour of mucilage. The influences of mucilage concentration, temperature and shear frequency were analysed using oscillation dynamic rheology tests. The mucilage was found to be characterised as a weak gel according to its viscoelastic properties. The rheology parameters (η, G', G'', τ_f and τ_y) were measured and their relationship with mucilage concentration is fitted by power law. These results also provided information for further mathematical modelling in the following chapters.

Based on the unique findings of seed mucilage, I carried out a series of experiments to analyse the role of seed mucilage or myxospermous seeds on soil physical properties. I measured the soil water retention, hydraulic conductivity and stability with different mucilage or seed concentration. The effect of seeds without mucilage was also measured to compare with that of seeds with mucilage.

Finally, the effect of seeds mucilage on water flow in soil is simulated by numerical methods. In the numerical model, the water flow was simulated by Darcy's law with continuum equation. The mucilage clogging effect was modelled by reducing the relative permeability of soil. The reduction of relative permeability was considered by introducing a term which accounting for the mucilage saturation in soil. Mucilage swelling degree and rheology parameters obtained in the experiments were used in this numerical model. To summarise, all the experimental tests and numerical modelling found that:

(1) The mucilage had a high swelling degree in water (16 g water g^{-1} mucilage dry weight) and a low osmotic pressure of-0.54 MPa (equivalent to 0.11 M or 6.6 g L^{-1} NaCl). The swelling was very rapid which finished within seconds.

(2) The water extractable mucilage was shear thinning with high viscosity. The viscosity of seed mucilage was usually higher than root and fruit mucilage. The rheology properties increased as mucilage concentration increased and were also slightly frequency dependent. The influence of temperature was small when temperature was under 40 ^{o}C.

(3) Seeds, whether myxospermous or not, increased sandy-loam soil water retention and rheology properties while reducing the soil hydraulic conductivity. The addition mucilage will increase water retention and stability as well.

(4) The water flow in sandy-loam soil can be greatly reduced by applying seeds in soil. The numerical modelling suggested that 2 – 4 % [w/w] MS uniformly distributed was the most effective amendment to sandy-loam soil.

The experimental and numerical investigations presented in this these is the first attempts to characterise the seed/seed mucilage properties and its application as soil conditioner.

7.2 Future work

Future research should include both experimental and numerical work based on the research findings presented here. As this project is multidisciplinary, collaboration between different departments and institutes is required. Firstly, chemical analysis, especially a polysaccharide linkage analysis, should be carried out to have detailed information of seed mucilage composition. In this thesis, mucilage composition was only analysed superficially by staining for pectin, cellulose and hemicellulose. Therefore, collaboration with a specialist plant cell wall biochemist will be required to carry out such analyses and from the balance of functionally distinct polymers inform the seed mucilage modelling process. In addition, this information will inform the manufacture of synthetic mucilages and extending this current work for comparative analyses with other plant mucilages.

More experimental tests on mucilage swelling properties under different environmental conditions should also be conducted. The influence of mucilage shape, size, the ion concentration and temperature are important factors for mucilage swelling. The experimental data may also be used to validate the numerical model. However, the current numerical models should also be extended to consider the influence of ion and

temperature. Also, the experiments and numerical modelling at this stage will be helpful for studying the clogging or blocking effect in soil.

The experiments of effect of mucilage or seed on soil properties should be improved too. Testing more mucilage or seed concentrations on more soil types will be important, as it will allow identification the optimal values of mucilage or seed concentration in soil. These tests can be conducted both in the laboratory and in field. In this context, and in relation to soil priming, the effect of seed mucilage and other mucilage including root or bacterial mucilage and commercial superabsorbent gels should be carried out in a comparative analysis. This could also assess soil formation and soil microbial diversity and function.

Numerical models for studying the water flow in mucilage amended soil could also be improved. In this study, the swelling process of mucilage was ignored and the blocking effect was considered by reducing the relative permeability of soil. It might be better to simulate the swelling process and considering mucilage degradation and loss at the same time. The microbial growth in soil related to mucilage also affects the water flow and should be important to be included in the model. The validation of the numerical model should be carried out too.

References

Acarkan, A., Rossberg, M., Koch, M. and Schmidt, R. 2000. Comparative genome analysis reveals extensive conservation of genome organisation for *Arabidopsis thaliana* and *Capsella rubella*. *The Plant Journal* **23,** 55–62.

Agaba, H., Orikiriza, L. J. B., Obua, J., Kabasa, J. D., Worbes, M. and Hüttermann, A. 2011. Hydrogel amendment to sandy soil reduces irrigation frequency and improves the biomass of *Agrostis stolonifera*. *Agricultural Sciences,* **2,** 544–550.

Akhter, J., Mahmood, K., Malik, K. A., Mardan, A., Ahmad, M. and Iqbal, M. M. 2004. Effects of hydrogel amendment on water storage of sandy loam and loam soils and seedling growth of barley, wheat and chickpea. *Plant, Soil and Environment,* **50,** 463–469.

Aksoy, A., Dixon, J. M. and Hale, W. H. G. 1998. *Capsella bursa-pastoris* (L.) Medikus (*Thlaspi bursa-pastoris* L., *Bursa bursa-pastoris* (L.) Shull, *Bursa pastoris* (L.) Weber). *Journal of Ecology,* **86,** 171–186.

Al-Darby, A. M. 1996. The hydraulic properties of a sandy soil treated with gel-forming soil conditioner. *Soil Technology,* **9,** 15–28.

Al-Darby, A. M., Al-Omran, A. M., El-Shafei, Y. Z. and Shalaby, A. A. 1996. Influence of a highly swelling gel-forming conditioner (Acryhope) on hydrophysical properties of layered sandy soils. *Journal of the King Saudi University,* **8,** 173–188.

Al-Darby, A. M. and AlSheikh, A. A. 1995. The combined effect of soil gel-conditioner and irrigation water quality and level on: 1. Soil water retention and availability, water and salt distribution in sandy soil. *Arab Gulf Journal of Scientific Research,* **13,** 719–748.

Alfrey, T., Gurnee, E. F. and Lloyd, W. G. 1966. Diffusion in glassy polymers. *Journal of Polymer Science Part C: Polymer Symposia,* **12,** 249–261.

Andry, H., Yamamoto, T., Irie, T., Moritani, S., Inoue, M. and Fujiyama, H. 2009. Water retention, hydraulic conductivity of hydrophilic polymers in sandy soil as affected by temperature and water quality. *Journal of Hydrology,* **373,** 177–183.

Arbona, V., Iglesias, D. J., Jacas, J., Primo-Millo, E., Talon, M. and Gómez-Cadenas, A. 2005. Hydrogel substrate amendment alleviates drought effects on young citrus plants. *Plant and Soil,* **270,** 73–82.

Arsovski, A. A., Villota, M. M., Rowland, O., Subramaniam, R. and Western, T. L. 2009. *MUM ENHANCERS* are important for seed coat mucilage production and mucilage secretory cell differentiation in *Arabidopsis thaliana*. *Journal of Experimental Botany,* **60,** 2601–2612.

Balhoff, M. T. and Thompson, K. E. 2004. Modeling the steady flow of yield-stress fluids in packed beds. *AIChE Journal,* **50,** 3034–3048.

Barré, P. and Hallett, P. D. 2009. Rheological stabilization of wet soils by model root and fungal exudates depends on clay mineralogy. *European Journal of Soil Science,* **60,** 525–538.

Begg, G. S., Wishart, J., Young, M. W., Squire, G. R. and Iannetta, P. P. M. 2011. Genetic structure among arable populations of *Capsella bursa-pastoris* is linked to functional traits and in-field conditions. *Ecography,* **34,** 1–12.

Bejan, A. 2000. *Shape and structure, from engineering to nature,* Cambridge, UK, Cambridge University Press.

Bengough, A. G. 2012. Water dynamics of the root zone: rhizosphere biophysics and its control on soil hydrology. *Vadose Zone Journal,* **11,** vzj2011.0111.

Bhardwaj, A. K., Shainberg, I., Goldstein, D., Warrington, D. N. and Levy, G. J. 2007. Water retention and hydraulic conductivity of cross-linked polyacrylamides in sandy soils. *Soil Science Society of America Journal,* **71,** 406–412.

Biot, M. A. 1941. General theory of three-dimensional consolidation. *Journal of Applied Physics,* **12,** 155–164.

Birgersson, E., Li, H. and Wu, S. 2008. Transient analysis of temperature-sensitive neutral hydrogels. *Journal of the Mechanics and Physics of Solids,* **56,** 444–466.

Boivin, K., Acarkan, A., Mbulu, R. S., Clarenz, O. and Schmidt, R. 2004. The *Arabidopsis* genome sequence as a tool for genome analysis in *Brassicaceae*. A comparison of the *Arabidopsis* and *Capsella rubella* genomes. *Plant Physiology,* **135,** 735–744.

Boult, S., Hand, V. L., Lloyd, J. R., Vaughan, D. J. and Wilkins, M. J. 2008. Experimental studies of the influence of grain size, oxygen availability and organic carbon availability on bioclogging in porous media. *Environmental Science & Technology,* **42,** 1485–1491.

Bryant, S. J., Arthur, J. A. and Anseth, K. S. 2005. Incorporation of tissue-specific molecules alters chondrocyte metabolism and gene expression in photocrosslinked hydrogels. *Acta Biomaterialia,* **1,** 243-252.

Caesar-Tonthat, T. C. 2002. Soil binding properties of mucilage produced by a basidiomycete fungus in a model system. *Mycological Research,* **106,** 930–937.

Chang, Y. and Cui, S. 2011. Steady and dynamic shear rheological properties of extrusion modified fenugreek gum solutions. *Food Science and Biotechnology,* **20,** 1663–1668.

Chen, J. S. 1990. Rheological behavior of Na-montmorillonite suspensions at low electrolyte concentration. *Clays and Clay Minerals,* **38,** 57-62.

Chirino, E., Vilagrosa, A. and Vallejo, V. R. 2011. Using hydrogel and clay to improve the water status of seedlings for dryland restoration. *Plant and Soil,* **344,** 99–110.

Clark, A. and Ross-Murphy, S. 1987. Structural and mechanical properties of biopolymer gels. *Advances in Polymer Science,* **83,** 57–192.

Cui, W., Eskin, N. A. M. and Biliaderis, C. G. 1994a. Yellow mustard mucilage - chemical-structure and rheological properties. *Food Hydrocolloids,* **8,** 203–214.

Cui, W., Mazza, G. and Biliaderis, C. G. 1994b. Chemical structure, molecular size distributions, and rheological properties of Flaxseed gum. *Journal of Agricultural and Food Chemistry,* **42,** 1891–1895.

Czarnes, S., Hallett, P. D., Bengough, A. G. and Young, I. M. 2000. Root- and microbial-derived mucilages affect soil structure and water transport. *European Journal of Soil Science,* **51,** 435-443.

de Gennes, P. G. 1979. *Scaling concepts in polymer physics,* Ithaca, New York, Cornell University Press.

De Kee, D., Liu, Q. and Hinestroza, J. 2005. Viscoelastic (Non-Fickian) diffusion. *The Canadian Journal of Chemical Engineering,* **83,** 913–929.

Deng, W., Jeng, D.-S., Toorop, P. E., Squire, G. R. and Iannetta, P. P. M. 2012. A mathematical model of mucilage expansion in myxospermous seeds of *Capsella bursa-pastoris* (shepherd's purse). *Annals of Botany,* **109,** 419–427.

Eggert Jr., R. W., Willhite, G. P. and Green, D. W. 1992. Experimental measurement of the persistence of permeability reduction in porous media treated with Xanthan/Cr(III) gel systems. *Society of Petroleum Engineers Journal,* **7,** 29–35.

Ellner, S. and Shmida, A. 1981. Why are adaptations for long-range seed dispersal rare in desert plants? *Oecologia,* **51,** 133–144.

Engesgaard, P., Seifert, D. and Herrera, P. 2006. Bioclogging in porous media: Tracer studies. *Riverbank Filtration Hydrology,* **60,** 93–118.

Fahn, A. and Werker, E. 1972. Anatomical mechanisms of seed dispersal. *Seed biology,* **1,** 151–217.

Farahnaky, A., Askari, H., Majzoobi, M. and Mesbahi, G. 2010. The impact of concentration, temperature and pH on dynamic rheology of psyllium gels. *Journal of Food Engineering,* **100,** 294–301.

Fedeniuk, R. W. and Biliaderis, C. G. 1994. Composition and physicochemical properties of Linseed (*Linum usitatissimum* L.) mucilage. *Journal of Agricultural and Food Chemistry,* **42,** 240–247.

Fitch, E. A., Walck, J. L. and Hidayati, S. N. 2007. Germinating seeds of *Lesquerella perforata* and *stonensis*: substrate effects and mucilage production. *Native Plants Journal,* **8,** 4–10.

Frey-Wyssling, A. 1976. Encyclopedia of plant anatomy. Gebrüder Borntraeger, Berlin.

Gerhards, C. and Walker, F. 1997. Rheological properties of mustard mucilage isolated from raw and from processed mustard. *Nahrung-Food,* **41,** 96–100.

Ghezzehei, T. A. and Or, D. 2001. Rheological properties of wet soils and clays under steady and oscillatory stresses. *Soil Science Society of America Journal,* **65,** 624–637.

Gregory, P. J. 2008. *Plant roots: growth, activity and interactions with the soil,* Blackwell Publishing.

Grubert, M. 1974. Studies on the distribution of myxospermy among seeds and fruits of angiospermae and its ecological importance. *Acta Biologica Venezuelica,* **8,** 315–551.

Grubert, M. 1981. *Mucilage or gum in seeds and fruits of angiosperms. A review,* Műnchen, Minerva Publikation.

Guinel, F. C. and McCully, M. E. 1986a. Some physical properties of corn root-cap mucilage related to water. *American Journal of Botany,* **73,** 629–629.

Guinel, F. C. and McCully, M. E. 1986b. Some water-related physical properties of maize root-cap mucilage. *Plant, Cell & Environment,* **9,** 657–666.

Guo, Q., Cui, S. W., Wang, Q. and Young, C. J. 2008. Fractionation and physicochemical characterization of psyllium gum. *Carbohydrate Polymers,* **73,** 35–43.

Gutterman, Y. 1993. *Seed germination in desert plants (adaptations of desert organisms)*, Springer-Verlag, Berlin.

Gutterman, Y. and Shem-Tov, S. 1997. Mucilaginous seed coat structure of *Carrichtera annua* and *Anastatica hierochuntica* from the Negev Desert highlands of Israel, and its adhesion to the soil crust. *Journal of Arid Environments,* **35,** 695–705.

Hallett, P. D. and Young, I. M. 1999. Changes to water repellence of soil aggregates caused by substrate-induced microbial activity. *European Journal of Soil Science,* **50,** 35–40.

Haughn, G. W. and Western, T. L. 2012. Arabidopsis seed coat mucilage is a specialized cell wall that can be used as a model for genetic analysis of plant cell wall structure and function. *Frontiers in Plant Science,* **3,** 64.

Hawes, C., Begg, G. S., Squire, G. R. and Iannetta, P. P. M. 2005. Individuals as the basic accounting unit in studies of ecosystem function: functional diversity in shepherd's purse, *Capsella*. *Oikos,* **109,** 521–534.

Heard, M. S., Hawes, C., Champion, G. T., *et al.* 2003. Weeds in fields with contrasting conventional and genetically modified herbicide-tolerant crops. I. Effects on abundance and diversity. *Philosophical Transactions of the Royal Society London Series B,* **358,** 1819–1832.

Hietala, S., Strandman, S., Järvi, P., *et al.* 2009. Rheological properties of associative star polymers in aqueous solutions: effect of hydrophobe length and polymer topology. *Macromolecules,* **42,** 1726–1732.

Holthusen, D., Peth, S. and Horn, R. 2010. Impact of potassium concentration and matric potential on soil stability derived from rheological parameters. *Soil and Tillage Research,* **111,** 75–85.

Hong, W., Zhao, X., Zhou, J. and Suo, Z. 2008. A theory of coupled diffusion and large deformation in polymeric gels. *Journal of the Mechanics and Physics of Solids,* **56,** 1779–1793.

Hui, C. Y. and Muralidharan, V. 2005. Gel mechanics: A comparison of the theories of Biot and Tanaka, Hocker, and Benedek. *Journal of Chemical Physics,* **123,** 154905.

Hurka, H. and Haase, R. 1982. Seed ecology of *Capsella bursa-pastoris* (Cruciferae): dispersal mechanisms and the soil seed bank. *Flora,* **172,** 35–46.

Iannetta, P. P. M., Begg, G., Hawes, C., Young, M., Russell, J. and Squire, G. R. 2007. Variation in *Capsella* (shepherd's purse): an example of intraspecific functional diversity. *Physiologia Plantarum,* **129,** 542–554.

Iannetta, P. P. M., Begg, G. S., Valentine, T. A. and Wishart, J. 2010. Sustainable disease control using weeds as indicators: *Capsella bursa-pastoris* and Tobacco Rattle Virus. *Weed Research,* **50,** 511–514.

Jani, G. K., Shah, D. P., Prajaoati, V. D. and Jain, V. 2009. Gums and mucilages: versatile excipients for pharmaceutical formulations. *Asian Journal of Pharmaceutical Science,* **4,** 308–322.

Karadag, E., Saraydin, D., Caldiran, Y. and Guven, O. 2000. Swelling studies of copolymeric acrylamide/crotonic acid hydrogels as carriers for agricultural uses. *Polymers for Advanced Technologies,* **11,** 59–68.

Karmakar, S. and Kushwaha, R. L. 2007. Development and laboratory evaluation of a rheometer for soil visco-plastic parameters. *Journal of Terramechanics,* **44,** 197–204.

Kazanskii, K. S. and Dubrovskii, S. A. 1992. Chemistry and physics of agricultural hydrogels. *Advances in Polymer Science,* **104,** 97–133.

Khachatoorian, R., Petrisor, I. G., Kwan, C.-C. and Yen, T. F. 2003. Biopolymer plugging effect: laboratory-pressurized pumping flow studies. *Journal of Petroleum Science and Engineering,* **38,** 13-21.

Khachatoorian, R. and Yen, T. F. 2005. Numerical modeling of in situ gelation of biopolymers in porous media. *Journal of Petroleum Science and Engineering,* **48,** 161–168.

Kim, S. B., Ham, Y. J. and Park, S. J. 2007. Numerical experiments for bioclogging in porous media. *Environmental Technology,* **28,** 1079–1089.

Koocheki, A., Mortazavi, S. A., Shahidi, F., Razavi, S. M. A. and Taherian, A. R. 2009. Rheological properties of mucilage extracted from *Alyssum homolocarpum* seed as a new source of thickening agent. *Journal of Food Engineering,* **91,** 490–496.

Leeds-Harrison, P. B. and Youngs, E. G. 1997. Estimating the hydraulic conductivity of aggregates conditioned by different tillage treatments from sorption measurements. *Soil and Tillage Research,* **41,** 141–147.

Leeds-Harrison, P. B., Youngs, E. G. and Uddin, B. 1994. A device for determining the sorptivity of soil aggregates. *European Journal of Soil Science,* **45,** 269–272.

Li, Y. and Tanaka, T. 1990. Kinetics of swelling and shrinking of gels. *The Journal of Chemical Physics,* **92,** 1365–1371.

Loix, F., Orgéas, L., Geindreau, C., Badel, P., Boisse, P. and Bloch, J. F. 2009. Flow of non-Newtonian liquid polymers through deformed composites reinforcements. *Composites Science and Technology,* **69,** 612–619.

Lu, J., Tan, D., Baskin, J. M. and Baskin, C. C. 2010. Fruit and seed heteromorphism in the cold desert annual ephemeral *Diptychocarpus strictus* (Brassicaceae) and possible adaptive significance. *Annals of Botany,* **105,** 999–1014.

Macquet, A., Ralet, M.-C., Kronenberger, J., Marion-Poll, A. and North, H. M. 2007. *In situ,* chemical and macromolecular study of the composition of *Arabidopsis thaliana* seed coat mucilage. *Plant and Cell Physiology,* **48,** 984–999.

McCully, M. E. 1999. Roots in soil: unearthing the complexities of roots and their rhizospheres. *Annual Review of Plant Physiology and Plant Molecular Biology,* **50,** 695–718.

McCully, M. E. and Boyer, J. S. 1997. The expansion of maize root-cap mucilage during hydration. 3. Changes in water potential and water content. *Physiologia Plantarum,* **99,** 169–177.

Medina-Torres, L., Brito-De La Fuente, E., Torrestiana-Sanchez, B. and Katthain, R. 2000. Rheological properties of the mucilage gum (*Opuntia ficus indica*). *Food Hydrocolloids,* **14,** 417–424.

Mezger, T. 2006. *The rheology handbook,* Vincentz, Germany.

Michel, B. E. 1983. Evaluation of the Water Potentials of Solutions of Polyethylene Glycol 8000 Both in the Absence and Presence of Other Solutes. *Plant Physiol.,* **72,** 66-70.

Monsoor, M. A., Kalapathy, U. and Proctor, A. 2001. Improved method for determination of pectin degree of esterification by diffuse reflectance Fourier transform infrared spectroscopy. *Journal of Agricultural and Food Chemistry,* **49,** 2756–2760.

Morel, J. L., Habib, L., Plantureux, S. and Guckert, A. 1991. Influence of maize root mucilage on soil aggregate stability. *Plant and Soil,* **136,** 111–119.

Mostafa, M. and Van Geel, P. J. 2007. Conceptual models and simulations for biological clogging in unsaturated soils. *Vadose Zone Journal,* **6,** 175–185.

Mostafa, M. B. 2009. *Experimental and numerical investigations of conceptual models for biological clogging of unsaturated soils.* PhD, Carleton University.

Murbeck, S. 1919. *Beiträge zur biologie der wüstenpflanzen. Vorkommen und bedeutung von schleimabsonderung aus samenhüllen.* , Lunds Universitets Arsskrift.

Ndjouenkeu, R., Goycoolea, F. M., Morris, E. R. and Akingbala, J. O. 1996. Rheology of okra (*Hibiscus esculentus* L) and dika nut (*Irvingia gabonensis*) polysaccharides. *Carbohydrate Polymers,* **29,** 263–269.

O'Neal, A. M. 1952. A key fore valuating soil permeability by means of certain field clues. *Soil Science Society of America Journal,* **16,** 312–315.

Page III, C. R. and Barber, J. T. 1975. Interactions between mosquito larvae and mucilaginous plant seeds. II. Chemical attraction of larvae to seeds. *Journal of American Mosquito Control Association,* **35,** 47–54.

Paluszek, J. 2011. Physical quality of eroded soil amended with gel-forming polymer. *International Agrophysics,* **25,** 375–382

Penfield, S., Meissner, R. C., Shoue, D. A., Carpita, N. C. and Bevan, M. W. 2001. *MYB61* is required for mucilage deposition and extrusion in the Arabidopsis seed coat. *Plant Cell,* **13,** 2777–2791.

Peters, A. and Candau, S. J. 1988. Kinetics of swelling of spherical and cylindrical gels. *Macromolecules,* **21,** 2278–2282.

Peters, A., Hocquart, R. and Candau, S. J. 1991. Kinetics of swelling of polyacrylamide gels: concentration profiles and effect of an imposed strain. *Polymers for Advanced Technologies,* **2,** 285–294.

Philip, J. R. 1969. Hydrostatics and hydrodynamics in swelling soils. *Water Resoure Research,* **5,** 1070–1077.

Philip, J. R. 1972. Hydrostatics and hydrodynamics in swelling media. *In:* IAHR (ed.) *Developments in Soil Science.* Elsevier.

Rao, M. A. 1999. *Rheology of fluid and semisolid foods: principle and applications.*, Springer-Verlag.

Read, D. B., Gregory, P. J. and Bell, A. E. 1999. Physical properties of axenic maize root mucilage. *Plant and Soil,* **211,** 87–91.

Reeves, E. L. and Garcia, C. 1969. Mucilaginous seeds of the Cruciferae family as potential biological control agents for mosquito larvae. *Journal of American Mosquito Control Association,* **29,** 601–607.

Ross-Murphy, S. B. 1994. *Rheological methods,* London, Blackie Academic and Professional.

Sadowski, T. J. 1965. Non-Newtonian Flow through Porous Media. II. Experimental. *Transactions of the Society of Rheology,* **9,** 251-271.

Sadowski, T. J. and Bird, R. B. 1965. Non-Newtonian Flow through Porous Media. I. Theoretical. *Transactions of the Society of Rheology,* **9,** 243-250.

Singh, A., Sarkar, D. J., Singh, A. K., Parsad, R., Kumar, A. and Parmar, B. S. 2011. Studies on novel nanosuperabsorbent composites: swelling behavior in different environments and effect on water absorption and retention properties of sandy loam soil and soil-less medium. *Journal of Applied Polymer Science,* **120,** 1448–1458.

Singh, B. 2007. Psyllium as therapeutic and drug delivery agent. *International Journal of Pharmaceutics,* **334,** 1–14.

Singh, B., Chauhan, G. S., Kumar, S. and Chauhan, N. 2007. Synthesis, characterization and swelling responses of pH sensitive psyllium and polyacrylamide based hydrogels for the use in drug delivery (I). *Carbohydrate Polymers,* **67,** 190–200.

Singh, J. 1997. *Physical behavior of superabsorbent hydrogels in sand.* PhD, McGill University, Montreal, Ouebec, Canada.

Sochi, T. 2010a. Modelling the flow of yield-stress fluids in porous media. *Transport in Porous Media,* **85,** 489–503.

Sochi, T. 2010b. Single-phase flow of Non-Newtonian fluids in porous media. *Journal of Polymer Science Part B: Polymer Physics* **48,** 2437–2767.

Somerville, C., Bauer, S., Brininstool, G., *et al.* 2004. Toward a systems approach to understanding plant cell walls. *Science,* **306,** 2206–2211.

Spena, F. R. and Vacca, A. 2001. A Potential Formulation of Non-Linear Models of Flow through Anisotropic Porous Media. *Transport in Porous Media,* **45,** 405–421.

Squire, G. R., Rodger, S. and Wright, G. 2000. Community-scale seedbank response to less intense rotation and reduced herbicide input at three sites. *Annals of Applied Biology,* **136,** 47–57.

Suzuki, Y. Y., Tokita, M. and Mukai, S. 2009. Kinetics of water flow through a polymer gel. *The European Physical Journal E: Soft Matter and Biological Physics,* **29,** 415–422.

Syvertsen, J. P. and Dunlop, J. M. 2004. Hydrophilic gel amendments to sand soil can increase growth and nitrogen uptake efficiency of citrus seedlings. *Hortscience,* **39,** 267–271.

Tanaka, T. and Fillmore, D. J. 1979. Kinetics of swelling of gels. *Journal of Chemical Physics,* **70,** 1214–1218.

Tanaka, T., Hocker, L. O. and Benedek, G. B. 1973. Spectrum of light scattered from a viscoelastic gel. *Journal of Chemical Physics,* **59,** 5151–5159.

Temsiripong, T., Pongsawatmanit, R., Ikeda, S. and Nishinari, K. 2005. Influence of xyloglucan on gelatinization and retrogradation of tapioca starch. *Food Hydrocolloids,* **19,** 1054–1063.

Terpstra, R. 1995. Dormancy of seeds of shepherd's purse in alternating wet and dry, compressed aggregated soil: a laboratory experiment. *Jounal of Applied Ecology* **32,** 434–444.

Thomas, N. L. and Windle, A. H. 1980. A deformation model for Case II diffusion. *Polymer,* **21,** 613–619.

Thullner, M., Schroth, M. H., Zeyer, J. and Kinzelbach, W. 2004. Modeling of a microbial growth experiment with bioclogging in a two-dimensional saturated porous media flow field. *Journal of Contaminant Hydrology,* **70,** 37–62.

Toorop, P. E., Campos Cuerva, R., Begg, G. S., Locardi, B., Squire, G. R. and Iannetta, P. P. M. 2012. Co-adaptation of seed dormancy and flowering time in the arable weed *Capsella bursa-pastoris* (shepherd's purse). *Annals of Botany,* **109,** 481–489.

Torrance, J. K. 1999. Physical, chemical and mineralogical influences on the rheology of remoulded low-activity sensitive marine clay. *Applied Clay Science,* **14,** 199–223.

Traore, O., Groleau-Renaud, V., Plantureux, S., Tubeileh, A. and Boeuf-Tremblay, V. 2000. Effect of root mucilage and modelled root exudates on soil structure. *European Journal of Soil Science,* **51,** 575–581.

Uren, N. C. 1993. Mucilage secretion and its interaction with soil, and contact reduction. *Plant and Soil,* **156,** 79–82.

Uscilowska, A. 2008. Non-Newtonian Fluid Flow in a Porous Medium. *Journal of Mechanics of Materials and Structures,* **3,** 1151–1159.

van Genuchten, M. T. 1980. A closed-form equation for predicting the hydraulic conductivity of unsaturated soils. *Soil Science Society of America Journal,* **44,** 892–898.

van Rheede van Oudtshoorn, K. and Van Rooyen, M. W. 1999. *Dispersal biology of desert plants,* Berlin, Springer Verlag.

Vandebroek, I. 2006. *Capsella bursa-pastoris* (L.) Medik. . *In:* SCHMELZER, G. H. and GURIB-FAKIM, A. (eds.) *Medicinal plants/Plantes medicinales 1[CD-Rom]*. Prota 11.

Vincken, J.-P., Schols, H. A., Oomen, R. J. F. J., *et al.* 2003. If Homogalacturonan were a side chain of Rhamnogalacturonan I. Implications for cell wall architecture. *Plant Physiology,* **132,** 1781–1789.

Vrentas, J. S., Jarzebski, C. M. and Duda, J. L. 1975. A Deborah number for diffusion in polymer-solvent systems. *AIChE Journal,* **21,** 894–901.

Wang, C., Li, Y. and Hu, Z. 1997. Swelling kinetics of polymer gels. *Macromolecules,* **30,** 4727–4732.

Wang, Y. T. and Gregg, L. L. 1990. Hydrophilic polymers - their response to soil amendments and effect on properties of a soilless potting mix. *Journal of the American Society for Horticultural Science,* **115,** 943–948.

Wannerberger, K., Nylander, T. and Nyman, M. 1991. Rheological and chemical properties of mucilage in different varieties from Linseed (*Linum usitatissimum*). *Acta Agriculturae Scandinavica,* **41,** 311–319.

Watt, M., McCully, M. E. and Jeffree, C. E. 1993. Plant and bacterial mucilages of the maize rhizosphere: Comparison of their soil binding properties and histochemistry in a model system. *Plant and Soil,* **151,** 151–165.

Western, T. L. 2006. Changing spaces: the *Arabidopsis* mucilage secretory cells as a novel system to dissect cell wall production in differentiating cells. *Canadian Journal of Botany,* **84,** 622–630.

Western, T. L. 2012. The sticky tale of seed coat mucilages: production, genetics, and role in seed germination and dispersal. *Seed Science Research,* **22,** 1–25.

Western, T. L., Skinner, D. J. and Haughn, G. W. 2000. Differentiation of mucilage secretory cells of the *Arabidopsis* seed coat. *Plant Physiology,* **122,** 345–356.

White, I. and Sully, M. J. 1987. Macroscopic and microscopic capillary length and time scales from field infiltration. *Water Resources Research,* **23,** 1514–1522.

Willats, W. G. T., McCartney, L. and Knox, J. P. 2001. *In-situ* analysis of pectic polysaccharides in seed mucilage and at the root surface of *Arabidopsis thaliana*. *Planta,* **213,** 37–44.

Windsor, J. B., Symonds, V. V., Mendenhall, J. and Lloyd, A. M. 2000. *Arabidopsis* seed coat development: morphological differentiation of the outer integument. *Plant Journal,* **22,** 483–493.

Woolfe, M. L., Chaplin, M. F. and Otchere, G. 1977. Studies on the mucilages extracted from okra fruits (*Hibiscus esculentus* L.) and baobab leaves (*Adansonia digitata* L.). *Journal of the Science of Food and Agriculture,* **28,** 519–529.

Woudberg, S., Du Plessis, J. P. and Smit, G. J. F. 2006. Non-Newtonian purely viscous flow through isotropic granular porous media. *Chemical Engineering Science,* **61,** 4299–4308.

Wu, M., Li, D., Wang, L. J., Zhou, Y. G. and Mao, Z. H. 2010. Rheological property of extruded and enzyme treated flaxseed mucilage. *Carbohydrate Polymers,* **80,** 460–466.

Yang, X., Baskin, C. C., Baskin, J. M., Zhang, W. and Huang, Z. 2012. Degradation of seed mucilage by soil microflora promotes early seedling growth of a desert sand dune plant. *Plant, Cell & Environment,* **35,** 872–883.

Yang, X., Baskin, J. M., Baskin, C. C. and Huang, Z. More than just a coating: Ecological importance, taxonomic occurrence and phylogenetic relationships of seed coat mucilage. *Perspectives in Plant Ecology, Evolution and Systematics,* **in press,** http://dx.doi.org/10.1016/j.ppees.2012.09.002.

Yang, X., Dong, M. and Huang, Z. 2010. Role of mucilage in the germination of *Artemisia sphaerocephala* (Asteraceae) achenes exposed to osmotic stress and salinity. *Plant Physiology and Biochemistry,* **48,** 131–135.

Young, J. A. and Evans, R. A. 1973. Mucilaginous seed coats. *Weed Science,* **21,** 52–54.

Zhang, J. P., Zhao, X. H., Suo, Z. G. and Jiang, H. Q. 2009. A finite element method for transient analysis of concurrent large deformation and mass transport in gels. *Journal of Applied Physics,* **105,** 093522.

Zitha, P. L. J., Wouter Botermans, C., v. d. Hoek, J. and Vermolen, F. J. 2002. Control of flow through porous media using polymer gels. *Journal of Applied Physics,* **92,** 1143–1153.

Zohuriaan-Mehr, M. J. and Kabiri, K. 2008. Superabsorbent polymer materials: a review. *Iranian Polymer Journal,* **17,** 451–477.